Percorso dottorale sviluppato con il sostegno finanziario di NextGenerationEU:

Missione 4, Componente 2, Investimento 3.3, CUP B63D22000980008

Borsa MUR ex DM 35x/2022, cofinanziata da Bio4Nature

Dipartimento di Scienze della Vita

Dottorato in Life Sciences

XXXVIII° Ciclo

Coordinatrice: Prof.ssa Simona Maccherini

Characterisation of the Extracellular Fraction in some economically relevant fungi

Settore scientifico disciplinare: Biologia cellulare, Fisiopatologia e Farmacologia

Candidato

Marco Taddei

Sede di attività: Bio4Nature s.r.l. & Università degli Studi di Siena

Firma digitale del candidato

09/01/2026 09:53:28
MARCO TADDEI

Marco Taddei

Supervisore

Michele Pallaoro

Ente di appartenenza: Ex Direttore Scientifico di Bio4Nature s.r.l.

Co-supervisore

Prof. Luca Bini

Ente di appartenenza: Università degli Studi di Siena

Anno accademico di conseguimento del titolo di Dottore di ricerca

2024/2025

Università degli Studi di Siena
Dottorato in Life Sciences
XXXVIII° Ciclo

Data dell'esame finale
28 Gennaio 2025

Commissione giudicatrice

Prof. ssa Alessandra Moscatelli
Prof. Michele Perazzolli

A Benedetta,
Per il sostegno e l'amore ricevuto ogni
singolo giorno in questi tre anni.

ABSTRACT

Botrytis cinerea, also known as "grey mould ", is a necrotrophic fungus part of the large fungal Ascomycota family. Over the years, *B. cinerea* has raised several concerns because of its wide host range and major impact on crops such as tomato, strawberry and grapevine.

Despite much research, current management of *B. cinerea* is mostly based on chemical fungicides, raising environmental and health concerns. To explore innovative control strategies, this PhD project focused on the characterisation of the Extracellular Fraction (EF) of *B. cinerea* ungerminated macroconidia, because it represents the very first interface between the pathogen and its host at the beginning of the spring life cycle of the pathogen. The EF was defined as the entire repertoire of molecules, metabolites, extracellular vesicles (EVs) and proteins present outside the macroconidia, either associated with the cell wall surface (membrane-associated factors) or secreted via conventional and unconventional pathways, through active or passive mechanisms.

A proteomic workflow was optimised to extract the EF and characterise the proteome profile (exoproteome and surfaceome) from ungerminated macroconidia of two *B. cinerea* strains with two different pathogenic backgrounds (B05.10, more aggressive, and T4, less aggressive). Experimental conditions were adjusted to preserve cell viability to avoid contamination from intracellular proteins released by lysis or cell death. Proteins were identified after trypsin digestion using nanoUPLC–MS/MS under conditions that do not allow EV rupture as reported in literature and bioinformatic analysis, such as functional classification, protein-protein interaction networks, effector classification, secretion and membrane-association prediction. Complementary TEM and nanoparticle tracking analysis confirmed that both strains release extracellular vesicles within one hour of incubation, making this the first report of EV production directly from macroconidia.

Proteomic analysis revealed a common core of 80 proteins between the two strains. These proteins were clustered in different functional groups associated with protein folding, stress response, primary metabolism and intracellular trafficking. The presence of proteins involved in redox homeostasis, protein quality control and RNA-related processes highlights that macroconidia in an unstimulating environment, as a neutral buffer, appear to be metabolically active, releasing factors that may act as early virulence effectors. This core of proteins shared between the two strains highlighted an interesting functional conservation of these factors in the early steps of infection between B05.10 and T4.

To investigate the functional role of the EF, detached leaf assays were performed in tomato (*Solanum lycopersicum*) and grapevine (*Vitis vinifera*). In tomato a pilot assay three concentrations of EF (25, 50 and 100 µg/mL) were tested. Results revealed a modulation of host defence genes such as *PTI5*, *WRKY1* and *PR1*, indicating a plant immune-stimulating effect. Afterwards, in grapevine, pretreatment with EF prior to fungal inoculation resulted in a reduced development of necrotic lesions. This effect was supported by stereomicroscope observations performed at various time points (0, 6, 24, 30 and 54 hours post-infection) following 48 hours of immune stimulation. Gene expression analysis confirmed the induction of defence gene markers such as *VvMYB14*, *VvSTS1* and *VvJAR1*, plus highlighted differences between infection with B05.10 and T4. Altogether, these findings support the role of the *B. cinerea* macroconidia exoproteome as an immune elicitor in plants and a probable virulence determinant.

In conclusion, this work provides a first characterisation of the *B. cinerea* macroconidial exoproteome and surfaceome fraction from the EF, including likely EV-associated proteins with a bottom-up proteomic approach. The planta in-vivo assays results, instead, confirm that the entire EF acts as a priming

stimulus that can enhance plant defence responses; parallel studies suggest that EF could probably prepare the macroconidial environment independently of its host to favour the subsequent infection. Considering the advances in understanding the early host-pathogen interaction mechanism, this research points towards potential applications of *B. cinerea* EF as a base for new eco-friendly crop protection strategy development. This work contributes to the search for sustainable alternatives to chemical fungicides in the fight against *B. cinerea* and other necrotrophic pathogens.

INDEX

LISTS OF FIGURES

LIST OF TABLES

1 INTRODUCTION

1.1 Ascomycetes Fungi

Among the vast diversity of fungi, Ascomycetes represent one of the largest and most diverse groups. The phylum Ascomycota includes approximately 64,000 described species, making it the largest division within the fungal kingdom [1]. Together with the Basidiomycota, it constitutes the subkingdom of Dikarya [2].
Ascomycetes are generally classified into three subphyla: *Saccharomycotina* includes unicellular yeasts such as *Saccharomyces cerevisiae*, but also *Candida Albicans*; *Taphrinomycotina,* comprises both yeast and filamentous fungi (*Neolecta, Taphrina*), as well as anamorphic species that reproduce exclusively asexually; *Pezizomycotina,* multicellular filamentous fungi that produce ascocarps of various shapes, colours and sizes, such as truffles, ergot, ascolichens and cup fungi [3].

Ascomycetes naturally occur in different parts of the environment and ecosystem, contaminating different surfaces both indoors and outdoors.
Their ubiquitous presence has led to extensive investigations into their applications [4], [5].
Ascomycetes are, in fact, of particular interest for humans as a source of medically important compounds, such as antibiotics made from Penicillium species, as well as fermenting bread like Saccharomyces, to alcoholic beverages for winemaking. Also, they are important for enzymes, vitamins and lipids production and other interesting compounds which are used in food production [6].
Some Ascomycetes serve as crucial biological model organisms in science. For example, *Neurospora crassa* is a key model for molecular and developmental biology, particularly in RNA interference and DNA methylation-mediated epigenetic control. This fungus offers several advantages, including rapid

vegetative growth, shared techniques, and biological tractability, among others [7].

Nonetheless, numerous fungi belonging to the Ascomycetes division act as pathogens for various organisms, including humans and, notably, plants.

Ascomycetes, in fact, also contain several species of plant pathogenic fungi, some of them with a very large host range, such as *Sclerotinia sclerotiorum [8]*. *S. sclerotium* is a close relative of *Botrytis cinerea*, leading to what is called "white mould" or "stem rot" on more than 400 plant species; it forms persistent sclerotia and gross necrosis on infected tissues, often covered by cottony mycelium [9]. Another emblematic Ascomycete plant pathogen is *Magnaporthe oryzae,* the causative agent responsible of the rice blast disease, considered the most serious fungal disease of rice.

Responsible for devastating yield losses that can feed tens of millions of people each year, *M. oryzae* has become a model system for studying molecular plant-pathogen interactions[10], [11]. *M. oryzae* displays a hemibiotrophic lifestyle: it initially establishes a biotrophic relationship with the rice host cells, suppressing plant defences, before switching to the necrotrophic phase, which leads to extensive tissue damage [12], [13]. Central to its virulence, the appressoria is considered a specialised infection structure which generates enormous turgor pressure used to penetrate the plant cell wall. Once there, the pathogen delivers effector proteins to invert host immunity and reprogram plant metabolism [14].

Equally significant are *Fusarium* species, which include a complex mix of soil pathogens such as *Fusarium oxysporum*, *Fusarium graminearum*, and *Fusarium verticillioides* [15]. These fungi cause root rots and head blights on cereals and vegetables, leading to severe economic and food security concerns. Generally, they produce mycotoxins, which contaminate crops, posing a serious risk to human and animal health [16].

Taken together, these pathogens exemplify the diverse arsenal of strategies developed by these species of pathogenic fungi to colonise plants. Against this backdrop, *B. cinerea* emerges as a particularly versatile and destructive

necrotrophic pathogen. *B. cinerea* distinguishes itself by its extraordinary host range, among 1,400 species. Its remarkable adaptability to different environmental conditions makes *B. cinerea* one of the most successful and damaging pathogens in agriculture [17], [18].

1.2 The pathogenic fungus B. cinerea

B. cinerea, commonly known as "grey mould" because of the characteristic grey sporulation covering infected tissues, is an airborne plant pathogen that attacks more than 200 human food plant species, including highly remarkable crops such as tomato, grapevine and strawberry [19]. Taxonomically, it's classified under the kingdom: Fungi, phylum: Ascomycota, subphylum: Pezizomycotina, class: Leotiomycetes, order: Helotiales, family: Sclerotiniaceae, genus: Botryotinia [20].

B. cinerea is considered one of the top 10 most dangerous fungal pathogens [21]. This type of pathogenic fungus generally lives a necrotrophic lifestyle. After killing the plant cells and macerating the plant tissue, it develops in it and reproduces by forming a large number of (asexual) spores on the infected tissue.

B. cinerea life cycle, in fact, can be divided into two phases, which are generally described as the asexual phase and the sexual phase.

During the asexual phase, the fungus produces macroconidia at the end of particular structures called conidiophores, which are specialised hyphae [22].

Conidia are specialised fungal structures whose survival and germination are strongly influenced by environmental conditions such as temperature, nutrient availability, exposure to sunlight, and humidity conditions [23]. Macrospores are asexual and generally represent the first and main structure, making contact with the host, and start the infectious life cycle every year.

They are metabolically dormant fungal structures and are considered survival structures.

When the living conditions for the fungus are not particularly favourable, it will instead form stone-like structures called sclerotia [22]. Sclerotia are a different survival structure, formed by the fungus, generally used for overwintering. These particular structures are resistant to adverse environmental conditions and are formed by melanising resting bodies [23]

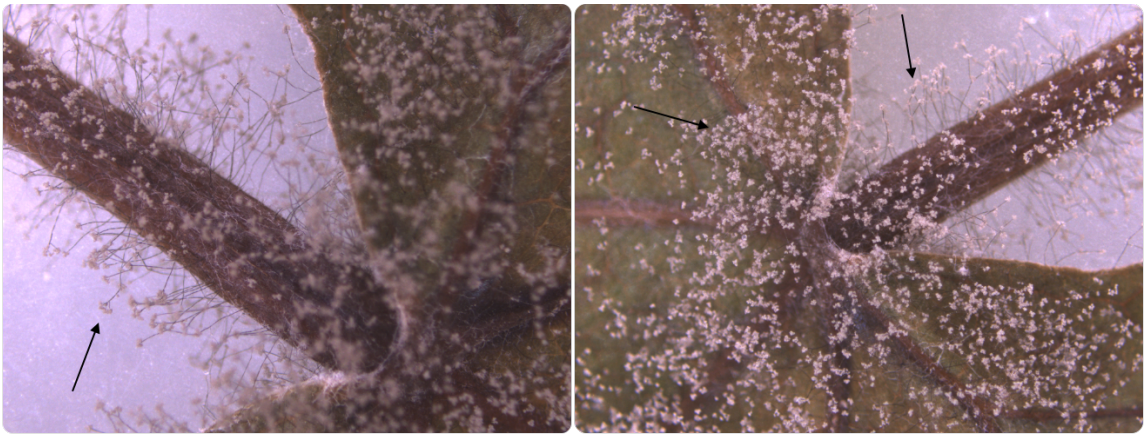

Figure 1.1 Stereoscope images of grapevine leaves infected by B. cinerea producing conidiophores with macroconidia on top. Macroconidia are indicated by black arrows.

On the other hand, the sexual life cycle structure of *B. cinerea* is not so common in nature. The most important structure in sexual cycle are microconidia, small conidia of 1 um, that act as spermatia for *B. cinerea* sexual reproduction. Microconidia are produced by old macroconidia, old hyphae and sclerotia [24]. Sclerotial structure, in fact, during sexual cycle can be fertilised by microconidia, producing apothecia from which ascospores are produced [24].

Although traditionally classified as necrotrophic, evidence is increasing that *B. cinerea* can also colonise asymptomatically as an endophyte, without generating disease symptoms and also eliciting little or no response from the host. Generally, they can establish latent infections that become evident at later development stages or during postharvest storage [25], [26].

1.3 B. cinerea cell wall structure

B. cinerea is characterised by a dynamic, multi-layered cell wall structure that provides both mechanical support and a barrier against external stresses, while also functioning as an interface with the host [17], [19]. It is composed primarily of polysaccharides (as β-1,3-glucans, β-1,6-glucans and chitin), structural glycoproteins, and a small fraction of uronic acids [27], [28], [29].

B. cinerea possesses a complex repertoire of membrane-associated proteins that play fundamental roles in signal transduction, environmental perception, virulence and maintenance of cell integrity [30]. Recent proteomic studies, for example, described how important membrane-associated proteins are in pathogens such as *B. cinerea*. Escobar-Niño *et al.* 2019, with a proteomic study, obtained from *B. cinerea* more than 2500 proteins, of which 46% were classified as membrane-associated thanks to bioinformatics prediction based on algorithms and databases for transmembrane domains or lipidation patterns, for example [31].

Transporters, including ATP-binding cassette (ABC), are one of the major components of the fungal membranome. These proteins are essential for exporting toxic compounds and for importing nutrients released during host tissue degradation. Their activity allows the fungus to survive hostile conditions [32].

Another important class of membrane-associated proteins are the signal receptors and transducers. These include G-protein coupled receptors (GPCRs) and histidine kinase, which detect environmental stress signals, fungicides and host-derived molecules triggering downstream signalling cascades [28]. Among these, mitogen-activated protein kinases (MAPKs) and membrane calcium channels regulate the formation of infection structures and virulence, stress responses and oxidative stress tolerance, enzyme secretion and fungal development during infection, respectively [33]. Small GTPases are another class of important transducers, acting as molecular switches in regulating cell polarity,

morphogenesis and cytoskeletal organisation. Proteins, as BcSec4, are described to be involved in conidiophore development, membrane integrity and autophagy [34].

Other important membrane-associated proteins are represented by enzymes embedded in or associated with the membrane, fundamental to play direct roles in host colonisation. Enzymes such as cutinases, lipases, and cell wall-degrading enzymes (CWDEs) are considered important pathogenic proteins, often tethered to the membrane to facilitate local degradation of the host cell wall and plant cuticle [35].

Finally, on the *B. cinerea* cell wall, structural and adhesion proteins are fundamental components ensuring both physical robustness and the capacity to establish contact with the host surface. Glycoproteins are attached to the cell wall by covalent and non-covalent linkages. The two most important covalently linked proteins found are glycosyl phosphatidylinositol (GPI-dependent wall proteins) and PIR proteins (proteins with internal repeats) [36]. Glycoproteins generally contain both N- and O-linked oligosaccharides. GPI usually anchor to β1,3-glucan or β1,6-glucan or the plasma membrane, while PIR proteins are highly O-glycosylated and are attached directly to β1,3-glucan [37]. This class of proteins taken together provides physical support, contributes to virulence, facilitates surface recognition and protects from host defences.

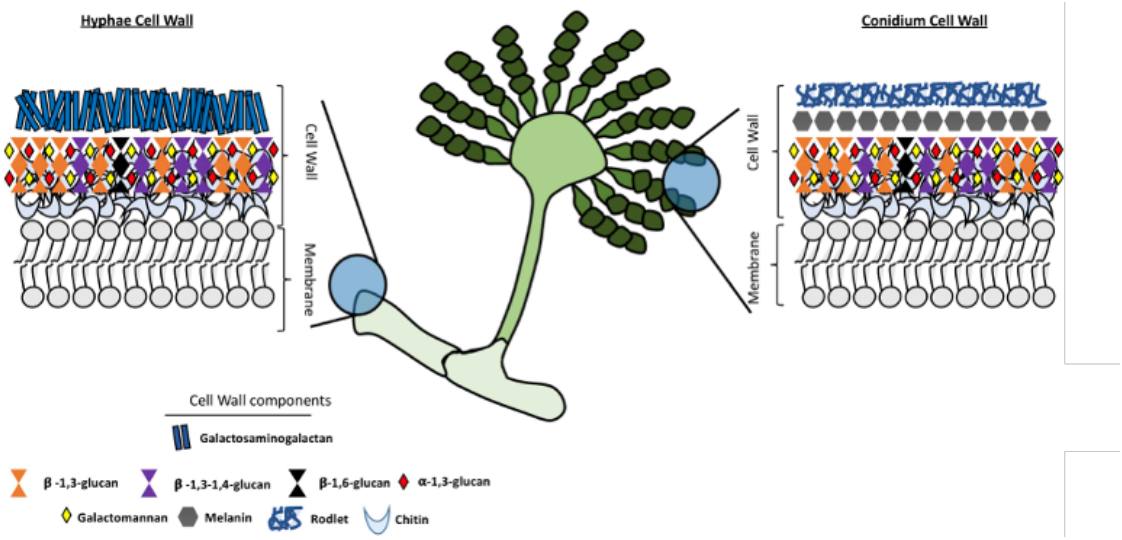

Figure 1.2. Structural organisation and composition of the ascomycete cell wall, such as B. cinerea. Adapted from Garcia-Rubio R. et al. 2020. [38]

1.4 The virulence arsenal of B. cinerea

B. cinerea employs a multifaceted arsenal of virulence factors that lead to its pathogenic success. Central to its infection strategy are specialised structures known as infective cushions (IC) and appressoria. IC are multicellular structures that facilitate host penetration, upon contact with leaves, flowers or fruit, by concentrating mechanical turgor force and secreting a plethora of virulence factors [39]. Those types of structures are also described for other ascomycete pathogens, such as *Magnaporthe oryzae*, which developed highly specialised appressoria to generate turgor pressure to enter the host surface [40].

Upon host contact, *B. cinerea* secretes an array of plant cell wall-degrading enzymes (PCWDEs), including proteins such as cutinases, cellulases, xylanases and pectinases [41]. These enzymes are fundamental as they destroy the plant's cuticle and polysaccharide network, creating an entry point to invade the host [17]. Other necrotrophic fungi, such as *Sclerotinia sclerotiorum,* rely on a broad spectrum of PCWDEs to promote tissue maceration and colonisation [8]. There are approximately 275 predicted secreted CAZymes (carbohydrate-active

enzymes) from *B. cinerea*, which help the fungus degrade different types of sugars and polymers in the plant cell wall [42]. These secreted PCWDEs help the fungus overcoming the cell wall barrier and utilise cell wall materials for nutrition [43].

Beyond enzymatic degradation, *B. cinerea* produces a repertoire of low-molecular-weight metabolites (secondary metabolites) and toxins, some of which have been shown to contribute to virulence. These include well-known molecules such as botrydial, a phytotoxic bicyclic sesquiterpene which contributes to virulence in some *B. cinerea* strains but not in others [44]. One of the most studied is Oxalic Acid (OA), reported to be produced at the late stage of colonisation; however, differently from *S. sclerotiorum*, in which oxalic acid is essential for pathogenicity, the role of OA in *B. cinerea* pathogenicity is unclear [45]. Other organic acids are described to be secreted by *B. cinerea* as citric acid to acidify the tissue, or even succinic acid, followed by accumulation of ammonia, to alter the local pH environment during infection. This secretion of organic acids helps fungi to adapt to different environmental conditions [46].

The arsenal further includes enzymes that generate reactive oxygen species (ROS), creating localised oxidative stress that helps the pathogen accelerate tissue decomposition, contributing to programmed cell death (PCD) [41]. ROS are highly reactive molecules produced both by plants and fungi during their interaction. Due to their high reactivity, they can cause molecular damage such as protein oxidations or DNA mutations, but they also serve as important signalling molecules within cells [47], [48]. Intracellular ROS primarily originate in the mitochondria; In particular, during host-pathogen interactions, ROS are of key importance for plant defence but also for fungal attack [49]. In plants, in fact, ROS help to strengthen the cell wall and trigger PCD. Botrytis, instead, not only copes with this oxidative stress, generated by the plants, but also contributes to it by generating its own ROS [41]. These fungal ROS help damage host tissue and

support infection. However, as ROS are also a problem for fungal cells, *B. cinerea* also provides strong antioxidant defences to control redox balance. Enzymes such as catalase, peroxidases and superoxide dismutases, together with the glutathione and thioredoxin systems [50], detoxify excess ROS.

1.5 The secretome and the surfaceome as the integrative virulence arsenal

All these virulence factors converge in what is collectively termed the secretome of *B. cinerea*: the entire set of proteins, metabolites and molecules actively released into the extracellular environment. The secretome has been given relevant importance in recent years because it represents the functional interface between the fungus and the host, carrying the molecular arsenal that is responsible for colonisation and pathogenicity [51], [52], [53], [54].
In *B. cinerea*, protein export in the extracellular environment follows two distinct pathways: the classical ER (endoplasmic reticulum)-Golgi pathway and several unconventional routes [41]. Different proteomic and genomic surveys have already described a multifaceted secretome. Early during the hyphal and infection phases, *B. cinerea* releases a rich mixture of carbohydrate-active enzymes, proteases, and other virulence factors carrying N-terminal signal peptides consistent with the classical ER-Golgi pathway. However, these studies also reported that a notable fraction of extracellular proteins lacks the canonical signal peptide, suggesting a parallel non-classical export pathway [54], [55].

The conventional pathway depends on the ER, the Golgi apparatus, and the final release of vesicles fused at the plasma membrane. This process is organised, and the secretory vesicles content is generally directed towards infection structures used by the fungus to penetrate host tissue [39]. A large set of proteins acts as the "machinery" that drives the process. Important are Rab GTPases, the exocyst complex that tethers the vesicles to the plasma membrane and the

SNARE proteins, which mediate the actual fusion with the membrane, allowing the cargo to be secreted outside [56], [57], [58]. Different studies on *B. cinerea* underscore how conventional pathway proteins such as BcSec4 (a Rab GTPase) or BcExo70 (exocyst subunit) are essential for secretion and pathogenicity [34], [59].

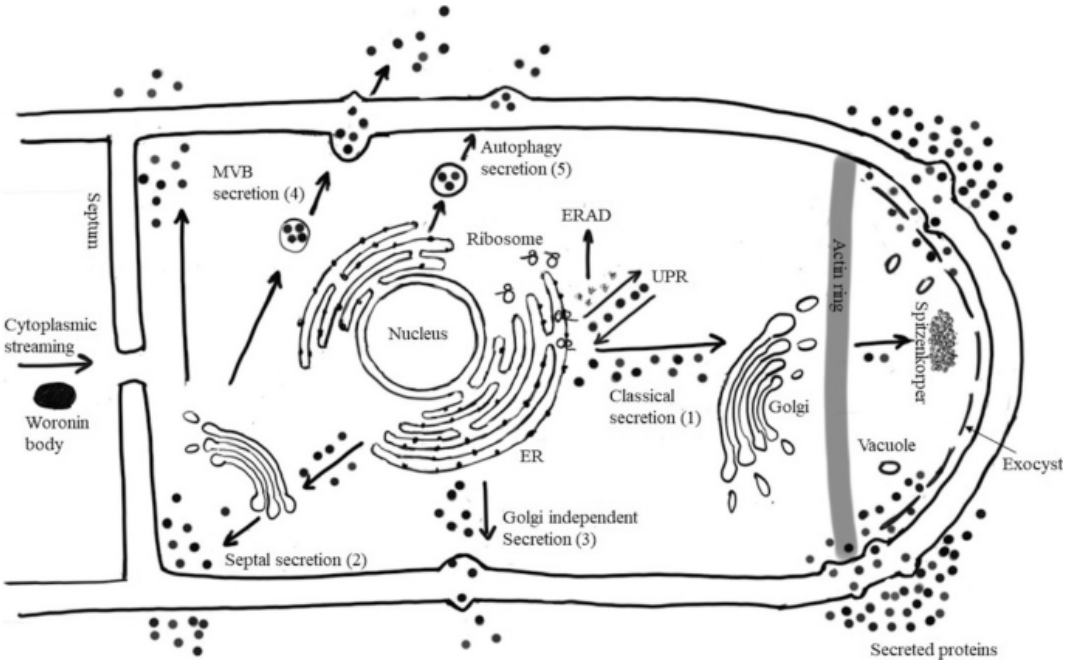

Figure 1.3. Pathogen secretory pathway. Adapted from Sakekar, A et al. 2021 [60]

Not all proteins secreted by *B. cinerea* follow the classical ER-Golgi pathway. In recent years, in fact, it has become increasingly clear that fungi, as *Candida Albicans*, but also *B. cinerea,* rely on unconventional secretion mechanisms [61], [62].

Some proteins, in fact, are directly translocated outside the cell because they lack the N-terminal leader signal peptides required for ER-targeting. In fungi and yeast, unconventional secretion depends on different mechanisms like: ESCRT-dependent secretion through specialised compartments, secretory autophagy or plasma-membrane shedding [54], [63].

Among all unconventional pathways, extracellular vesicles (EVs) have emerged as particularly relevant to *B. cinerea* biology and virulence. EVs are heterogeneous lipid spherical nanoparticles secreted by cells [64]. They can be classified into exosomes, microvesicles and apoptotic bodies. Exosomes are

small structures in the 30 to 100 nm diameter range that originate from an intracellular endocytic trafficking pathway involving the fusion of late endosomes (multivesicular bodies [MVBs]) with the plasma membrane. After such fusion, the intraluminal vesicles of MVBs are released into the extracellular space as exosomes [65], [66]. Microvesicles range from 100 nm to 1000 nm in size, and they are formed by budding of the plasma membrane. Apoptotic bodies are instead the largest vesicle structures (1 μM to 5 μM) observed only in cells that undergo apoptosis.[67]. EVs can carry different molecules, from nucleic acids to proteins and lipids and are proposed as critical mediators of cell-to-cell communication.

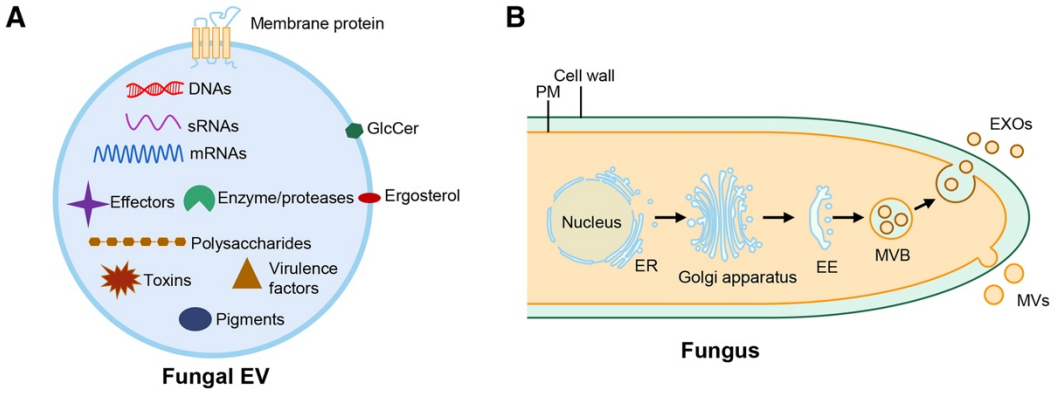

Figure 1.4. Extracellular vesicle (EV) composition and biogenesis. A, Fungal EVs contain a complex mix composition as enzymes, nucleic acids, virulence factors, toxins and other molecules that can be released outside the cells. B, Fungi produce EVs by generating multivesicular bodies (MVBs) or budding from the plasma membrane (PM). Adapted from Wang et al. 2023 [65].

Different studies described the isolation from hyphae of different fungi, as *C.albicans, Ustilago maydis, Fusarium graminearum, Fusarium oxysporum and Colletotrichum higginsianum* [61], [68], [69], [70], [71], [72]. More recent studies instead described the release of EVs even from hyphae of *B. cinerea* B05.10 strain [73], [74].

EVs have emerged as a fundamental and highly versatile mechanism for delivering virulence factors [70], but also for their roles in regulating plant-microbe interactions; however, their complete roles in host-pathogen interactions remain largely unknown. In *B. cinerea* EVs isolated from 5-day-old hyphae, Escobar-Nino *et al.* 2023 [75]), identified an enrichment in cell wall metabolism and proteolysis, but also many virulence factors and proteins

implicated in important steps of invasion, such as pectin degradation, redox state, and signalling.

Beyond proteins and metabolites, it has been shown that *B. cinerea* utilises EVs to secrete small RNAs (sRNAs), which are then internalised by plant cells through clathrin-mediated endocytosis (CME) [76]. This highlights the under-appreciated role of EVs in cross-kingdom communication. It's also widely described that *B. cinerea* transfers virulent sRNA effectors into host plant cells to suppress host immunity genes in Arabidopsis and tomato and achieve infection [77], increasing the arsenal of weapons used by this pathogenic fungus.

The protein pool of the secretome has become a central concept in fungal pathogenicity research, as it represents an important part of the polypeptidic weaponry used by the pathogen to modulate host immunity and establish infection. However, the classical definition of "secretome" does not totally describe and include the diversity of proteins encountered outside the fungal cell wall [78]. In fact, many proteins defined as membrane-bound and cell wall-anchored proteins, such as GPI-anchored proteins, glycoproteins and cell wall-surface hydrolases, are described to play equally important roles in the fungus-host interface, mediating adhesion and direct interactions with the host receptors, but are generally define as "surface proteome" or "proteomic surfaceome" [79]. Different approaches have been optimised to reach and uncover new proteins, linked with the cell wall involved in cell wall integrity and host-pathogen interaction [80] or mediating the signalling pathway from the outside to the inside of the cell, triggered by abiotic and biotic stress stimuli [79]. Recently, in *B. cinerea*, a G protein-coupled receptor (GPCR) BcEst has been identified, playing a key role in signalling and cellular responses and involved in hyphal growth, virulence and stress tolerance [81].

While the term 'secretome' refers to the pool of proteins, but also metabolites and molecules that are actively secreted through classical or non-classical pathways, or via the release of exosomes, as well as to the secretion machinery

itself (including EVs), the term “surfaceome” specifically denote all membrane-anchored proteins and cell-wall modifying enzyme that can be released through enzymatic cleavage, considering all the possible proteins or protein domains accessible to enzymatic digestion [80], [82], [83], [84], [85]. Similarly, the term “exoproteome” instead describes the specific subset of extracellular proteins (and proteases) that can be found in the extracellular proximity of the cell or spore surface, arising from both active and inactive release mechanism, including cell lysis, EV-associated proteins, or proteins accidentally released during manipulation or centrifugation [78], [86] (Fig. 1.5). According to these definitions, the secretome, exoproteome and the surfaceome can be defined as the total “Extracellular Fraction” (EF). Thus, EF can be considered as a complementary component of the pathogen’s virulence arsenal, allowing it to interact with the external environment, approach the hosts and initiate its infection strategy.

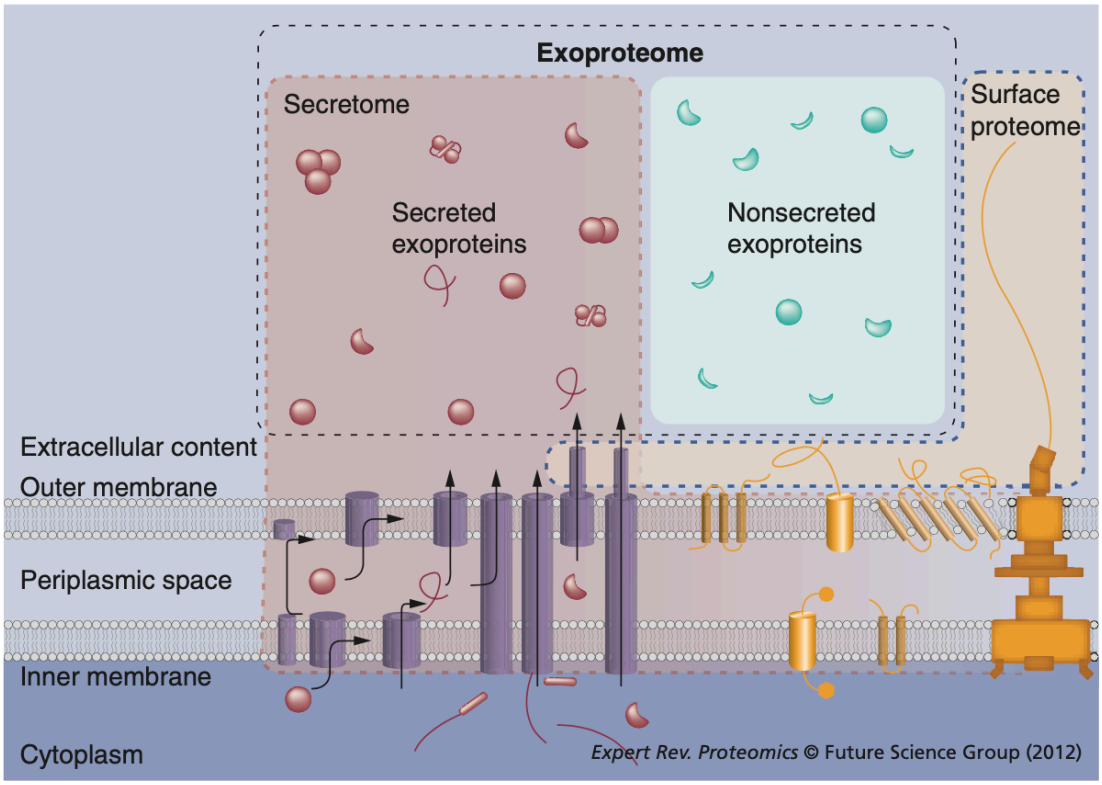

Figure 1.5. Secretome, surfaceome and exoproteome concepts illustrated with a eukaryotic cell model: The exoproteome (black dotted line) regroups the so-called 'secreted exoproteins' and 'non-secreted exoproteins' (among them, proteins from cellular lysis or fragments from proteomic surfaceome due to abrasion). The secretome (red dotted line) regroups the so-called 'secreted exoproteins', most membrane proteins here shown in orange, and the diverse secretion systems here drawn in purple, considering also molecules and metabolites secreted by the cell, including EVs. The surface proteome (blue dotted line) comprises the fraction of proteins inserted in the membrane in contact with the extracellular environment, accessible to enzymatic digestion. Adapted from Armengaud J, et al. 2012 [78].

With this view in mind, proteomics has played a dominant role in the study of specific proteins involved in the virulence of plant pathogens [57], [87]. While genomic and transcriptomic data outline the potential coding capacity of the organism, only proteomics can reveal which proteins are effectively produced to interact with the environmental situations. This makes proteomics an indispensable approach to studying the pathogenic fungi exoproteome.

The most widely applied methodology in this field is the bottom-up proteomics approach. Generic sample proteins are first enzymatically digested into peptides (usually through trypsin), then the mixture is separated by ultra high-performance liquid chromatography (UPLC) and analysed by tandem mass spectrometry (MS/MS)[51]. Bottom-up proteomics is highly sensitive, robust and capable of analysing complex mixtures, making it ideal for EF proteomic analysis.

Although the EF (or part of it) of *B. cinerea* hyphae have been studied in different stages of infection or under specific stimuli [51], [54], [87], [88], [89], very little is known about the very early events before spore germination. The need for new strategies against *B. cinerea* is underscored by its enormous economic impact. This necrotrophic fungus is responsible for grey mould disease in more than 200 human alimentation plant species, with severe consequences for vegetable crops and viticulture in pre- and post-harvest situations. In tomato, *B. cinerea* can cause post-harvest losses exceeding 20-30% under inadequate storage [90]. In viticulture, grey mould remains one of the most diffuse diseases worldwide. Recent estimates suggest that *B. cinerea* is responsible for billions of euros in losses annually in Europe, both through yield reduction and deterioration of grape and wine quality[91]. To compensate, intensive fungicide applications remain the main strategy to control the disease. According to the Food and Agriculture Organization (FAO) and EU monitoring reports, fungicides represent nearly 40% of all pesticides use in Europe [92], [93], [94]. Fungicides not only increase the resistance of pathogens but also have potential hazards to the environment, soil microorganisms and human health [91].

By exploring the early EF of *B. cinerea* macroconidia, this study aims to expand the current understanding of fungal adaptation strategies in the initial phase of development. Macrospores, in fact, are considered the very first line of the pathogen's structures, making contact with the future host. Every year, generally, the infectious life cycles start from the release of macrospores in the environment by the sporulated overwintered sclerotia. Considering the low amount of information generated in the literature towards this type of structure of *B. cinerea* (different from hyphae or others), this study aimed to provide greater clarity regarding the macrospores of this pathogen. Applying a proteomic approach to the EF in a very early-stage window offers the opportunity to detect proteins that may act as early sensors, environmental modulators, or "stealth" virulence factors, that may allow infection in later stages, the massive release of

enzymes and virulence effectors to complete the infection process. Identifying these proteins could improve our understanding of the early infection stages and provide new molecular targets for the development of innovative and eco-friendly crop protection strategies.

1.6 Grapevine and Tomato as Model Systems for Studying B. cinerea Interactions

Grapevine (*Vitis vinifera*) is one of the most economically important fruit crops worldwide, cultivated on more than 7 million hectares with a global production exceeding 70 million tons of grapes per year [95].

Approximately 70% of the harvest is destined to winemaking, while the remaining is used for fresh consumption and dried products. In 2024, wine production was estimated to be 237 million hectolitres, and the Italian viticulture sector exported wine for total earnings of 8,1 billion just in the last year [95], [96].

Beyond its economic relevance, viticulture is deeply influenced by soils, climate, and vineyard management, but especially is highly susceptible to a wide range of fungal pathogens, including downy mildew, powdery mildew and *B. cinerea [91]*. Viticulture, in fact, is often associated with high inputs of agrochemicals, especially fungicides, which account for a disproportionate use relative to its cultivated surface area [92], [93].

For these reasons, the grapevine is a particularly relevant model for studying plant-pathogen interactions. The economic value, with its vulnerability to *B. cinerea*, makes it a good crop for testing innovative strategies such as priming and the use of *B. cinerea* exoproteome as a potential elicitor for plant immunity.

Tomato (*Solanum lycopersicum*) is another important agronomically and scientifically important plant system, offering relevant insights into plant-pathogen interaction. Compared to grapevine, it is an annual crop widely used as a model for plant immunity studies, due to its well-characterised genetics, short life cycle and susceptibility to different pathogens such as *B. cinerea* [97], [98], [99].

Concerning *B. cinerea*-grapevine interaction, this fungus is a common component of the natural microflora in most vineyards. The pathogen's life and its disease cycle have been described by Elmer and Michailides [100].

The fungus is generally able to overwinter as sclerotia and/or mycelium in plant debris. When environmental conditions become favourable, these soil structures produce conidia, which serve as the primary inoculum that is capable of infecting grapevine, but also tomato and other plant tissues [58].

B. cinerea infection can occur at any stage of fruit development, but generally, primary infections most often occur during blooming, remaining asymptomatic until berry ripening. This is because, often, the primary infection occurs when infected tissues are not immediately infectious. Different factors seem to influence this quiescent phase, such as nutrient-limited availability, thick and firm cell walls, and inactivation of fungal virulence factors [101]. However, during ripening, physicochemical changes in berries, as cuticular changes or cell-wall loosening, together with a substantially different signalling network activated by the fungus, lead to an aggressive fungal colonisation [101].

B. cinerea infection is predominantly initiated by macroconidia, which attach and germinate over the plant surface, as flowers, leaves or fruit. After macroconidia germination and germ tube and hyphae elongation, *B. cinerea* is able to develop appressoria and IC, to colonise the inside of the tissue [90].

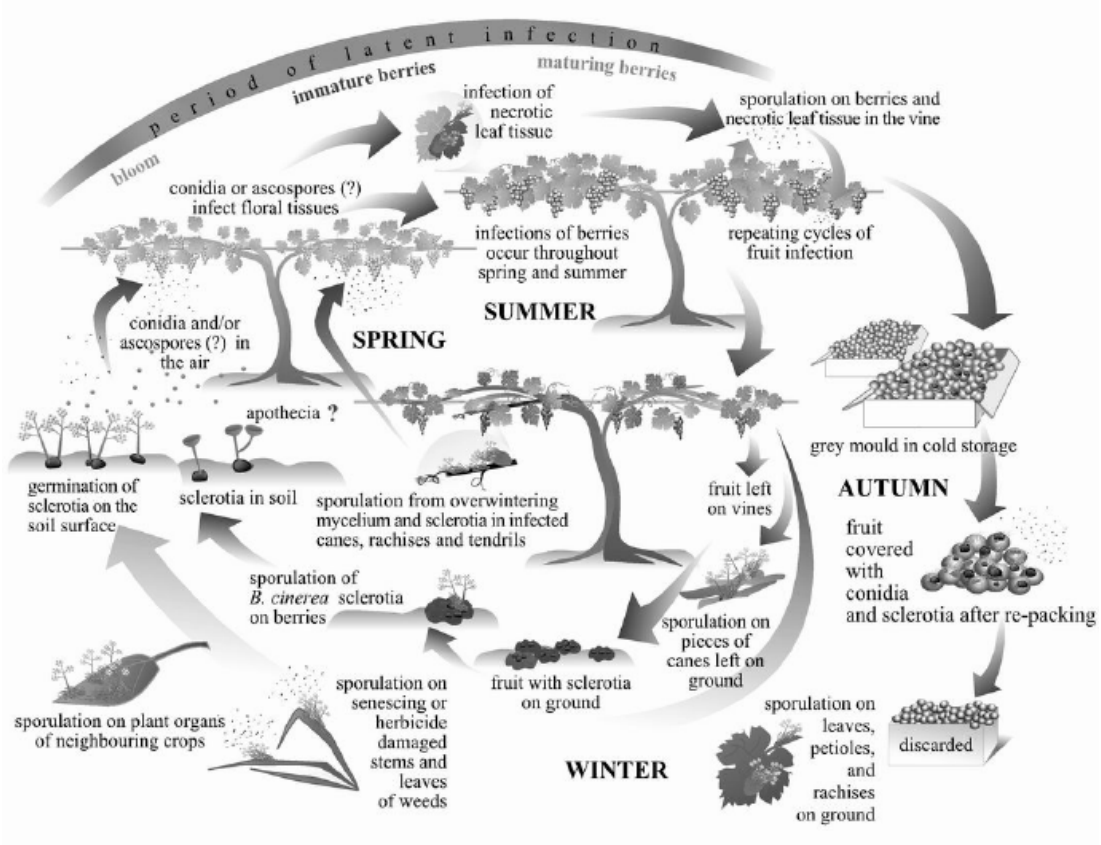

Figure 1.6. B. cinerea life cycle and disease cycle in grapevine and vineyards. Adapted from Elmer et al. 2007 [97]

Following the initial contact with grapevine, two distinct phases have been described: an early phase characterised by the formation of a non-spreading infection, and a later stage, where an abundant fungal biomass is produced and the lesion is spread [41], [90].

However, important details about the initial events following spore contact and germination are not completely clear. A short "non-destructive" phase, similar to a transient biotrophy as described for *S. sclerotiorum* [102], may occur, as *B. cinerea* could invade living cells and kill them after, or invade after it is killed via secreted molecules [41]. However, both scenarios create an infection space that allows fungal biomass accumulation. Evidence suggests that spreading lesions involve diffusible fungal agents and manipulation of the host hypersensitive response pathway [41], [103].

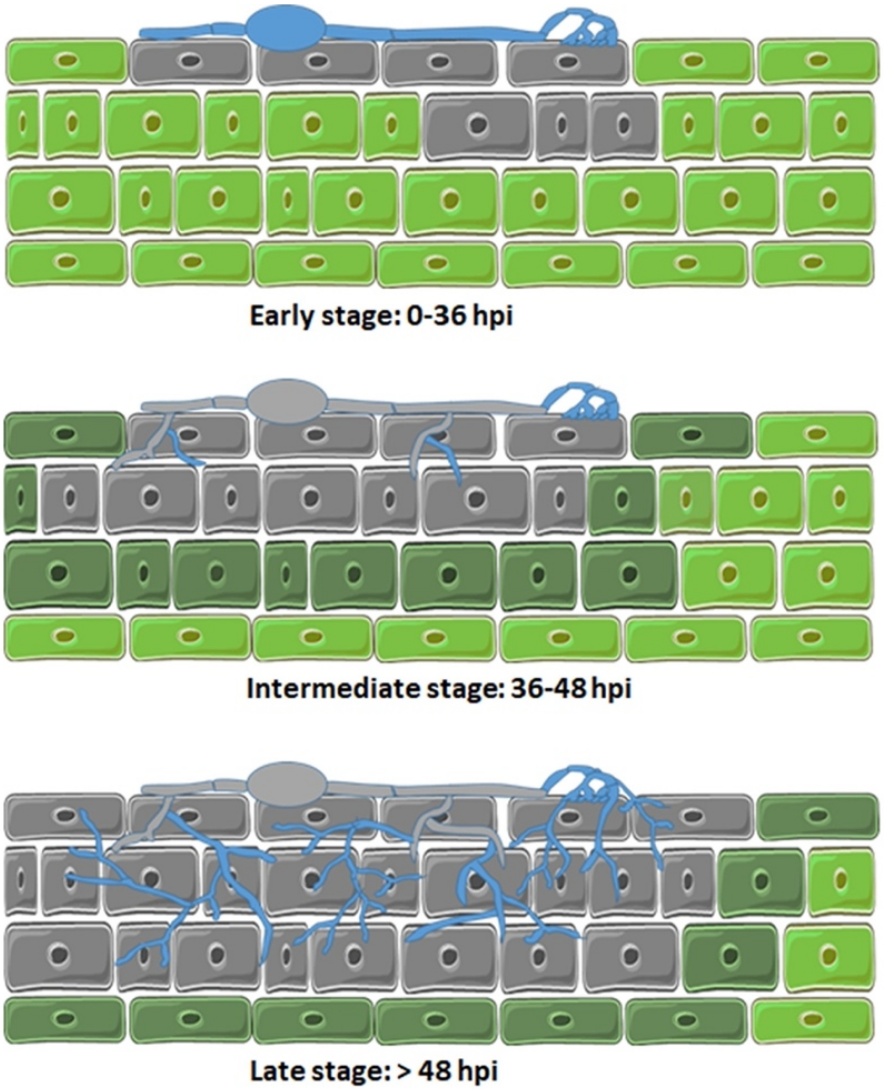

Figure 1.7. Principal steps in B. cinerea infection stages. Adapted from Bi et al. 2023 [41]

From the other side of the plant-pathogen interaction, plants, unlike animals, lack mobile immune cells and an adaptive immune system based on antibodies or memory lymphocytes. Instead, they developed a sophisticated and multilayered innate immune system that allows them to perceive pathogens' presence and activate a rapid defence. Basically, their system is characterised by membrane-localised receptors, intracellular defence proteins, and complex hormonal signalling pathways to generate a local and systemic resistance [104].

1.7 Plant immunity model

A widely accepted model to describe plant immunity is the “zig-zag “ model, firstly proposed by Jones and Dangl (2006) [105]. This model shows how the first phase of plant defence is the “Pattern-Triggered Immunity (PTI), activated when cell-surface Pattern Recognition Receptors (PRRs) recognise pathogen-associated molecular patterns (PAMPs) or damage-associated molecular patterns (DAMPs), such as chitin, polysaccharides and/or flagellin for bacterial [106]. PTI then tries to restrict pathogens’ invasion through basal defences like oxidative bursts, callose deposition and transcriptional activation of defence genes. In response, pathogens secrete effectors that suppress PTI, leading to the second part of the zig-zag model, the Effector-Triggered Susceptibility (ETS) phase. Plants, in fact, have evolved intracellular Nucleotide-Binding Leucine-Rich Repeat (NLR) receptors that detect these effectors and activate a stronger defence response known as Effector-Triggered Immunity (ETI), upon direct or indirect recognition of effectors by NLRs [107], [108]. ETI is often associated with the hypersensitive response (HR) that represents a localised programmed cell death (PCD) that tries to restrict pathogen growth together with ROS burst, mitogen-activated protein kinase (MAPK) cascades, calcium flux and phytohormone signalling [107].

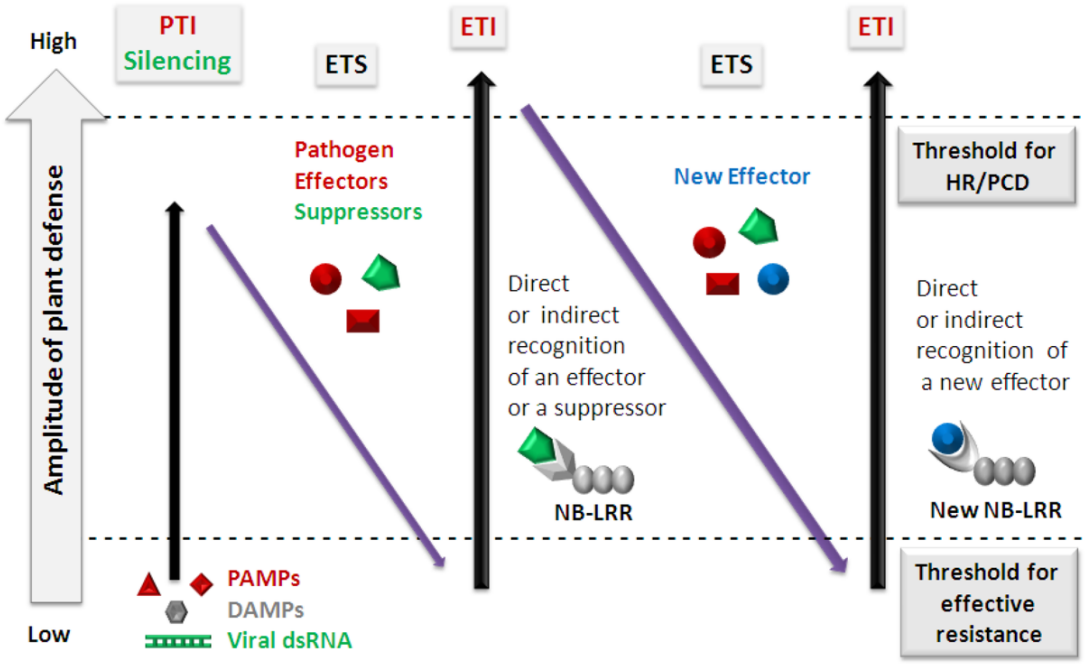

Figure 1.8. Zig-zag model description for the innate immunity system against pathogens. In phase 1, plants detect pathogen-associated molecular patterns (PAMPs) and damage-associated molecular patterns (DAMPs) via pattern-recognition receptors (PRRs) to induce pattern-triggered immunity (PTI). In phase 2, pathogens deliver effectors/suppressors that interfere with PTI, resulting in effector-triggered susceptibility (ETS). Then effectors are recognised directly or indirectly by an NLR protein (NB-LRR), activating effector-triggered immunity (ETI), an amplified version of PTI leading to hypersensitive response (HR) and programmed cell death (PCD). Adapted from Zvereva et al. 2012 [109]

Within this context, plant hormones play a pivotal role: salicylic acid (SA), jasmonic acid (JA) and ethylene (ET) are the three main phytohormones that orchestrate the immune response [110].

Phytohormones are central regulators of plant immunity, coordinating local and systemic responses against pathogens with different lifestyles. During PTI, ETS and ETI plant hormones trigger extensive transcriptional reprogramming and thereby tightly regulate defence responses [110]. Generally, SA is primarily associated with defence against biotrophic and hemibiotrophic pathogens, where its accumulation triggers HR and PCD, trying to restrict pathogen's growth at the infection site [111]. However, in grapevine, for instance, infection by *B. cinerea* triggers the SA-dependent pathway and production of stilbenes such as resveratrol and phytoalexins (molecules produced for plant defence) that inhibit fungal growth, through the activation of defence genes like *STS* and *PAL* [112]. SA

also activates systemic acquired resistance (SAR), which represents a long-lasting immune state, where defence responses are propagated throughout the plant after local infection.

In contrast, JA and ET act synergistically to orchestrate defences against necrotrophic pathogens, as *B. cinerea*. The JA/ET signalling pathway regulates the induction of pathogenesis-related (PR) proteins, for example, through *PR1*, protease inhibitors and secondary metabolites that limit fungal colonisation [113], [114].

JA is a lipid-derived phytohormone synthesised through the octadecanoid pathway, mainly from linolenic acid released from chloroplast membranes [115]. However, the bioactive form of JA is the one conjugated to isoleucine, forming jasmonoyl-isoleucine (JA-Ile) produced by the enzyme JAR1 [116]. The bioactive form JA-Ile, when it is produced, promotes the degradation of JAZ repressors, thereby activating transcription factors that regulate defence-related genes[117]. JA signalling pathway regulates the production of antimicrobial secondary metabolites, such as phytoalexins and protease inhibitors, contributing also to the reinforcement of the cell wall [118]. However, some researchers revealed that JA is involved in several other physiological processes, like root growth and plant senescence [118]. In grapevine, JA signalling is strongly linked to the induction of stilbene synthases (*VvSTS*) and regulators like *VvMYB14*. Together, they contribute to resveratrol production [119], [120]. Resveratrol, in fact, is produced through the activity of STS, condensed p-coumaroyl-CoA and malonyl-CoA, and with its derivatives, exhibits potent antifungal activity [121].

On the other side, ET is a gaseous phytohormone synthesised from methionine via aminocyclopropane-1-carboxylic acid (ACC), catalysed by ACS (1-Aminocyclopropane-1-Carboxylic acid Synthase) and ACO (1-Aminocyclopropane-1-Carboxylic acid Oxidase) in response to multiple environmental stresses, both abiotic and biotic [122]. ET can also act as a developmental hormone, but in immunity, its role is tightly linked to defence against necrotrophic pathogens and modulation of JA responses. ET can act

synergistically with JA to enhance resistance, through ethylene response factors (ERFs), activating related defence genes [122]. The interplay between JA and ET is considered a cornerstone of plant immunity, activating a branch of defence gene expression. In contrast, as for JA, ET may also interact antagonistically with SA signalling, prioritising defences against necrotrophs [123]. However, these two systems (JA/ET and SA) don't work independently, but it seems that they can talk to each other. Generally, when one is active, it can suppress the other. But sometimes, at low levels, SA and JA can even work together to boost defence. Overall, the balance between SA and ET/JA seems to be crucial. Plants can probably regulate which pathway is stronger depending on the pathogen type and environmental conditions. This hormone crosstalk ensures the plants do not waste energy and prepare the right defence for the right pathogens.

1.8 The plant primed state

Beyond direct defence responses, plants can establish a "primed" state that enhances their ability to respond to future challenges. Priming is an adaptive strategy that improves the defensive capacity of plants. After an initial stimulus, from pathogens, beneficial microbes, as well as chemical and abiotic cues, plants can establish a priming state, allowing them to respond faster and more robustly upon subsequent pathogen attacks [124]. Upon stimulus perception, changes may occur in the plant at the physiological, transcriptional, metabolic, and epigenetic levels [106]. Priming can be durable, and plants can maintain the effect through all plant's life cycle or transmit it to generations, indicating an epigenetic component of transgenerational defence priming [125]. In particular, pathogen-derived molecules can act as priming stimuli in plants. This can be of different biochemical natures (peptides, polysaccharides or lipids) and are perceived by the plant through PRR.

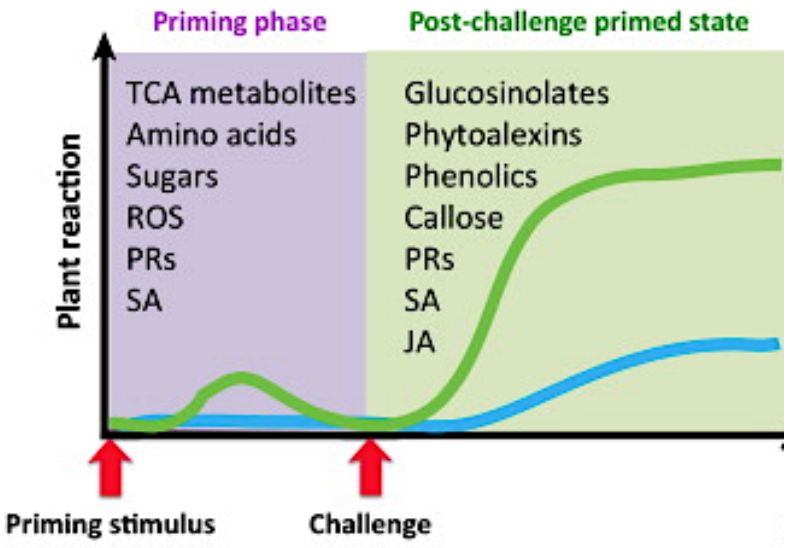

Figure 1.9. Example of primed and unprimed state levels in plants. A stimulus triggers the priming state and lasts until the plant is subsequently exposed to challenging stress. During the priming phase, the plant enters in a standby state, and secondary metabolites, enzymes and hormones are slightly altered. During the real challenge with a stress, the plants entered the post-challenge primed state, in which all the factors to combat the given stress are induced rapidly. The green line represents primed plants, and the blue line shows the unprimed plants.

Priming events are characterised by three main criteria: (i) memory, the plants are able to remember the priming stimulus [126], (ii) potentiated response, primed plants, in fact, can activate stronger or faster defences when challenged (through accumulation of phytoalexins or ROS burst), putting the plant in a standby state (accumulation of amino acids, sugars, Pathogen Related (PRs) proteins and SA)[127], (iii) improved performance, since primed plants typically show higher tolerance, survival, or yield under stress conditions, with a low fitness cost [128]. Priming is associated with changes also in signal transduction pathways, involving SA, JA and ET as well as epigenetic modifications [125].

Overall, the literature reviewed underscores the complexity of plants' immune regulation, from pathogen perception to the hormone regulators' signalling pathway, in which SA, JA and ET play a decisive role, and their crosstalk can determine the outcome of the plant-pathogen interactions. In this framework, priming has emerged as a central concept, as the capability of the plants to establish a "ready-to-respond" state that enables a stronger, faster and more efficient defence response upon pathogen challenge, while minimising

metabolic cost. With this idea in mind, the experimental section of the in-vivo plant test aims at evaluating the priming potential of the Extracellular Fraction (EF) (including both the secretome (proteins, EVs, metabolites...etc), exoproteome and surfaceome) fraction obtained from two strains of *B. cinerea* (B05.10 and T4) in two different hosts: tomato (Solanum lycopersicum) as a preliminary model to understand the first effects of this fraction and its necessary concentrations; and grapevine (*Vitis vinifera*) a perennial species of major economic importance and natural host of *B. cinerea*. By integrating macroscopic phenotyping with molecular analysis of defence-associated marker genes, these experiments seek to provide new insights into the role of the fungal EF in modulating the host's immunity and into its possible application as a tool for developing sustainable crop protection strategies.

2 Materials and methods

2.1 Fungal Strain and Culture Conditions

B. cinerea B05.10 (VTT Culture Collection) and T4 strain (kindly provided by Dr. Muriel Viaud) were used. Each strain was grown on "MYPA" medium (30 g/L Malt extract; 5 g/L Yeast extract; 5 g/L Peptone; 15 g/L agar). Spores of each strain were inoculated on Petri plates at $0{,}02x10^5$ sp/mL concentration solution and incubated under lab light for 72 Hrs. followed by complete darkness until collection at 14 days p.i. (*Post inoculation*). All strains were grown at 21-23°C for the incubation period.

After mycelium sporulation, conidia were harvested in 154 mM NaCl solution, filtered through a 40 µm nylon filter (Avantor, VWR) and centrifuged three times for 10 min at 2000 x g, then resuspended in NaCl solution at $10x10^6$ /mL concentration and stored at 4°C until use.

For long period storage, conidia were resuspended in 10% (v/v) Glycerol, 154 mM NaCl solution at $0{,}1x10^6$/mL concentration and stored at -80°C [74].

Spore solutions were counted using the Neubauer chamber and vitality assessed with trypan blue.

2.2 Extracellular Fraction Isolation

For the optimisation of the EF isolation, three protocols were used as references, but with some modifications. [73], [74], [129]

Briefly, conidial samples were centrifuged at 2000 x g for 10min, conidia pellet was resuspended in 154 mM NaCl solution and centrifuged again, but then resuspended in sterile water, to clean all the substances released by the spores during storage and to eliminate any other possible cell debris. Conidia were centrifuged for the last time and then resuspended in an incubation buffer

solution of HEPES 5 mM pH 8.0, NaCl 154 mM and DTE 50 µM to a 300x10^6/mL conidia concentration.

The conidia suspension was then incubated at 25°C for one hr in the dark.

After the incubation period, conidia were removed by centrifugation at 4000 x g (4°C) for 15min and then at 20000 x g (4°C) for 20 min. Afterwards, all the possible remaining conidia were removed by filtration with a 0.45 µm filter, an aliquot was also plated on MYPA to check the absence of any residual macroconidia.

EF solution, appearing clear, was then stored at -80°C after addition of trehalose to a final 25 mM concentration [129]. Cell lysis and spore vitality were monitored before and after incubation period using a Trypan Blue solution to ensure no cell death.

For the tomato and grapevine detached leaves assay, three independent preparations of EF for each strain were concentrated with Vivaspin20 3 KDa (Merck) and pooled together. Protein concentration for both EF strains was determined by Bradford protein assay in microplates, to adjust the EF to the concentration needed.

2.3 Monodimensional Gel Electrophoresis Analysis

Mono-dimensional gel electrophoresis analysis was performed with four EF samples from both *B. cinerea* strains. Aliquots of EF were prepared using 45 µL by first concentrating the samples in SpeedVac and then resuspending them in Laemmli buffer (100 mM Tris–HCl pH 6.8, 2% (w/v) SDS, 20% (v/v) glycerol, 4% (v/v) β-mercaptoethanol) and heated at 95 °C for five minutes. Specifically, 3 to 5 µg of proteins for each sample were loaded and separated on 10% polyacrylamide gel. Ammoniacal silver staining was then used to visualise the mono-dimensional gels. The resulting gels were scanned with Image Scanner III laser densitometer run by the LabScan 6.0 software (GE Healthcare). Image Master 2D Platinum 6.0 software (GE Healthcare, Uppsala, Sweden) was used to carry out image analysis.

2.4 Cryo-TEM analysis

For cryo-TEM analysis EF solution obtained from filtration was centrifuged at 100.000 x g for 1 hour. After centrifugation most of the supernatant was revomed, leaving only to 50 µL, where the possible pellet, if present, was resuspended. Then an aliquot of 2,3 µl of sample solution was applied to glow-discharged holey carbon grids (Quantifoil Cu R2/1, 300 mesh, Quantifoil Micro Tools GmbH), blotted for 3 s, and plunge-frozen in liquid ethane using an FEI Vitrobot Mark IV plunge freezer to achieve sample vitrification. Frozen samples were stored in liquid nitrogen until EM imaging in a Philips CM200FEG microscope operating at 200 kV, equipped with a TVIPS TemCam-F224HD CCD camera and a Gatan 626 Cryo-Holder.

2.5 EF measurement by NTA analysis

Measurements of EVs concentration and size in the entire EF were performed by NTA using a NanoSight NS 300 particle analyser (Malvern Instruments Ltd., Malvern, UK). EF direct samples were injected into the flow cell at a flow rate of 0.05 mL/sec through an automated syringe pump. Five measurements (30 seconds each) were obtained for each sample, and the average was plotted as a representation of size distribution and concentration (particles/ml). Three measurements of EF for each strain were performed, and a table of average results was reported. A representation of size distribution and concentration was chosen for each strain and described.

2.6 Macrospore EF shaving preparation

For spores shaving optimisation of the, a proteomic strategy previously described for *C. albicans* [85] has been optimised to identify the EF.

Briefly, conidia suspension samples were centrifuged at 2000 x g for 10 min, the drained conidia pellet was resuspended in 154 mM NaCl solution, centrifuged again twice and then resuspended in sterile water and centrifuged for the last time. The Conidia pellet was then resuspended with HEPES 5 mM pH 8.0, NaCl 154 mM, DTE 50 µM to a $300x10^6$/mL concentration and incubated at 25°C. A total amount of 10 ug Trypsin (Seq. Grade modified Trypsin, Promega) was added for $150x10^6$ spores only for the "TRY" sample.

After incubation, samples were centrifuged at 20000 x g for 20 min, spores separated, and the supernatant was taken up carefully and centrifuged again two times. The supernatant was then filtered using 0.45 µm pore-size filters (Millipore). At each sample (shaving and control with no spores) 2 µg/mL of Trypsin was added and incubated again overnight at 37°C. Proteolytic reactions were stopped by adding 0.1% TFA (v/v). Samples were then concentrated in SpeedVac and stored at -80°C until use.

Cell lysis and spore vitality were monitored before and after the incubation period using a Trypan Blue solution to ensure no cell death.

2.7 Proteomic Analysis by nanoUPLC-MS/MS analysis

Digested samples (that comprised only the exoproteome and surfaceome) were reconstituted in 0.1% formic acid in water. LC-MS/MS analyses were performed using Q-Exactive HF-X Orbitrap mass spectrometer coupled with UltiMate 3000 RSLCnano UHPLC System (Thermo Scientific). Peptide separation was carried out at 35°C using a PepMap RSLC C18 column, 75 um × 15 cm, 2 µm, 100 Å (Thermo Fisher) at a flow rate of 300 nl/min. The mobile phases A and B used for the analysis were 0.1% formic acid in water and 0.1% formic acid in acetonitrile, respectively. The gradient started with 5% of B, and then it was increased up to 90% in 120 min. The experiment was performed using a data-dependent analysis (DDA) setting to select the "top twenty" most abundant ions for MS/MS analysis. Protein identification was performed using MaxQuant software (Version 1.6.50,

https://maxquant.net/maxquant/ (accessed on January 2024) using the following parameters: Enzyme Trypsin, unique peptide ≥1; minimum length: 7 amino acids, FDR threshold for both peptides and protein identification: 0.01; Missed cleavage: 2; Modification: Oxidation; Mass tolerance: 10 ppm; Fragment mass tolerance: 0.5 Da; Peptide to use: Unique + Razor. MS/MS spectra were searched against *Botrytis cinerea B05.10 and T4* entries in the UniProtKB/Swiss-Prot database. From all the proteins obtained from MaxQuant analysis, only those with a "score" value higher than 10 were considered for the analysis, generating a high-confidence quality data.

2.8 Bioinformatic analysis

To compare all the accession numbers obtained from MaxQuant identifications between the three independent experiments, and between the two B. *cinerea* strains, the online website Interactive Venn (http://www.interactivenn.net/) was used (accessed February 2024), generating an immediate visualisation of the common and specific protein groups [130]. Considering the different Accession numbers between the two *B. cinerea* strains, to facilitate protein comparison, protein accession numbers from the T4 strain (*Botryotinia fuckeliana 999810*) were converted to the B05.10 accession number (*Botryotinia fuckeliana 332648*) by BLAST tool in UniProt database https://www.uniprot.org/blast (accessed April 2024), and only the proteins with an overlap over 95% were taken.

STRING database v12.0 (accessed May 2024) was used to generate a protein interaction network of the 80 common proteins identified from B05.10 and T4. The protein-protein network was obtained, and the highest confidence interaction score ≥ 0.9 was used to reduce false-positive interactions [131]. This network was subsequently divided into clusters, divided by colours, based on the Markov Clustering (MCL) option, in order to obtain highly connected and biologically meaningful clusters. The inflation value was set to 2.0 as the default.

GO enrichment was performed using STRING, and the results were considered significant at FDR < 0.05 using the Benjamini–Hochberg method.

For the functional analysis of the 80 common proteins, different bioinformatic tools online were used. Effector P 3.0 (accessed June 2024) was used to predict the potential pathogenic effect of the proteins [132]. Alpha and Beta transmembrane domains were predicted using Deep TMHMM [133]. Signal peptides were predicted by SignalIP 5.0 (accessed June 2024) [134]. Net-GPI 1.1 (accessed June 2024) was used to study different kinds of protein-membrane association [135]. For the subcellular localisation of the proteins Cello v2.5 (accessed June 2025) was used [136].

The common proteins were further analysed using the Conserved Domain tool from NCBI [137] and all the default parameters. For uncharacterized proteins with unknown domains, BlastP was used to obtain as much information as possible.

For the Gene Ontology (GO) classification, for each protein, a GO ID was obtained using QuickGO (accessed July 2025) [138].

Then, to avoid GO redundancy and better visualise the most important biological and functional groups REVIGO software v1.8.1 (accessed July 2025) was used [139].

2.9 Tomato detached leaves protocol

Tomato (*Solanum Lycopersicum* cv. *RedCherry*) was used for the experiment for the first *in vivo* plant approach for the EF fraction. 5 plants were used for the experiment, grown under greenhouse conditions. The leaves were collected, but due to unforeseen problems, only two leaves for each condition could be used. All the leaves were sterilised by immersion in 5% sodium hypochlorite for 2 minutes, followed by three washes with sterile distilled water. Sterilised leaves were then randomly placed on petri dishes (245 mm x 245 mm), divided into 4

squares, one for each condition, with two leaves on each over 1% agar solution. Each leaf was placed with the adaxial side uppermost on the agar.

For each *B. cinerea* strain, two leaves were treated with the corresponding EF with a droplet method of 10 µL, then spread all over the leaves' surface with three different concentrations of EF: 25 µg/mL, 50 µg/mL and 100 µg/mL, considering the EF availability. For controls, two leaves for each strain were spread with mock (EF buffer solution), and two leaves were spread with 10 µL of a $1x10^6$ sp/mL B. cinerea solution (positive control INF). Leaves were incubated at room temperature in the dark. Samples were collected at only two time points, 24 and 48 hpi (hours post inoculation), and immediately frozen in liquid nitrogen, stored at -80°C until further analysis as described in [140]. Two biological replicates were collected for each sample.

2.10 Grapevine detached leaves protocol

Vitis vinifera cultivar susceptible to B. cinerea B05.10 and T4 strains, Trincadeira (**ViVC number 15685)** was selected for this work. Plants were grown under greenhouse conditions (22 °C/ day and 18 °C/ night).

A total of 30 plants from this cultivar were used. Leaves were collected from the third to the fifth leaf from the shoot apex. All the leaves were sterilised by immersion in 5% sodium hypochlorite for 2 minutes, followed by three washes with sterile distilled water. Sterilised leaves were randomly placed on Petri dishes (245 mm x 245 mm) containing 150 mL of 1% Agar solution. For each dish, which represents a different condition, 4 leaves were placed with the adaxial side uppermost on the agar.

The experimental design was made to enhance plant immune response prior to pathogen inoculation.

For each *B. cinerea* strain, four leaves were treated with the corresponding extracellular protein fraction using a droplet method at 50 ug/mL concentration, and randomly applied 125 uL divided in drops and spread all over the leaf surface.

After EF application, leaves were incubated at room temperature under a 12h light / 12 h dark cycle for 48 Hrs.

Following this first immunity boost phase, leaves were inoculated with a spore suspension $1x10^6$ sp/mL (125 uL) of the respective *B. cinerea* strain (EF + INF) [141].

The experimental design included Immunity control (EF only), where leaves were pre-treated with EF and then inoculated only with spore suspension buffer without spores. Positive control, where leaves were pre-treated with EF buffer only, followed by inoculation with *B. cinerea spores* (INF). Negative controls were leaves treated only with EF buffer throughout the entire incubation period without spores (CTRL).

After the inoculation, all the leaves were maintained at room temperature in the dark for the first 24 hrs and then under the same 12h/12h light/dark cycle. Samples were collected at 0, 6, 30 and 54 hours post inoculation (hpi) and immediately frozen in liquid nitrogen, stored at -80°C until further analysis as described in [140]. Three biological replicates were collected for each condition. For each leaf at each time point, before collection, a leaf disk was taken and visualised directly under the stereomicroscope.

2.11 RNA extraction and cDNA synthesis

Total RNA was isolated from 100 mg of frozen leaves from each condition with the Spectrum™ Plant Total RNA Kit (Sigma-Aldrich, USA), according to manufacturer's instructions. Residual genomic DNA was digested with DNase (TURBO DNA-free™ Kit, Thermo Scientific, USA).

RNA purity and concentration were measured at 260/280 nm using a spectrophotometer (NanoDrop-1000, Thermo Scientific) while RNA integrity was verified by agarose gel electrophoresis (1.2% agarose in TAE buffer). To check for genomic DNA contamination, crude total RNA samples were subjected to quantitative real-time Polymerase Chain Reaction (qPCR) targeting a reference

gene, Actin7 for tomato assay and Elongation Factor 1-alpha (EF1α) for grapevine assay. Complementary DNA (cDNA) was synthesised from 500 ng of total RNA using RevertAid®H Minus Reverse Transcriptase (Fermentas, Ontario, Canada) anchored with Oligo(dT)23 primer (Fermentas, Ontario, Canada), according to the manufacturer's instructions.

2.12 Gene expression analysis

Gene expression experiments were conducted using a StepOne™ Real-Time PCR system (Applied BiosystemsTM, Sourceforge, USA) with the iTaq™ Universal SYBR® Green Supermix, (Bio-Rad Laboratories, Inc, USA), following manufacturer's instructions. Each reaction had a 10 µL volume, containing 2.5 mM $MgCl_2$, 2 µM of each primer, and 1 µL of cDNA as a template. A control without cDNA template was included in each reaction set. Primer sequences are provided in (Table S1). Thermal cycling began with a 95 °C denaturation step for 10 minutes, followed by 40 cycles of denaturation at 95 °C for 15 seconds and a single annealing/extension step at a specific temperature for 30 seconds.

Three biological replicates and two technical replicates were used. Gene expression (fold-change) was calculated as previously described [142]. Actin7 for tomato assay and Elongation Factor 1-α (EF1α) gene for grapevine assay [143] were used for expression data normalisation, as outlined in Monteiro et al. [144]. All methods were carried out in accordance with relevant institutional, national, and international guidelines and legislation guidelines complying with the Convention on Biological Diversity (https://www.cbd.int/convention/).

2.13 Statistical analysis

Due to the lack of data normality and homogeneity of variances, the statistical analysis of the data was based on a non-parametric test. Statistical analysis was performed using the Kruskal-Wallis test to compare all groups with each other at

each time point of the analysis, with R software (v. 4.5.1) and RStudio (2025.05.1+513). Results yielding $p<0.05$ were considered statistically significant.

3 RESULTS

3.1 Optimisation of B. cinerea macrospore EF shaving conditions

The main object of this first work section was to characterise with a proteomic approach the EF from the macrospores of the pathogenic fungus *B. cinerea*. This fraction contains different set of proteins, including glycoproteins [145], transmembrane proteins and/or membrane GTP-anchored proteins, which are generally the ones making the first contact with the host surface [146], [147], proteins secreted through classical and non-classical pathways [73], [75], but also inactive secreted proteins.

To achieve this, it was very important to set up experimental conditions allowing access to the EF fraction via enzymatic digestion with trypsin while maintaining cell integrity.

The technique used is known as "surface shaving" and is based on the controlled use of one or more proteolytic enzymes, like Trypsin or Proteinase K, that digest all the accessible proteins that are outside the cell or on the surface of the cell wall [80], [148]. At the same time, it's important not to compromise the integrity of the fungal cell membrane and the vitality of the cell.

B. cinerea, both stains, B05.10 and T4, were grown on MYPA (Malt – Yeast – Peptone – Agar), a standard sporulation medium, rather than a medium that mimics the host plant tissue. This choice allows for the identification of EF proteins that may be relevant in a broader spectrum of host-pathogen interactions, making our results applicable for diverse infection scenarios.

The second step, after optimising macrospore sporulation production for both strains, was to remove cellular debris accumulated during spore collection since the technique requires scratching as much fungal mycelium as possible from the

plate. Although the 40 µm filtration step was very functional in separating the macrospores from mycelium, a lot of debris were still present in the collection buffer, together with some seldom microconidia. This contamination was solved by three centrifugation steps at 2000 g x 10 min, which eliminated all the debris by confining them in the supernatant, as shown in Figure 3.1.

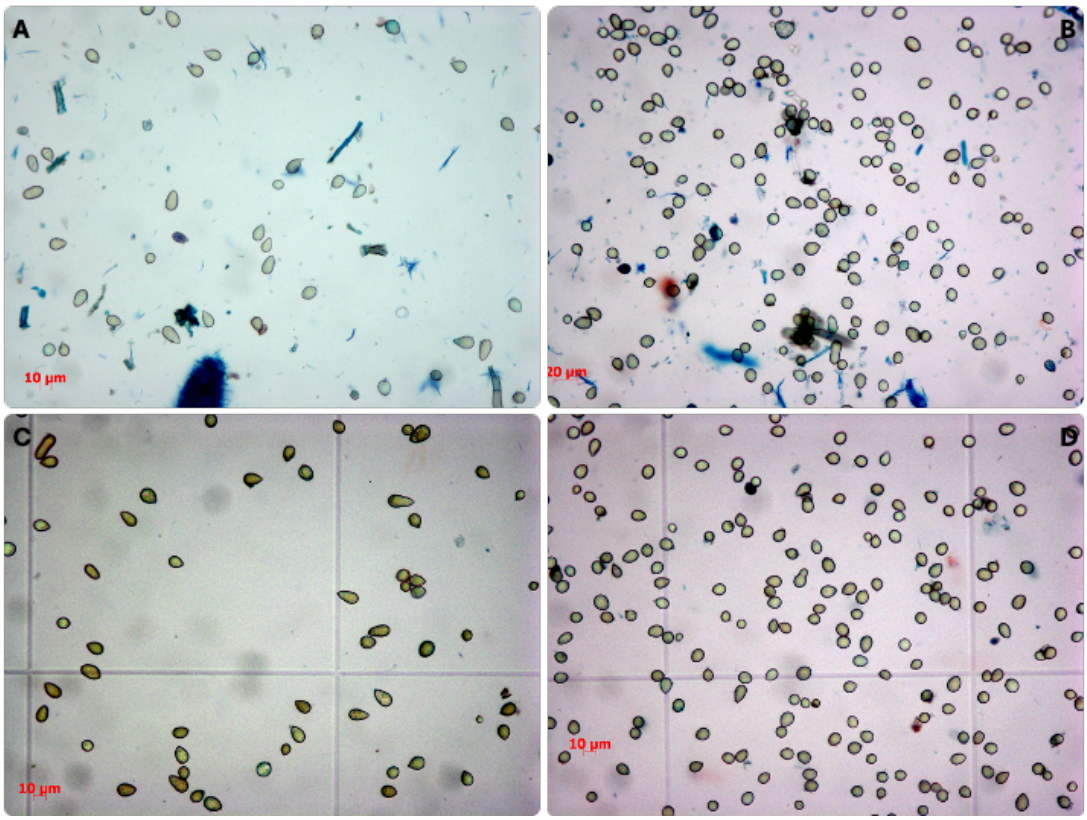

Figure 3.1. B. cinerea B05.10 and T4 macrospores cleaning. A and C represent B05.10 macrospores pre- and after the three centrifugation washes, respectively. B and D represent T4 macrospores pre- and after three centrifugation washes, respectively.

Then, multiple conditions to optimise the proteolytic digestion were tested to define a 1-hour incubation window, in order to capture the macroconidia exoproteome and surfaceome prior to germination. This is a critical point because hyphae, which are the primary infection structure, emerge directly from germinating macroconidia, which, however, are the very first pathogenic cycle starting point, and may play a major role in the host-fungal interaction.

To facilitate enzymatic access, especially to cell-wall surface proteins, DTE (1,4-dithioerythritol) was used at a final concentration of 50 uM. DTE promotes disulfide bond reduction with a minimal cell viability impact [149].

The buffer solution was maintained, as the collection buffer, at a physiological concentration of 150 mM NaCl to avoid osmotic stress. Incubation temperature was set at 25°C, which is a definite non-stress temperature for *B. cinerea* growth conditions [150]. Although trypsin activity is optimal at 37°C, 25°C represents a valid compromise condition between enzymatic efficiency and preservation of macrospores' viability to avoid intracellular protein contamination.

The final optimised macrospore shaving conditions use 5 mM HEPES buffer (pH 8.0) containing 50 uM DTE, 150 mM NaCl, spores were incubated 1 hour at 25°C with 10 µg of Trypsin at $300x10^6$ sp/mL concentration.

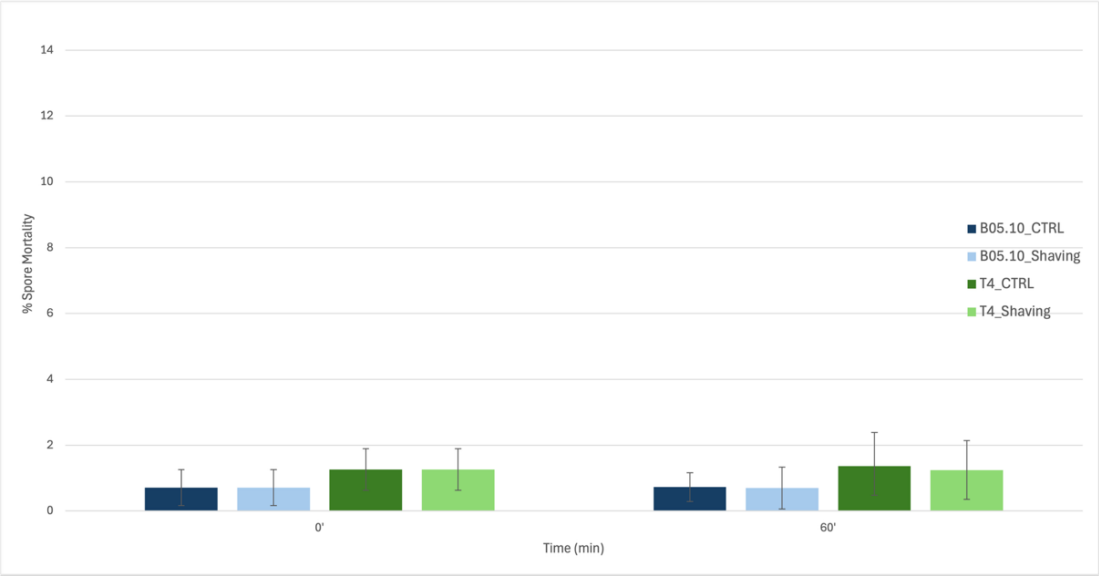

Figure 3.2. Percentage of macrospore mortality before and after 1-hour incubation period of both strains B05.10 (blue) and T4 (green). The bar chart represents the average of 3 different experiments for each strain with Standard Deviation bars.

As shown in Figure 3.2, these conditions maintain spore mortality below 2%.

Cell mortality and integrity through the shaving process, but also during protocol experimental set-up, were monitored using Trypan blue staining [151]. As shown in Figure 3.3, Trypan blue clearly stains dead macrospores compared to the live ones, as was proved with a heat-treated spore positive control at 95°C for 5min.

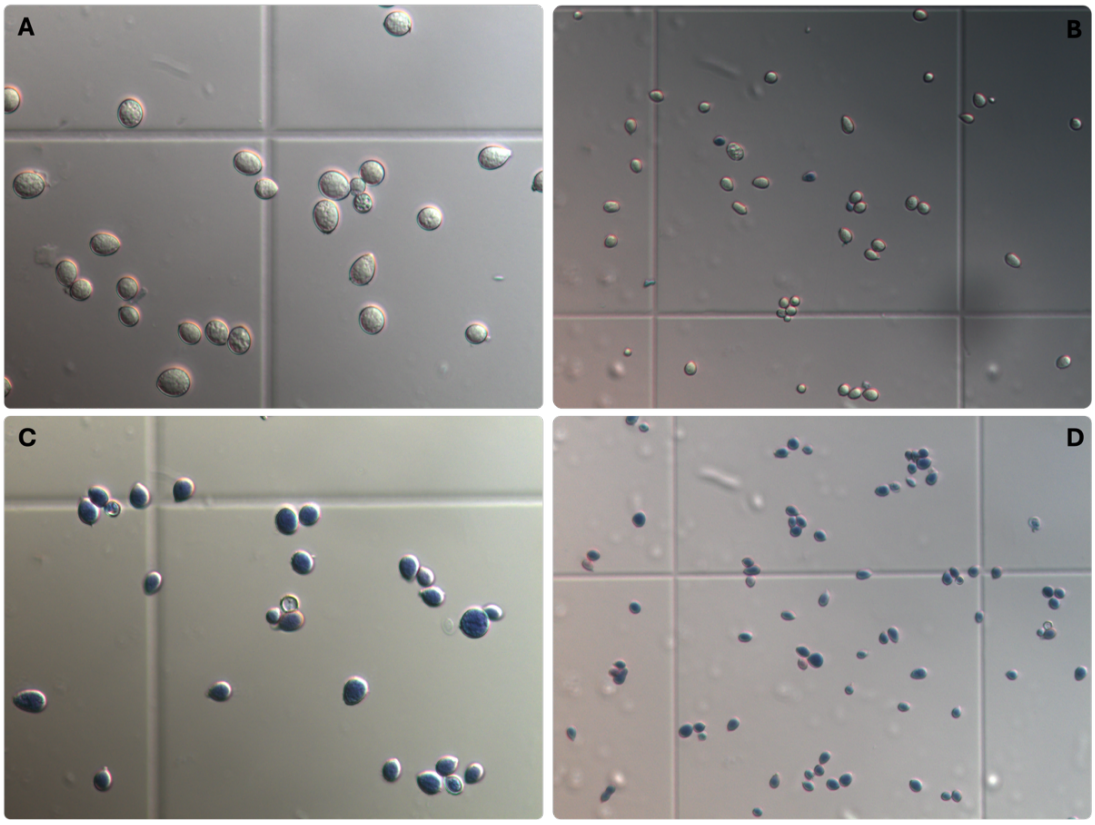

Figure 3.3. Macrospores Trypan Blue staining mortality test at 95°C for 5min: Panel A (20x) and B (10x) represent macrospores before the heating period. Panel C (20x) and D (10x) represent macrospores after the heating test.

Another important point was to confirm the absence of germinated macrospores during and after the incubation window. Samples at 0 and 1 hour (Figure 3.4) were observed under the microscope. As shown, no germinated macrospores were detected, confirming that the EF extraction analysis was conducted under control of intact, ungerminated macroconidia, with a mortality percentage consistently under 2%.

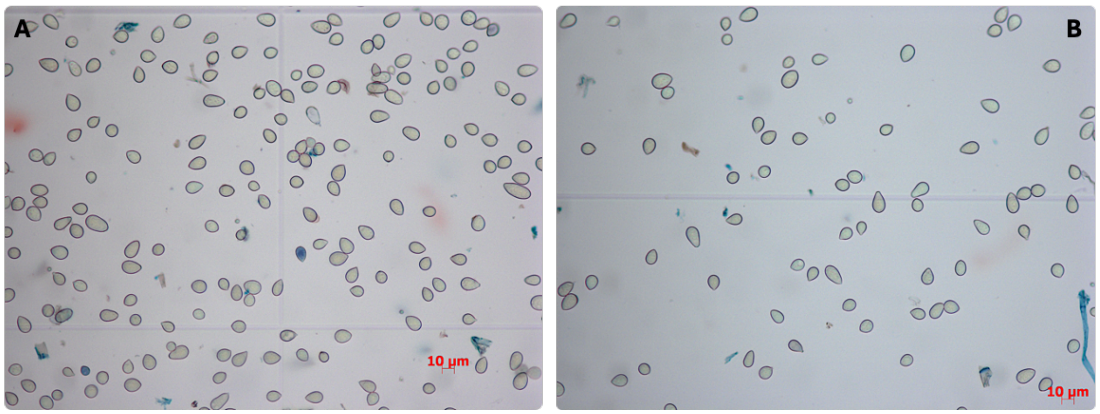

Figure 3.4. B. cinerea macrospores observation under the microscope at 0 (A) and 1 (B) hours of incubation in the experimental shaving conditions.

The reproducibility and solidity of the protocol were validated by one-dimensional SDS-PAGE analysis of four independent samples for both *B. cinerea* strain B05.10 and T4. As shown in Figures 3.5 and 3.6, protein profiles for each strain, but also between the two strains, were consistent for all biological replicates, even if in some preparations, some differences are notable. This is generally accepted by the biological diversity from one preparation to another. Notably, EF appears to be totally different from a cellular lysate, confirming the particularity of this fraction. Major bands were observed around 75kDa, 60kDa and 37 kDa with an intense band around 10kDa, observed in both strains. This probably suggests an abundant production and/or release of a small protein common to both *B. cinerea* isolates.

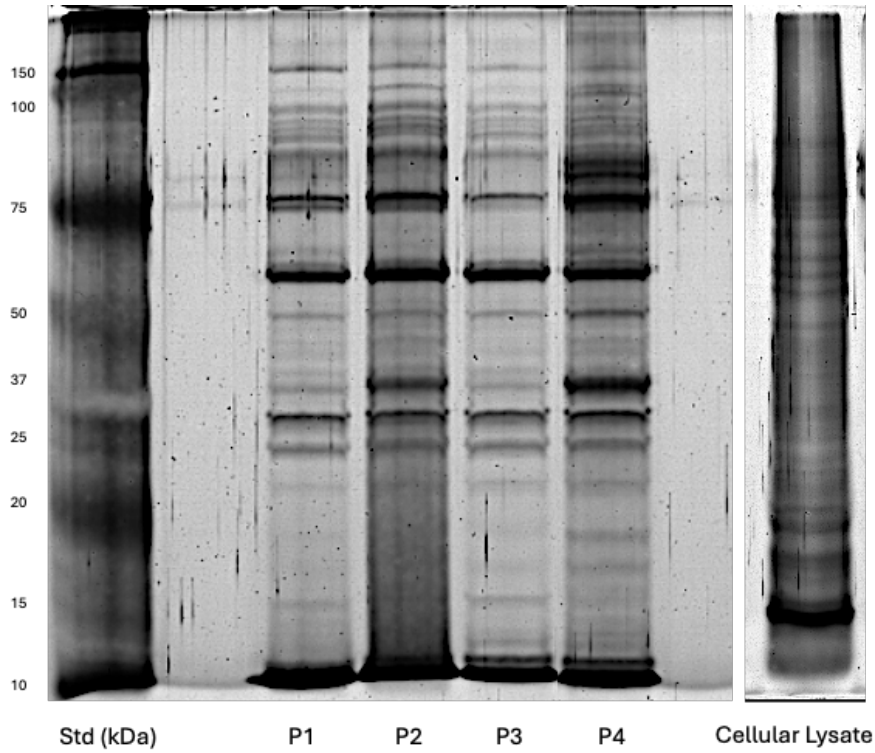

Figure 3.5. Silver-stained one-dimensional 12% polyacrylamide SDS-PAGE analysis of the EF from B. cinerea B05.10 incubated 1 hour in buffer at 25°C from four independent exoproteome preparations (P1 – P2 – P3 – P4) compared to B. cinerea B05.10 cellular lysate. EF was separated from macrospores, and 50 µL of EF was concentrated using SpeedVac and loaded onto the gel in a total volume of 20 µL. Relative molecular weights from standards are given on the left side of the gel.

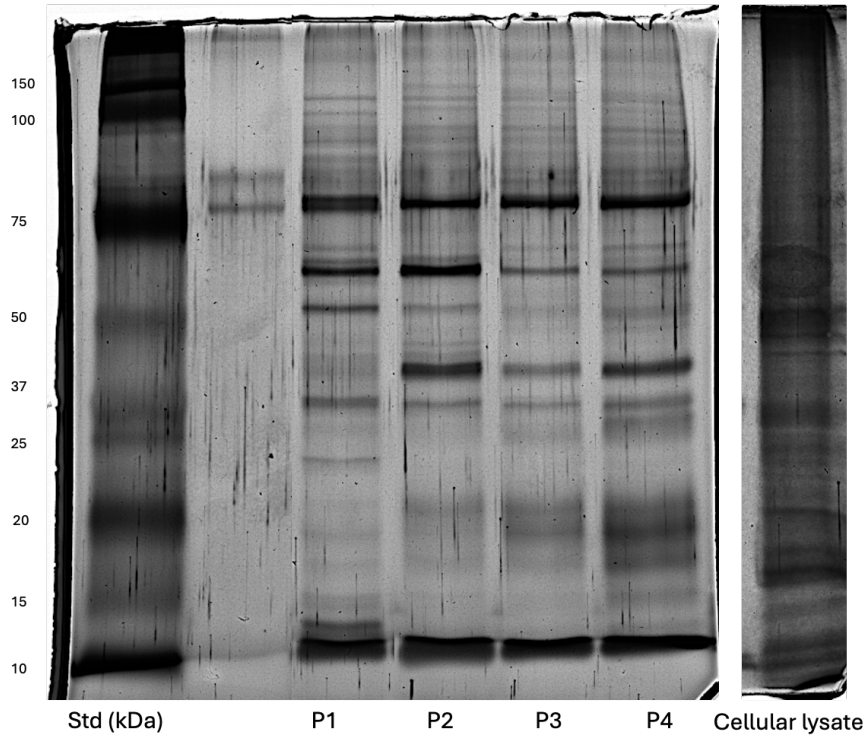

Figure 3.6. Silver-stained one-dimensional 12% polyacrylamide SDS-PAGE analysis of the EF from B. cinerea T4 incubated 1 hour in buffer at 25°C from four independent exoproteome preparations (P1 – P2 – P3 – P4) compared to B. cinerea T4 cellular lysate. EF was separated from macrospores, and 50 µL of EF was concentrated using SpeedVac and loaded onto the gel in a total volume of 20 µL. Relative molecular weights from standards are given on the left side of the gel.

Fig. 3.7 describes the main steps of the EF shaving protocol from a proteomic bottom-up approach and also the EF analysis by cryo-TEM and SDS-PAGE.

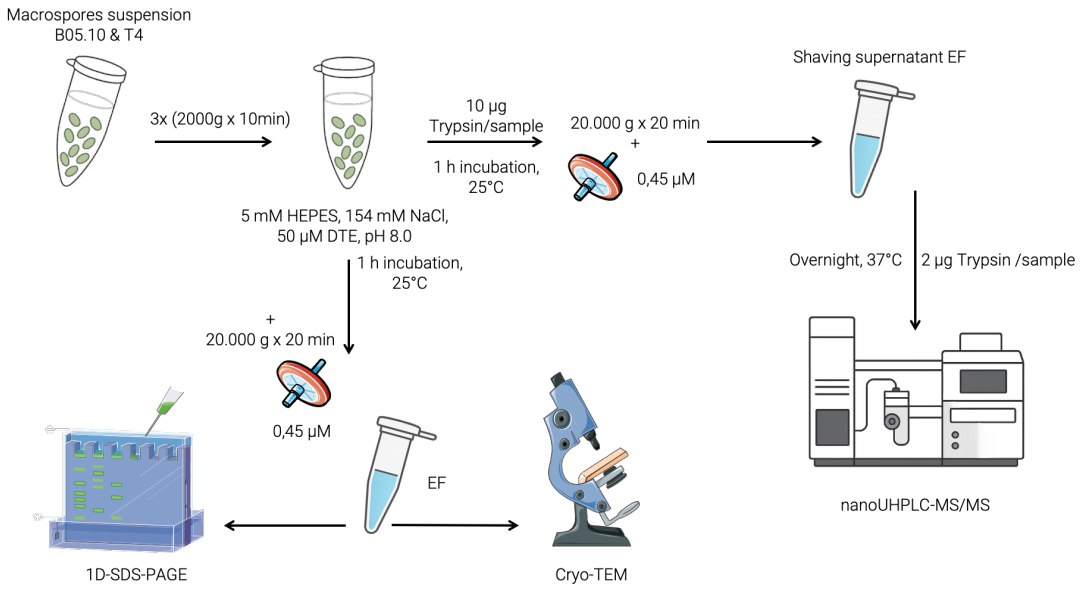

Figure 3.7 Macrospores B05.10 & T4 analysis for exoproteome and surfaceome shaving bottom-up proteomic approach and EF monodimensional SDS-PAGE gel, and Cryo-TEM analysis

3.2 *B. cinerea* Extracellular Fraction revealed Extracellular Vesicles presence

Extracellular fraction (EF) produced by both *B. cinerea* strains revealed the presence of Extracellular vesicle (EVs) structures. Following the two most recent studies [73], [74] that described the production of EVs from the same pathogen after liquid hyphal growth under mild agitation for a few days, we tested our EF samples for the possible presence of EVs.

The most relevant thing is that EVs are present in the EF from both strains of *B. cinerea* B05.10 and T4, which probably indicates that these structures, for themselves, are not responsible for the different pathogenicity of these two strains, but at the same time, could be the EVs' content or the remaining EF's components to be responsible for the pathogenicity differences.

Nanoparticle Tracking Analysis (NTA), conducted over EF preparation of the B05.10 strains, revealed a range of dimensions of the EVs of 155 nm for B05.10 and 266 nm for the T4 strain. Span value of 1,7 and Dev. Std of 117,7 nm suggest a moderate heterogeneous population with dimension variability that goes from 70 nm to 275 nm. The distribution of the particles seems to be highly concentrated around 100 nm, as shown in Figure 3.8.

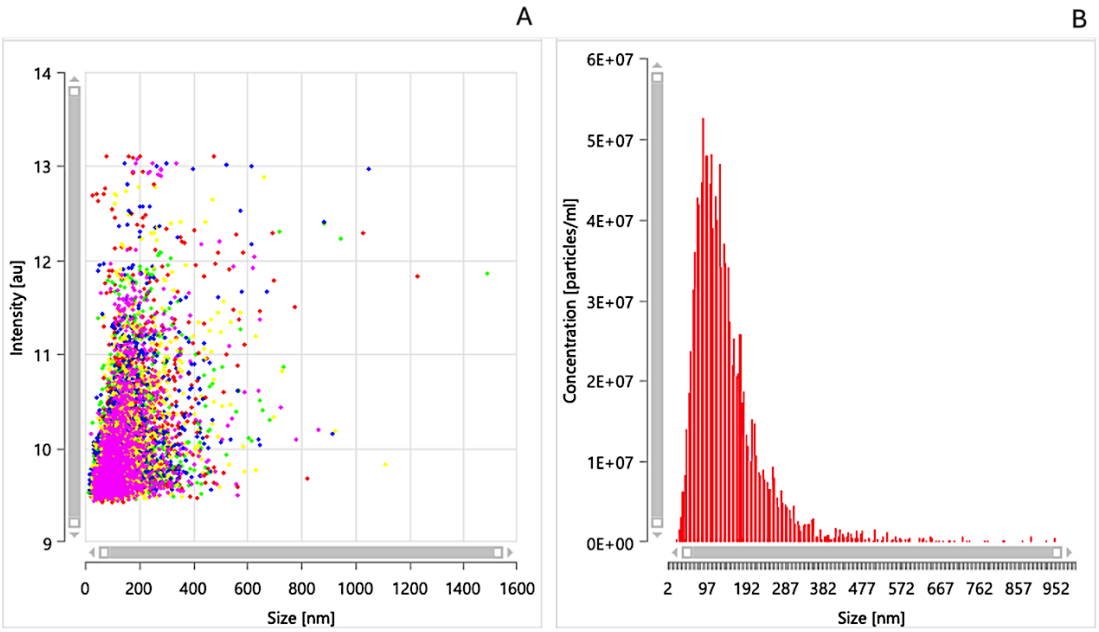

Figure 3.8. Nanoparticles Tracking Analysis of EF fraction release from B. cinerea B05.10 strain, revealed the presence of EVs distributed around 100 nm in dimension. (A) represent Intensity Plot; (B) represent Size Distribution Histogram

EF from T4 strain instead show a more heterogeneous population (Figure 3.9), with the most frequent distribution around 95-100 nm as B05.10, but when we look at the average size dimension (266 nm) EVs seem to present a high number of bigger particles. In this case, the EVs go from 81 to 520 nm. Span value higher than 2 delineates a much more polydisperse population respect to B05.10.

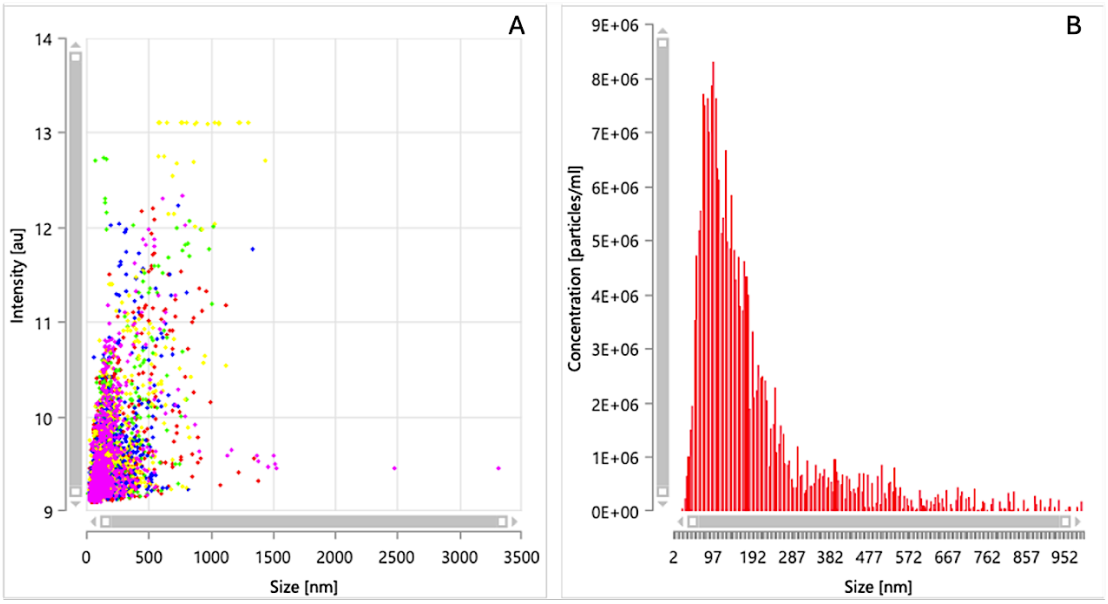

Figure 3.9. Nanoparticles Tracking Analysis of EF fraction release from B. cinerea T4 strain, revealed the presence of EVs distributed around 100 nm in dimension. (A) represent Intensity Plot; (B) represent Size Distribution Histogram

Tabella 3-1. Average value of NTA analysis from B05.10 and T4 EFs.

	B05.10			**T4**	
	Average	Std.Dev		Average	Std.Dev
Mode (nm)	90,8	15,3		97,5	5,3
Mean (nm)	155,3	8,0		266,0	89,1
Std.Dev (nm)	117,7	31,8		253,5	71,4
Conc.particles/mL	6,93E+08	5,05E+08		1,95E+08	5,23E+07
D10 (nm)	70,0	9,2		81,5	17,7
D50 (nm)	121,7	11,7		199,5	84,1
D90 (nm)	275,3	23,4		520,0	130,1
Valid tracks	8051,3	3323,8		4524,5	2017,4
Total particle tracks	36034,7	10319,4		30155,5	3618,3
Average particles per frame	55,3	23,4		33,1	13,3
Bin size (nm)	5,0	1,4		5,0	0,9
Span	1,7	0,4		2,3	0,4

EVs' presence in the EF of both *B. cinerea* strains B05.10 and T4 is confirmed by the images obtained from Cryogenic Transmission electron Microscopy (cryo-TEM) that revealed preserved spherical vesicles surrounded by lipid membrane, mono and bilayered (Figures 3.10 and 3.11, respectively).

Both multilamellar and monolamellar vesicles were observed in both strains after an incubation period of just 1 hour, suggesting different possibilities related to the biogenesis pathway and functional roles.

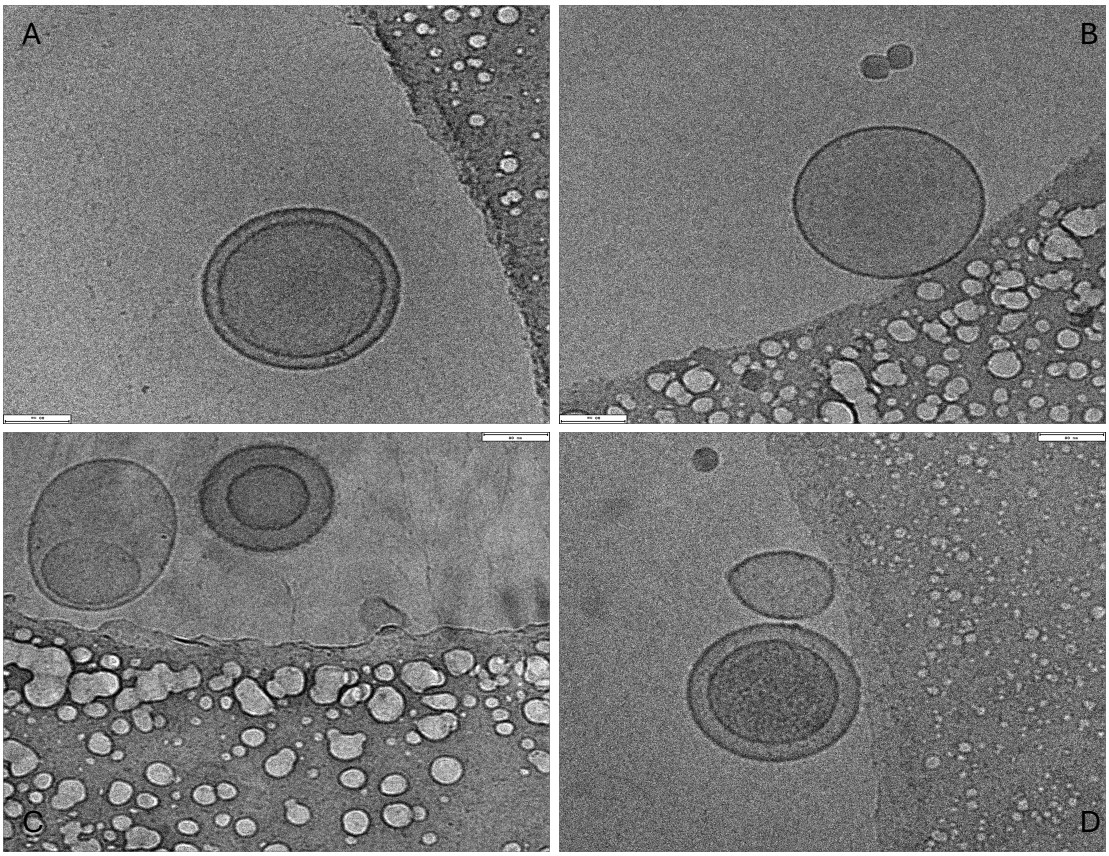

Figure 3.10. EF from B. cinerea B05.10 releases EVs in 1 hour of incubation. Cryo-TEM images of B05.10 EVs, composed of multilamellar (A – C – D) and unilamellar (B) structures. Scale bar dimension of (A - B – C – D) is 80 nm;

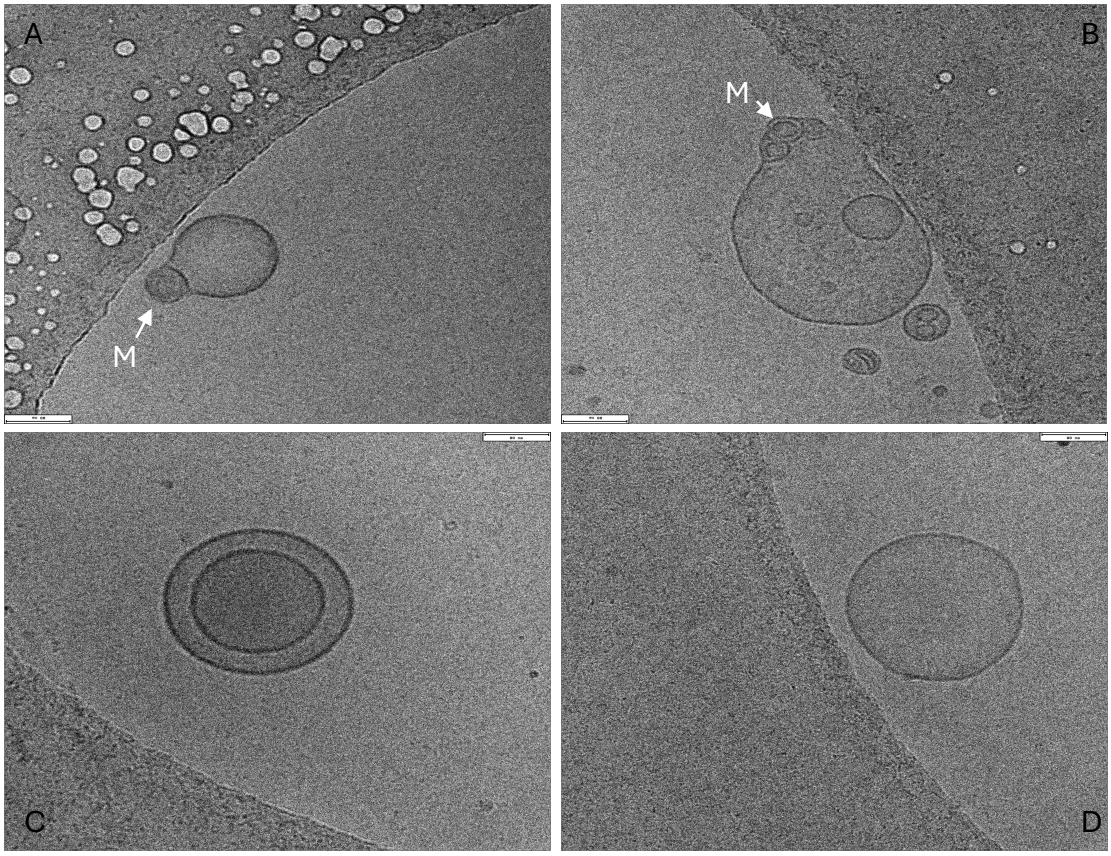

Figure 3.11. EF from B. cinerea T4 release EVs in 1 hour of incubation. Cryo-TEM images of T4 EVs, composed of multilamellar (C), unilamellar (D). In (B) multivesicular bodies (MVB) structures are visible on the side of the EVs, probably ready to be released to the outside. In (A) in the same way, a multivesicular body appears to be in the proximity of expulsion to the outside of the EVs. MVB are indicated. Scale bar dimension of (A -B – C – D) is 80 nm.

As shown in Figure 3.11, notably in the T4 strain, multivesicular bodies (MVB) were detected adjacent to the internal membrane of a vesicle, probably in the moment of fusion with the vesicle membrane and release to the outside. Even if they were not detected in these photos, MVBs are also supposed to be present in the other *B. cinerea* strain, the B05.10, as reported in literature [73]. The vesicle sizes observed by cryo-TEM were consistent with those obtained from NTA analysis.

Altogether, these results indicate that both strains of *B. cinerea* b05.10 and T4 release EVs in the incubation buffer after just 1 hour of incubation. Overall, both strains produce morphologically similar EVs. To our knowledge, this is the first time that EV production is reported from non-germinated macroconidia of this fungus from two different strains, B05.10 and T4, similar to what has been reported for the yeast-like phase of other ascomycetes.

3.3 Proteomic analysis of B. cinerea EF reveals intracellular protein signatures and metabolic activity

When performing a bottom-up proteomic analysis, it must be considered that the proteins identified at the end of the mass spectrometry workflow are only those that have been cleaved and sequenced by trypsin. In our case, since the EF was digested using trypsin, but without any denaturing agents (in order to preserve the structural integrity of the macrospores) the structure of the EVs was also maintained intact, consistent with several observations reported in literature. This differs from the SDS-PAGE analysis, where EF was treated with Laemmli buffer. Indeed, trypsin alone, in the absence of a detergent such as Triton X-100, is unable to hydrolyse any type of lipid bilayer [152], including that of EVs. Considering this, trypsin has access only to the proteins actively or passively secreted and/or released into the extracellular space (**exoproteome**), including proteins anchored to the EV membrane, as well as those exposed to the outer spore surface (**surfaceome**). Therefore, the proteins identified in this proteomic analysis exclusively correspond to the exoproteome and surfaceome fractions.

The proteins obtained from the exoproteome and surfaceome of three independent biological preparations for each *B. cinerea* strain, B05.10 and T4, were run on nanoUPLC-MS/MS analysis. Protein IDs obtained shared among biological replicates were entered into a Venn diagram in order to identify both strain-specific and common proteins.

As illustrated in Figure 3.12 in the Venn diagram, 80 common IDs were identified for B05.10 and 123 for T4 from three independent experiments performed for each strain. The Venn diagram was used subsequently to compare the IDs between the two strains, resulting in 8 and 51 proteins specific to B05.10 and T4, respectively. A core set of 72 proteins was found to be in common between the two strains (Fig 3.13). Notably, the 8 specific proteins for B05.10 were also present in two of the three replicates of the T4 strain, supporting the hypothesis of a shared core exoproteome of 80 proteins.

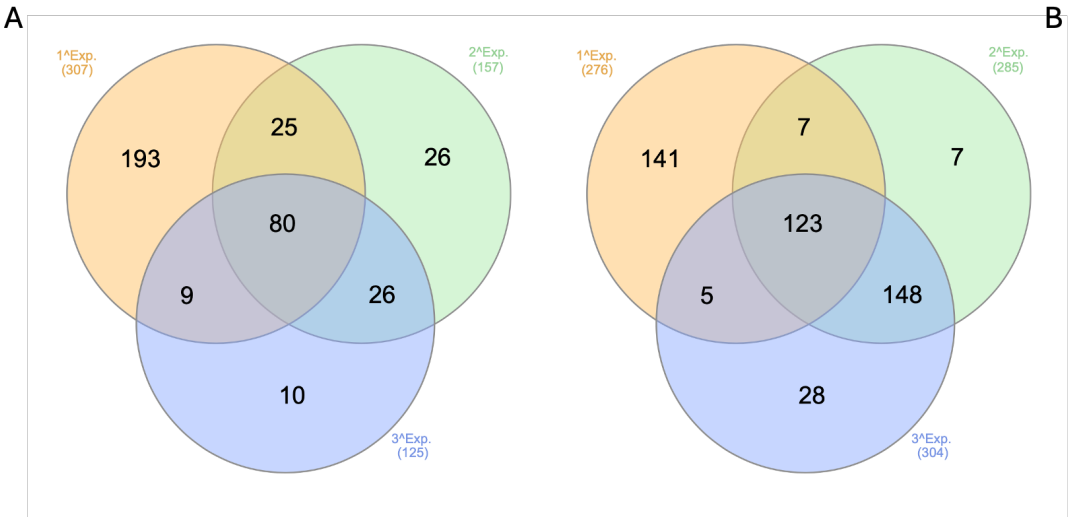

Figure 3.12. Venn Diagrams of the common proteins obtained from 3 independent biological samples for each strain of B. cinerea. (A) represents IDs obtained from three independent experiments of B05.10. (B) represents IDs obtained from three independent experiments of T4.

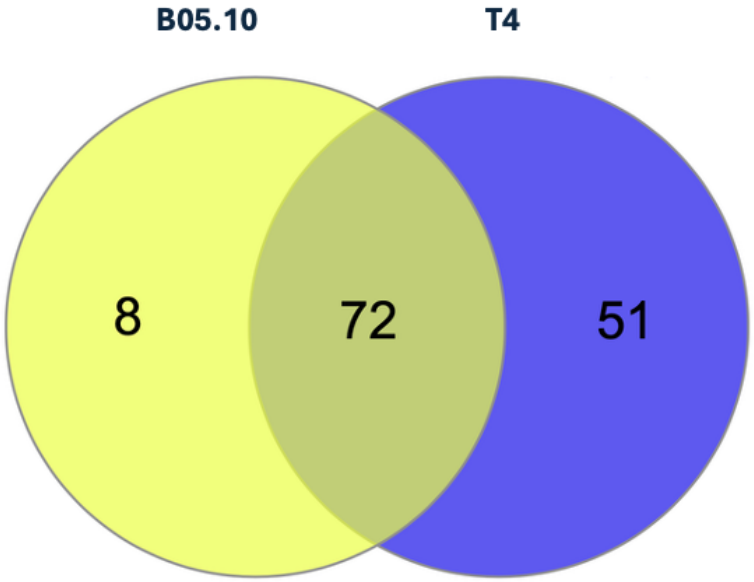

Figure 3.13. Venn Diagram of the common proteins obtained from 3 independent biological preparations revealed a set of 72 common proteins, plus 8 specifics for B05.10, but present in two of the three replicates of the T4 strain.

First of all, the 80 common proteins between the two strains were classified by Gene Ontology (GO) biological process classification (BP) as shown in Figure 3.14 GO analysis revealed a predominance of categories related to protein folding, maturation and quality control, represented by 26% of proteins, and primary metabolism (24%). A considerable proportion was associated with

energy production and respiration, represented by 16%, whereas a small fractions were involved in intracellular trafficking and secretion (7%), oxidative and environmental stress response (4%) and post-transcriptional regulation and RNA transport (3%). In addition, 11% were described as uncharacterized proteins and 9% were grouped into other functional categories.

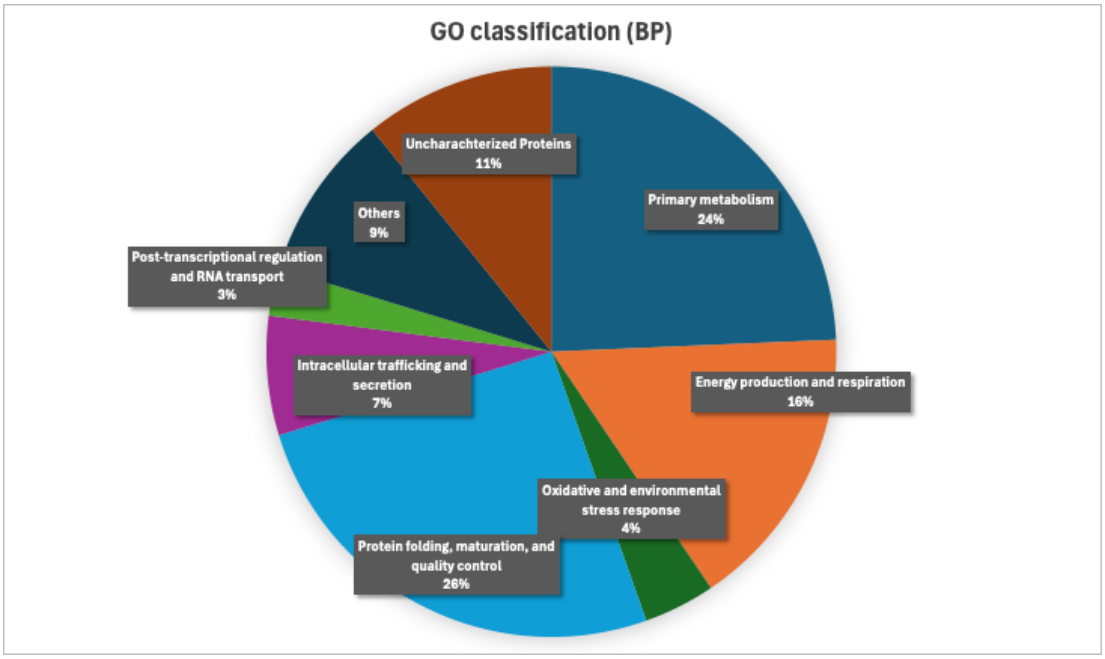

Figure 3.14. Gene Ontology (Biological Process) classification of the 80 common proteins. Proteins were grouped into major functional categories, including protein folding, maturation and quality control (26%), primary metabolism (24%), energy production and respiration (16%), intracellular trafficking and secretion (7%), oxidative and environmental stress response (4%), post-transcriptional regulation and RNA transport (3%), uncharacterized proteins (11%), and others (9%).

The 80 common proteins were then subjected to a protein-protein interaction (PPI) network analysis by the STRING online database (v. 12.0) [153].

The resulting network showed 125 edges, significantly higher compared to the 53 edges expected by the software, with PPI p-value of 1.0e-16. This is a very significant value, suggesting a strong functional protein association and indicates that the proteins are at least partially biologically connected, as a group.

The proteins were then divided in clusters to understand the main role of this set of proteins by the Cluster analysis using MCL clustering, obtaining 8 different clusters divided by colours as shown in Figure 3.14.

STRING analysis revealed interesting results. The most prominent, cluster 1 (red), was enriched in proteins involved in protein folding, including chaperones and HSPs, Bcsti1 and BcKAR2.

On the other hand, cluster 2 and cluster 3, represented by 5 and 4 proteins, respectively, were described as clusters involved in translational elongation and the pentose phosphate pathway glycolytic process, respectively.

Cluster 4 represents proteins described to be involved in seleno-compound metabolism, and cluster 8 is involved in protein deubiquitination, with clusters 5, 6 and 7 with no specific description.

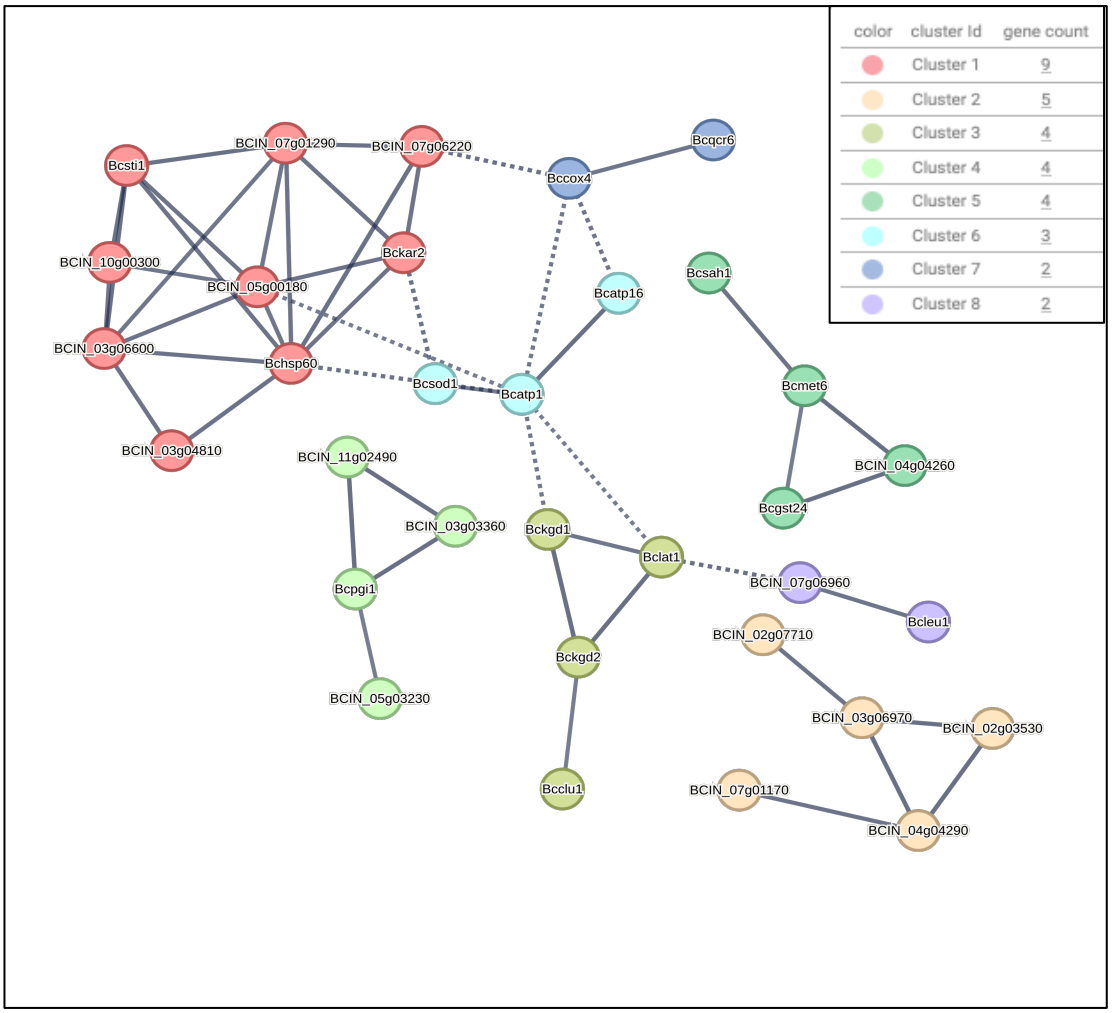

Figure 3.15. B. cinerea B05.10 and T4 common proteins STRING cluster analysis. STRING cluster analysis revealed the presence of 8 different clusters divided by colours in the 80 common set of proteins.

To clarify the role of the 80 common proteins identified, STRING was also used for the Gene Ontology (GO) enrichment analysis, and the proteins were classified

based on their Biological Process (BP), Molecular Function (MF), Cellular Component (CC) and Reactome Pathways (RP).

Figure 3.16 shows 9 BP in which the set of 80 proteins form the exoproteome and surfaceome are involved in organonitrogen compound biosynthetic process, amide biosynthetic process, protein folding, protein refolding, translational elongation and other metabolic processes, energy activation and generation of precursor metabolites, suggesting an important metabolism potential even in the absence of external stimuli in just 1 hour incubation.

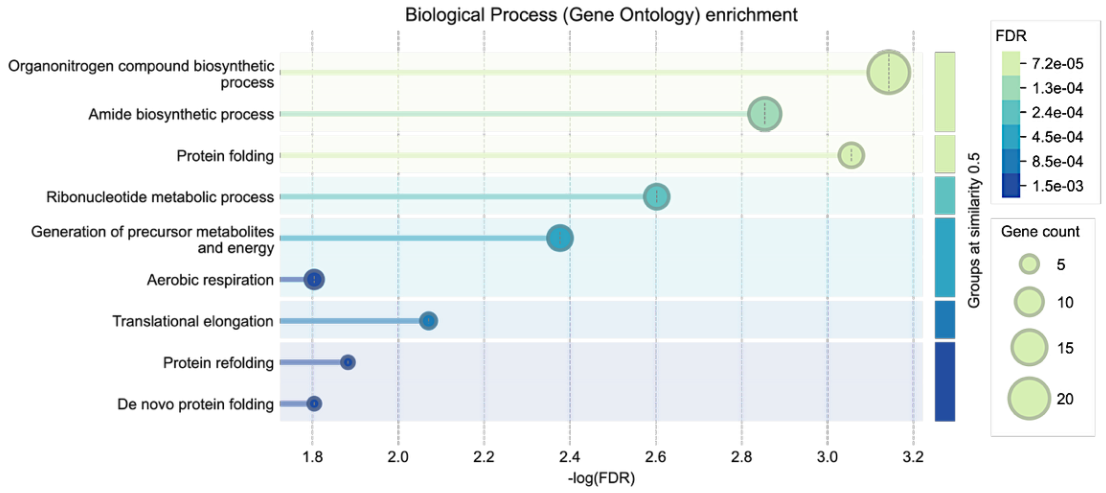

Figure 3.16. BP (Gene Ontology) enrichment analysis of the 80 common proteins released in the exoproteome and surfaceome fraction of both B. cinerea strains.

One of the most interesting results of this exoproteome and surfaceome analysis, which could confirm the presence of intracellular structures released to the outside of the macrospores as EVs, is the CC enrichment analysis shown in Figure 3.17, which describes most of the protein groups in the network as cytosolic proteins. This means that most of these represent proteins that are present inside the macrospore and are released to the outside, probably during EV secretion, by other secretory pathways or even anchored to the surface of the EVs.

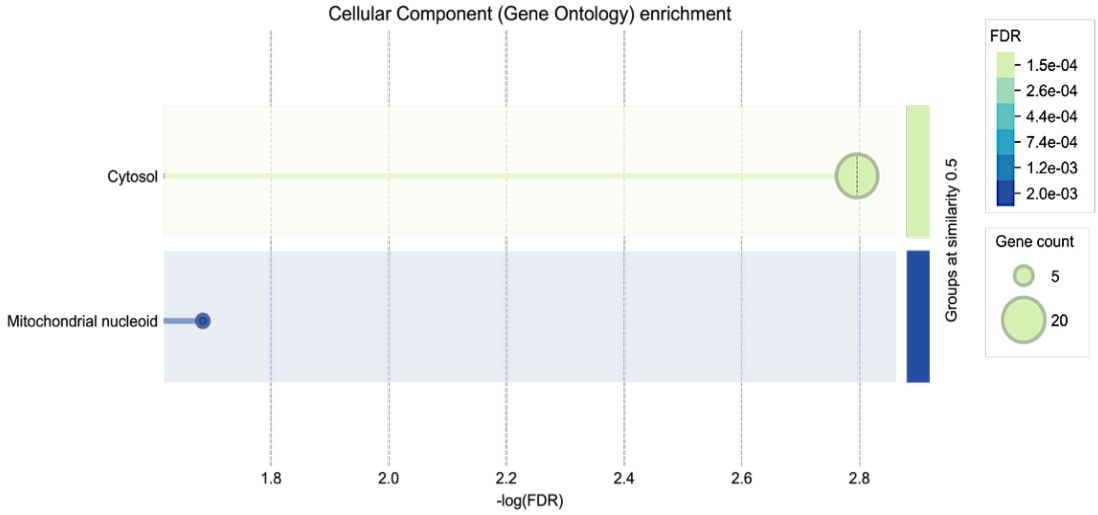

Figure 3.17. CC (Gene Ontology) enrichment analysis of the 80 common proteins released in the exoproteome and surfaceome fraction of both B. cinerea strains.

MF of the protein-protein interaction network (Fig. 3.18) instead revealed an ATP-dependent protein folding chaperone activity.

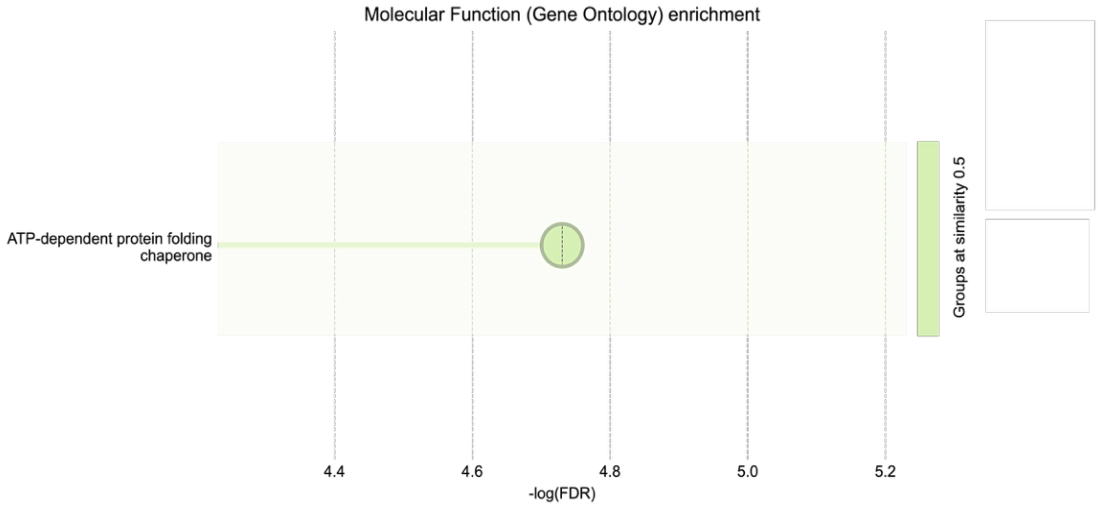

Figure 3.18. MF (Gene Ontology) enrichment analysis of the 80 common proteins released in the exoproteome and surfaceome fraction of both B. cinerea strains.

KEGG pathway analysis (Fig. 3.19) revealed significant enrichment pathways in carbon metabolism and secondary metabolite biosynthesis. Other pathways involved seem to be glycolysis/gluconeogenesis, the pentose phosphate pathway and the TCA cycle. These data could further confirm an early metabolic activation potential in this fraction under non-stimulatory conditions.

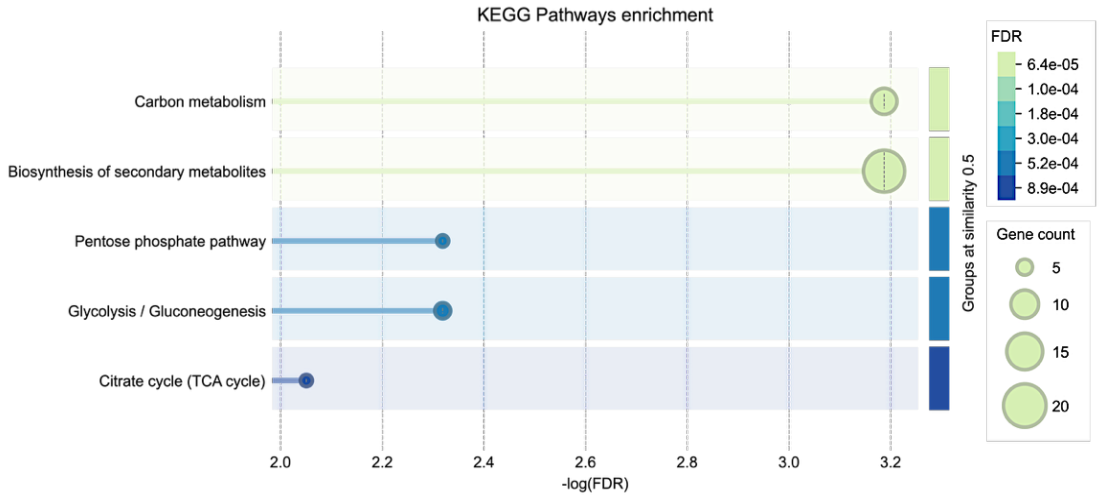

Figure 3.19. KEGG Pathways enrichment analysis of the 80 common proteins released in the exoproteome and surfaceome fraction of both B. cinerea strains.

The second step to clarify the role of this common set of proteins (exoproteome and surfaceome) obtained from the EF of both *B. cinerea* strains was to perform in silico analysis using different prediction algorithms to understand the features of these proteins.

EffectorP 3.0 was used to determine the presence of some type of effectors, suggesting a possible role in the plant-pathogen interaction. As shown in Figure 3.20, in fact, nearly half of the proteins, 50% are suggested by the software as cytoplasmic effectors, playing a role mainly at the cytoplasmic level in the plant-pathogen interaction, while only 3 proteins are suggested as apoplastic effectors. This result supports the idea that these proteins could have a defined role for the macrospores' development in the environment and may be involved in pathogenesis.

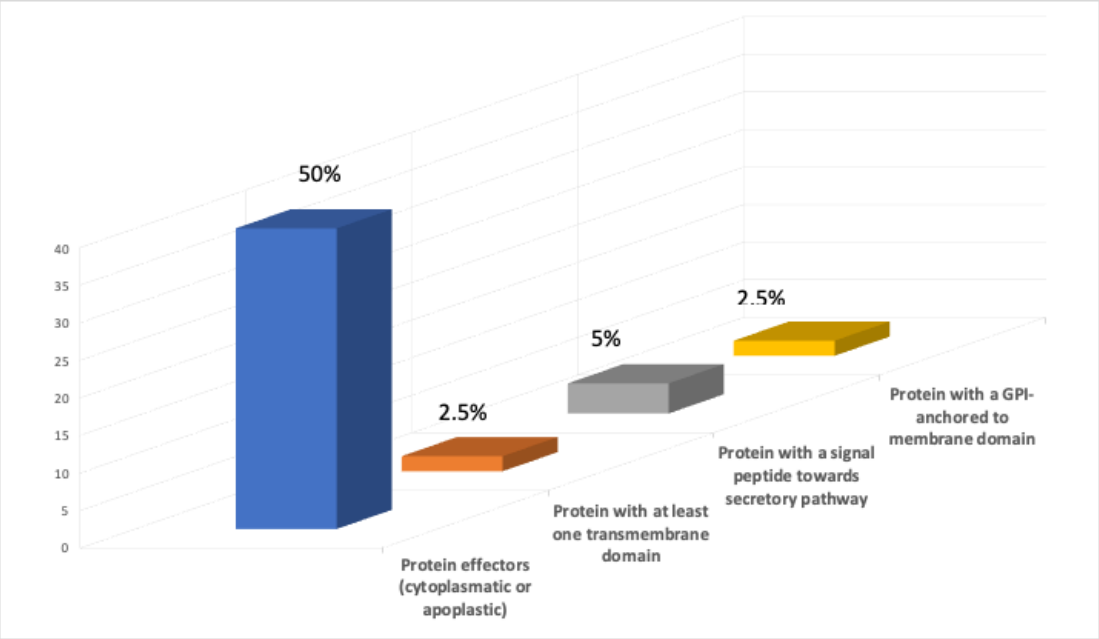

Figure 3.20. In-silico analysis of the 80 common set of proteins obtained from EF from both B. cinerea strains B05.10 and T4. (Blue bar) EffectorP 3.0, which revealed proteins described as effectors, cytoplasmatic or apoplastic, resulting in 50% of the total common proteins. (Orange bar) DeepTMHMM, which revealed proteins with at least one transmembrane domain, resulting in 2,5% of the total common proteins. (Grey bar) SignalIP, which revealed proteins with at least one signal peptide that directs proteins to the secretory pathway, resulted in 5% of the total common proteins. (Yellow bar) Net-GPI predicts proteins to be GPI-anchored to the membrane, resulting in 2,5% of the total common proteins.

DeepTMHMM identified two proteins (2,5%) with a transmembrane domain, and 9 proteins instead are revealed to be totally secreted outside of the macrospore. SinaglIP predicted four proteins (5%) to have a signal peptide that directs proteins to the secretory pathways, which could be outside the macrospores, inserted in the cell wall or targeted to the endoplasmic reticulum.

Another bioinformatic tool used was Net-GPI, which predicts two proteins (2,5) to be GPI-anchored to the membrane of the macrospores or EVs.

The last bioinformatic tool used was Cello (v2.5), which predicts the subcellular location of the proteins identified from EF fraction proteomic analysis

As shown in Figure 3.21, 49% of the proteins are described to be cytoplasmatic, confirming the Gene Ontology analysis consistent with literature data [74].

In contrast, 29% of the proteins are detected to be nuclear, with 13% as part of the Mitochondrial subcellular localisation.

Eight percent of the proteins are suggested to be localized in the extracellular space or on the Plasma membrane, with only 1% located in the Endoplasmic Reticulum (ER).

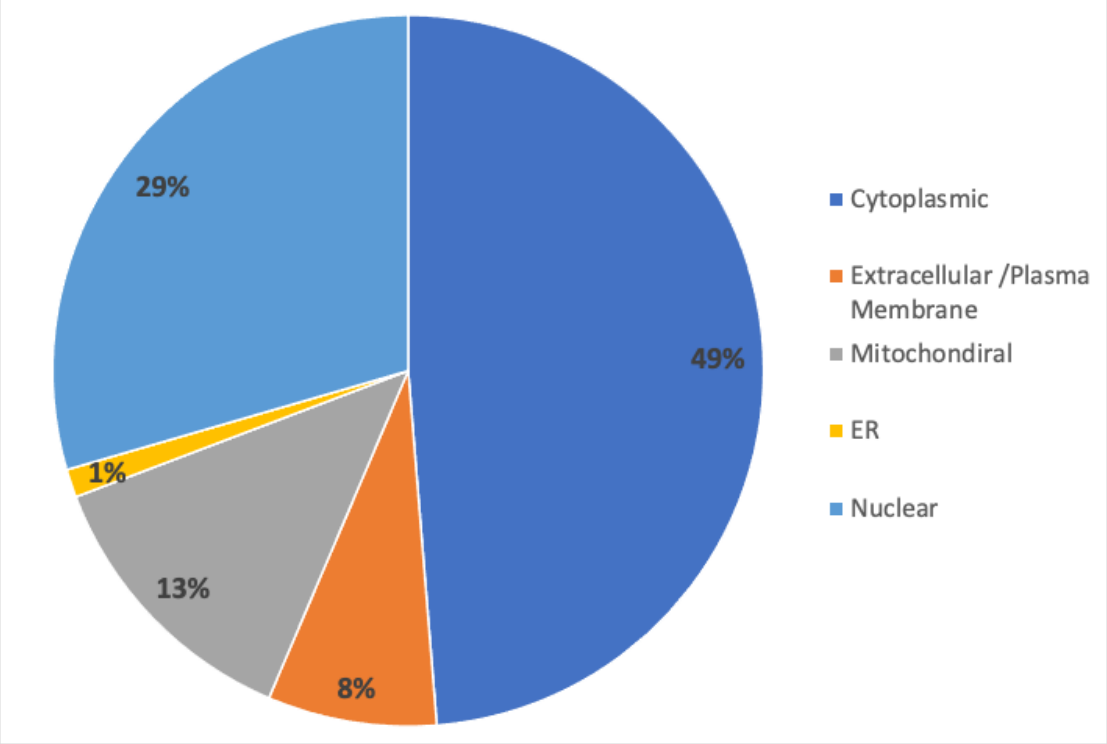

Figure 3.21. Predicted subcellular location by Cello (v2.5) bioinformatic online tool of the 80 common proteins obtained from the EF of the two B. cinerea strains B05.10 and T4. 49% located in the cytoplasm, 29% located in the nucleus, 13% located in the mitochondria, 8% located in the extracellular space or plasma membrane and 1% located in the ER.

To enhance the understanding of the possible functional relevance of this common set of proteins, a scientific literature review was conducted to assess if some of them had already been studied to be involved in some biologically relevant process of the *B. cinerea* physiopathology and development. It is interesting to note that this analysis found that seven of the 80 proteins present in the exoproteome and surfaceome common set had been previously described, and six of the seven as relevant in the pathological process, especially after studies from knock-out mutants.

Tabel 3.2 shows all the proteins selected, with Accession Number (AN) from the Uniprot database for both *B. cinerea* strain B05.10 and T4, function and mutant effects.

Tabella 3-2. Correlation of proteins identified in the EF protein common set with literature.

AN (B05.10 - 332648ID) Uniprrot	AN (T4 - 999810) Uniprot	Gene Name	Function	Effect on Mutation	Reference
A0A384J6I8	G258XZJ0	Bcass1	Argininosuccinate synthase is a urea cycle enzyme that catalyses the penultimate step in arginine biosynthesis: the ATP-dependent ligation of citrulline to aspartate to form argininosuccinate, AMP and pyrophosphate.	Reduce growth on French bean leaves, strawberries and tomatoes.	Patel et al. (2010)[154]
A0A384J6H0	G2XYV3	Bcenol1	Catalyses the reversible dehydration of 2-phospho-D-glycerate to phosphoenolpyruvate as part of the glycolytic and gluconeogenesis pathways.	Expression reduce when adenylate cyclase mutant is made, increasing abiotic stress sensitiveness	Pandey et al. (2009)[155]
A0A384K4A6	G2YFU1	BcekdA	Membrane protein involved in vegetative differentiation, adaptation to oxidative stress and virulence.	Reduce mycelial growth, conidiation and sporulation. Hyphae distortion and deformities growth. Reduce virulence in grapevine fruit and leaves, with an increased sensitivity to abiotic stress.	Zhang et al. (2023)[156]
A0A384J7A7	G2XQE6	Bcpsd	Phosphatidylserine decarboxylase catalyses the formation of phosphatidylethanolamine (PtdEtn) from phosphatidylserine (PtdSer).	Mitochondria protein not essential for hyphal growth or conidiation.	An et al. (2016)[157]
A0A384JED1	G2YHE5	Bcptc3	Catalyses the dephosphorylation of phosphoserine and phosphothreonine residues of specific protein substrates.	Reduce hypal growth, increase conidiation and impaired sclerotium development. Increased sensitiveto osmotic and oxidative stresses and decreased virulence on host plant cell.	Yang et al. (2013)[158]

A0A384JBV7	G2YHA8	Bcsod1	Catalyse the conversion of superoxide radicals to molecular oxygen.	Reduce virulence on tomato and Arabidopsis plant	Lòpez-Cruz et al. (2017)[159]
A0A384JG14	G2XXL3	Bcste7	(MAPKs) is a dual-specificity protein kinase that catalyses the transfer of the gamma-phosphoryl group from ATP to serine/threonine or tyrosine residues on protein substrates;	Defects in germination, delayed vegetative growth, reduced\ size of conidia, lack of sclerotia formation and loss of pathogenicity.	Schamber et al. (2010)[160]

The presence of some well-characterised proteins involved in the pathological process within the identified EF strongly supports the biological significance of this dataset. These proteins may contribute to the early fungal metabolic or pathogenic activity and suggest they are present even in the absence of particular host's stimuli. Furthermore, for some of them, these data suggest a moonlighting activity previously unnoticed.

3.4 Preliminary *in vivo* assay to assess the immunomodulatory activity of EF from B. cinerea in tomato plants.

After standardising EF production from both *B. cinerea* strains, understanding the compositions of the core proteins and discovering the presence of EVs in such an early phase, we sought to determine if the EF derived from this pathogenic fungus could stimulate immune-related responses in plants.

To study this, before designing a full-scale bioassay, we first wanted to test the immune-activating potential of the EF (considering all the secretome, exoproteome and surfaceome), also with the goal to identify the right working dose that would be biologically active without creating any phytotoxic effects on the plant.

First, a preliminary concentration-response pilot test was designed for a detached leaves assay in tomato plants (*Solanum lycopersicum cv. RedCherry)*. Three independent EF preparations were obtained from each *B. cinerea* strains B05.10 and T4 and pooled together to ensure biological consistency and reproducibility. Protein concentration was determined by Bradford protein assay in micro-plates, allowing us to prepare three treatment solutions of EF at 25 µg/mL, 50 µg/mL and 100 µg/mL, as tested in other studies [161], [162]. These concentrations were selected to study a low-to-high range of protein content to identify a possible dose-response pattern.

Tomato plants were cultivated under regulated greenhouse conditions. Leaves were harvested, sterilised and arranged on an Agar plate with a detached-leaf setup, the classical model system to study plant immune response under control and non-systemic conditions [163]. Each plate, containing from two to three leaves, received one of the EF from either B05.10 or T4. As positive control (INF), a plate for each strain where leaves were inoculated with *B. cinerea* $1x10^6$ sp/mL [141] was applied in a 10 µL droplet of EF buffer solution. As a negative control, mock treatment with only EF buffer was used to search for background effects.

Two time points, 24 and 48 Hpi (*Hours Post Infection*) were chosen to cap two possible different phases of tomato leaves signalling defence eaves [164], [165]. While resources limited the experiments to only two biological replicates per treatment, some preliminary data were, however, expected to help understand at least trends and help choose the concentration for further testing.

After 48 hours, just before collections, pictures of the leaves were captured, and EF was revealed to have some interesting effects on the leaves, clearly different from the negative and positive controls.
As illustrated in Figure 3.22, in the B05.10 plate, the positive control shows an increasing necrotrophic infection stage. In the EF leaves, instead, different black signs were clearly visible on the leaves compared to the negative control, in all three concentrations. After 7 days post-infection (Dpi) B05.10 shows complete necrotrophic infection and sporulation.

Figure 3.22. In-vivo detached leaves tomato assay of figure B05.10 with EF. (A) B05.10 positive control at 48 hpi. (B) Positive control at 7 dpi (Days-post-infection) confirmed the complete pathogen infection. (C) EF treatment at 25 µg/mL at 48 hpi. (D) EF treatment at 50 µg/mL at 48 hpi. (E) EF treatment at 100 µg/mL at 48Hpi. (F) negative control (mock leaf with EF buffer). HR symptoms are marked with blue circles.

In the same way, T4 shows (Fig. 3.23) a necrotrophic lesion on the positive control leaves at 48hpi (A). Interestingly, in the less aggressive strain (T4), the necrotrophic lesion seems to be worse compared to the most aggressive strain (B05.10), in the first 48 hours. In the EF concentration condition samples (C-D-E), as in the B05.10, some black dots are visible on the leaves, already described as a Hypersensitive Response (HR) [97], visible at 100 µg/mL (E) and 50 µg/mL (D).

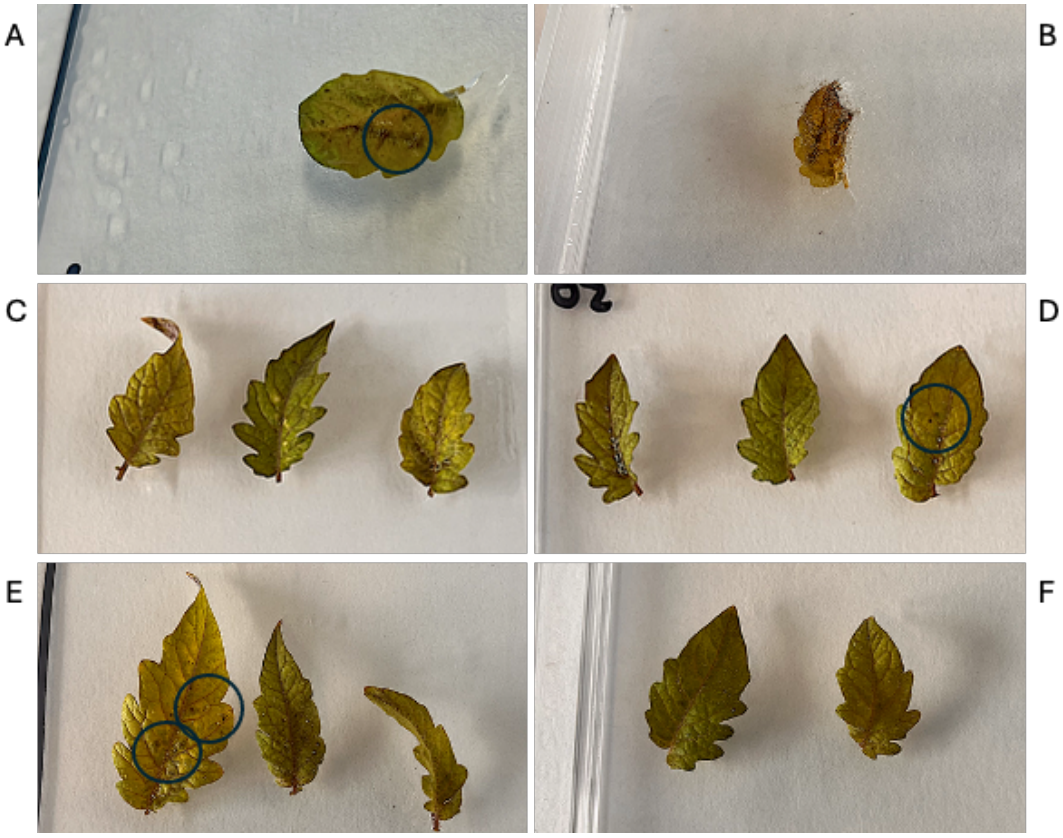

Figure 3.23. In-vivo detached leaves tomato assay of figure T4 with EF. (A) T4 positive control at 48 hpi. (B) Positive control at 7 dpi (Days-post-infection) confirmed the complete pathogen infection. (C) EF treatment at 25 µg/mL at 48 hpi. (D) EF treatment at 50 µg/mL at 48 hpi. (E) EF treatment at 100 µg/mL at 48Hpi. (F) negative control (mock leaf with EF buffer). HR symptoms are marked with blue circles.

To further investigate the possible immune activation and confirm what was seen on plates, five well-characterised defence-related genes were analysed by RT-qPCR gene expression. These genes were selected because they are described to be involved in the plant immune system, like *SlPTI5* and *SlWRKY1* transcriptional regulators implicated in PAMP-triggered immunity and communication between hormonal pathways [164], [166], [167]. *SlPR1*, a pathogen-induced gene, is generally used as a marker for SA-mediated responses, especially in SAR [96], [120], [164], the *SlSOD* marker of early oxidative burst [166], and *SlJAR1*, the central player in JA signalling [168].

SlPTI5 expression analysis (Fig 3.24) seems to present a similar profile at 24 hours between the positive control and 50 µg/mL and 100 µg/mL, then at 48 hours, the tendency of the *PTI5* gene in the positive control (INF) seems to increase,

reaching 12.6 ± 2.7 and 13.8 ± 0.6 of FC for B05.10 and T4, respectively while it does not increase further for the EF stimulated samples. At 50 µg/mL, the tendency at 48 hours seems to be a downregulation as the plant is already prepared for the defence.

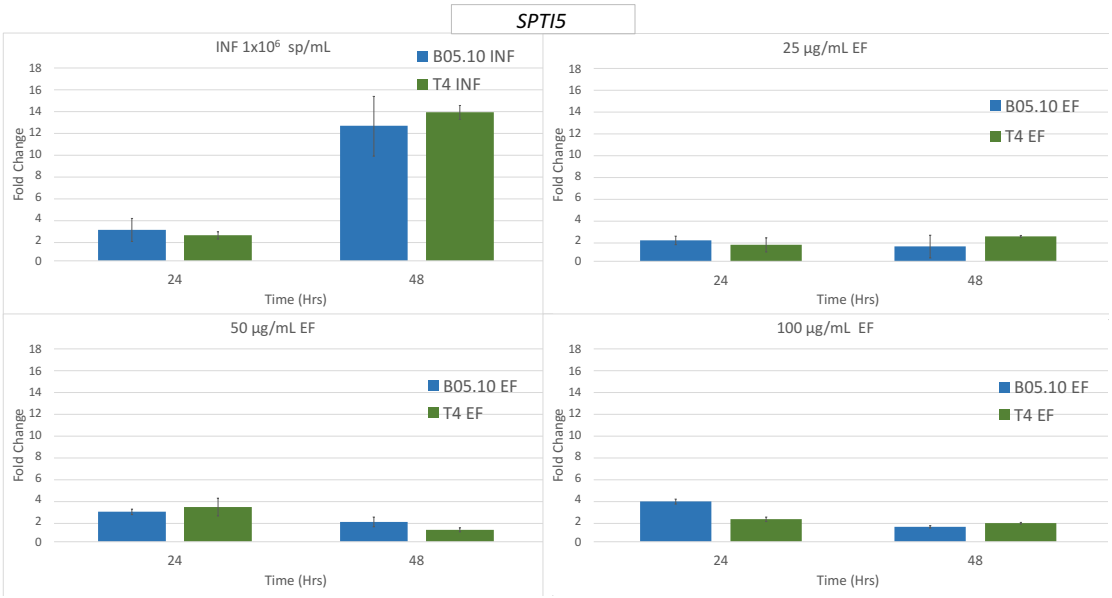

Figure 3.24. Relative expression of the SlPTI5 gene in tomato. Three different concentrations of EF from figure strains B05.10 (blue) and T4 (green) were inoculated over tomato detached leaves: 25 µg/mL, 50 µg/mL and 100 µg/mL. Samples were collected at 24 and 48 hpi. INF represent the positive control. Bar plots show fold change (FC) values in gene expression, and error bars indicate standard deviation (SD) values from two biological replicates. Expression levels were normalised to the reference gene SlACT and calculated relative to the negative control.

As a transcription factor involved in secondary compounds production and SA signalling for plant defence, *SlWRKY1* was expected to be activated, the positive control (INF), in the same way as the EF treatment. As illustrated in Figure 3.25, the tendency at 24 hours seems to be the same in all conditions and similar to with *SlPTI5*, the expression seems to rise at 48 hours in the positive control but is reduced or kept the same in the EF treatment. 50 µg/mL treatment seems to suggest a pathogen strain difference tendency, although the statistical power of the test does not allow determination of real differences but only trends.

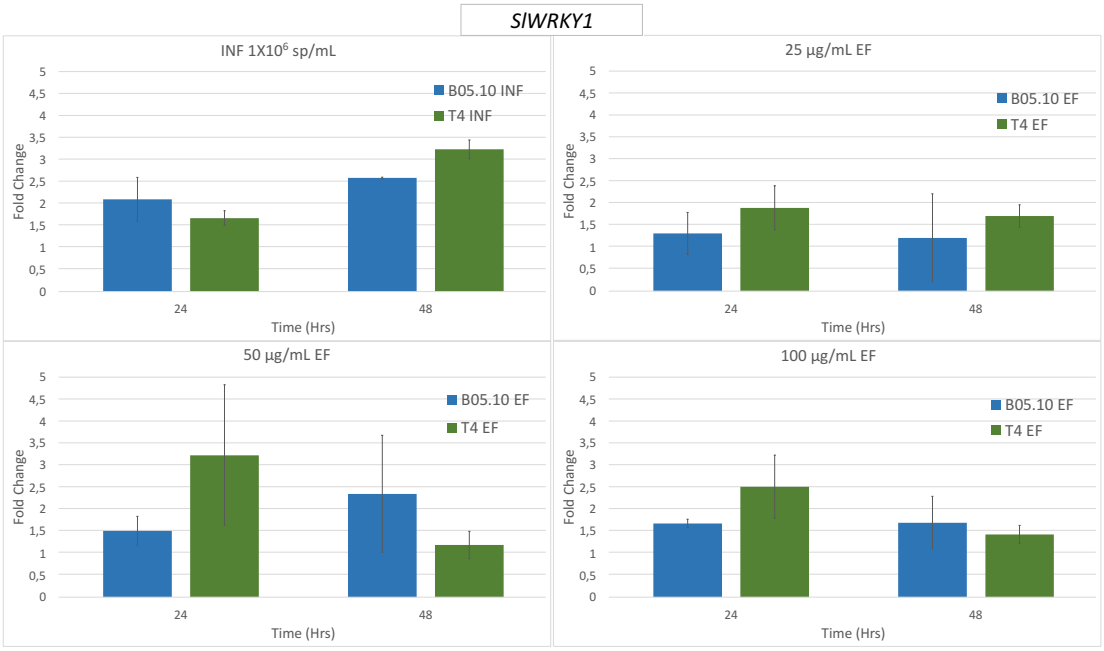

Figure 3.25. Relative expression of the SlWRKY1 gene in tomato. Three different concentrations of EF from figure strains B05.10 (blue) and T4 (green) were inoculated over tomato detached leaves: 25 µg/mL, 50 µg/mL and 100 µg/mL. Samples were collected at 24 and 48 hpi. INF represent the positive control. Bar plots show fold change (FC) values in gene expression, and error bars indicate standard deviation (SD) values from two biological replicates. Expression levels were normalised to the reference gene SlACT and calculated relative to the negative control.

The same pattern of expression tendency was shown by *SlPR1* (Fig. 3.26), where the response increased at 48 hours after inoculation, as presented in the C+ panel, but remained around basal level in the EF fraction treatments.

Figure 3.26. Relative expression of the SlPR1 gene in tomato. Three different concentrations of EF from figure strains B05.10 (blue) and T4 (green) were inoculated over tomato detached leaves: 25 µg/mL, 50 µg/mL and 100 µg/mL. Samples were collected at 24 and 48 hpi. INF represent the positive control. Bar plots show fold change (FC) values in gene expression, and error bars indicate standard deviation (SD) values from two biological replicates. Expression levels were normalised to the reference gene SlACT and calculated relative to the negative control.

Gene expression of the *SlSOD* gene is illustrated in Fig. 3.27, where the gene fold change value seems to be kept around basal levels, with a tendency to a mild increase in the 25-50 µg/mL concentration range between the two strains at 48 hpi.

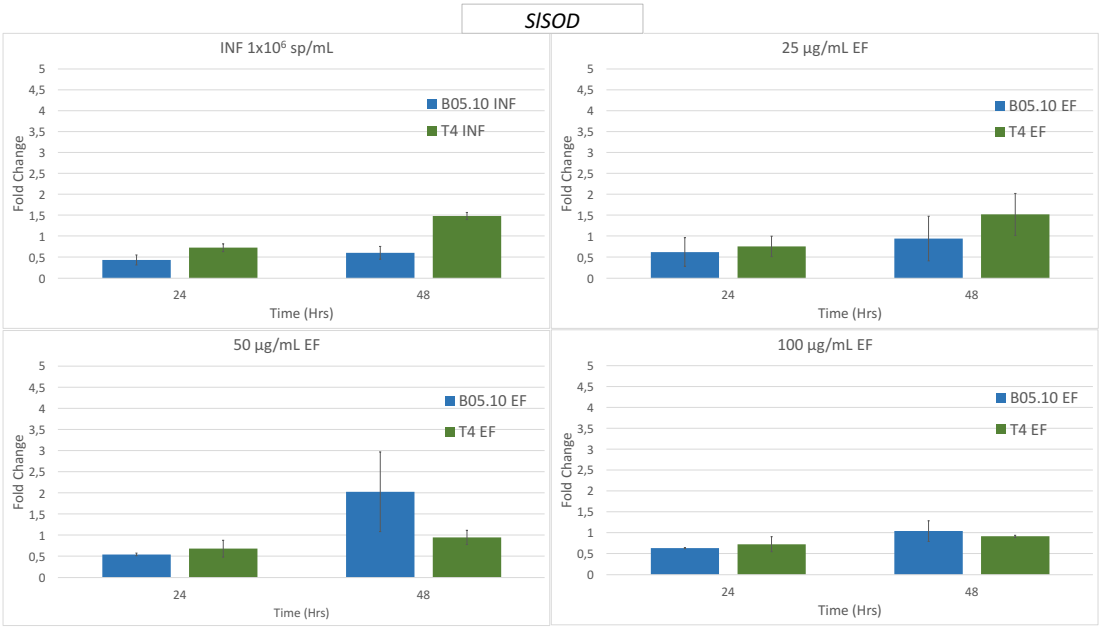

Figure 3.27. Relative expression of the SlSOD gene in tomato. Three different concentrations of EF from figure strains B05.10 (blue) and T4 (green) were inoculated over tomato detached leaves: 25 µg/mL, 50 µg/mL and 100 µg/mL. Samples were collected at 24 and 48 hpi. INF represent the positive control. Bar plots show fold change (FC) values in gene expression, and error bars indicate standard deviation (SD) values from two biological replicates. Expression levels were normalised to the reference gene SlACT and calculated relative to the negative control.

Finally, *SlJAR1* expression described the gene tendency of JAR1.

JAR1 codes for the enzyme that activates the active jasmonic acid form, conjugated with the Ile (Ile-JA) [98], [168]. *SlJAR1* shows apparently that in the positive control (INF) for both strains, the expression seems to remain the same or even slightly downregulated at 48 hours to $0.54 \pm 0.11$and 0.66 ± 0.07 FC for B05.10 and T4, respectively. However, the high standard deviation observed precludes definitive conclusions, even for the EF tendency shown in Figure 3.28. Apparently, it seems that tomato gene expression of JAR1 responds in the same way as the EF application, especially after 24 hpi.

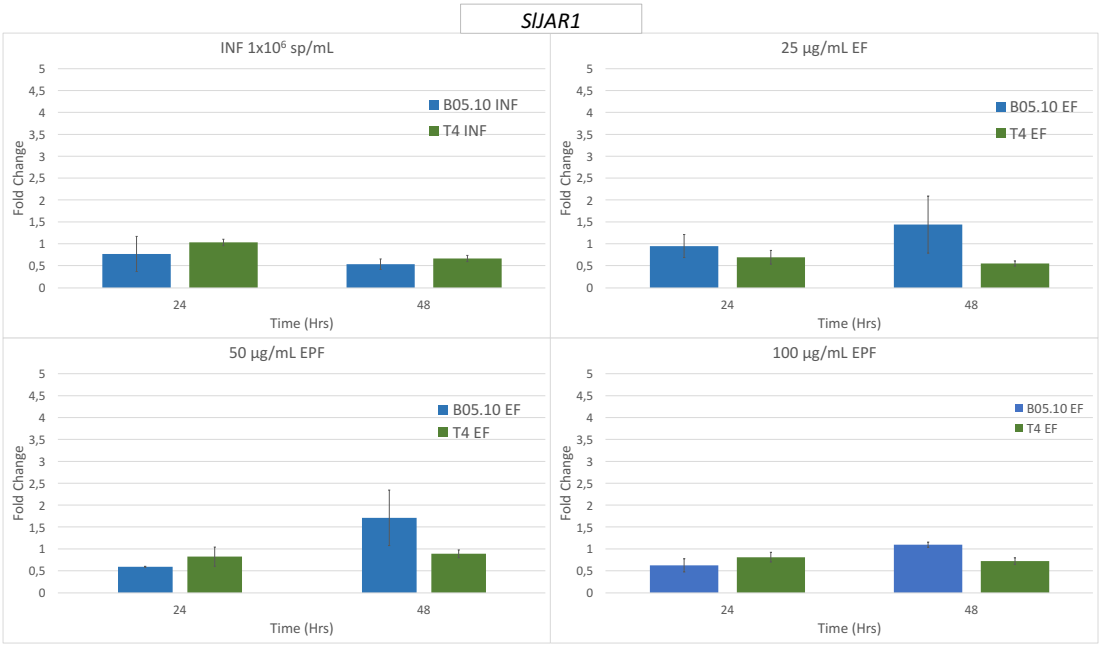

Figure 3.28. Relative expression of the SlJAR1 gene in tomato. Three different concentrations of EF from figure strains B05.10 (blue) and T4 (green) were inoculated over tomato detached leaves: 25 µg/mL, 50 µg/mL and 100 µg/mL. Samples were collected at 24 and 48 hpi. INF represent the positive control. Bar plots show fold change (FC) values in gene expression and error bars indicate standard deviation (SD) values from two biological replicates. Expression levels were normalised to the reference gene SlACT and calculated relative to the negative control.

Anyway, taken together, these results suggest a possible different plant interaction response between the pathogen inoculated and the elicitation EF treatment, especially in the later phase of response. This is expected as the pathogen still continues to infect and damage the plant, as shown in the detached leaves pictures. The elicitation instead seems to present a tendency to activate only the signalling pathway.

3.5 Evaluating EF as a priming agent in grapevine: a functional immune challenge on *Vitis vinifera*

Supported by the trends observed in the preliminary tomato detached leaves assay, the 50 µg/mL EF concentration of *B. cinerea* was selected as the working dose for the next test. In the tomato plant experiment, considering the high standard deviation, this concentration suggests more than the others, a possible activation of the immune system, comparable to the effects created by the real pathogen. At the same time, EF does not seem to cause an exaggerated damage to the leaves and shows a tendency to differentiate between the two pathogen strains (B05.10 and T4) in the later subsequent time point. Based on these results, a priming agent's possible activity was hypothesised from the EF, with the aim of sensitising the grapevine immune system in anticipation of subsequent *B. cinerea* attack.

Priming is a well-known strategy in plant immunity, whereby after being exposed to a certain stimulus, the plant can respond more rapidly and robustly upon future stress or pathogen invasion. [124], [125]

We therefore wanted to explore whether *B. cinerea* EF could have such a role in a more pathologically and economically relevant host as grapevine (*Vitis vinifera*), representing an important worldwide crop affected by grey mould disease.

To test this, a functional challenging assay using the *Trincadeira* cultivar was designed (Fig 3.29). Green-house grapevine leaves were excised and prepared for a detached leaf assay as in the tomato experiment previously described. Leaves were pretreated with EF at 50ug/mL concentration for 48 hours. This should give the plant sufficient time for immune activation prior to pathogen infection.

Following the priming phase of 48 hours, leaves were inoculated with the same conidial suspension used for the tomato assay, $1x10^6$ sp/mL for both strains B05.10 and T4 [169] (EF + INF).

Inoculation was carried out by dispensing a total volume of 125 µL over 4 leaves, from different plants, for each treatment, and evenly spread all over the surface.

Leaves were sampled at four time points: 0, 6, 30 and 54 hours post infection (hpi) as three biological replicates. To properly control the treatment's effects, three experimental controls were included: the negative control (CTRL) (treated with buffer only, without priming or pathogen exposure), the positive control (INF) (treated with buffer for 48 hours, then inoculated with the pathogen) and the priming control (EF) (treated with the EF for 48 hours, then mock-inoculated with water). Leaves were photographed under a stereomicroscope, and tissue was collected for RNA extraction and gene expression analysis as in the tomato experiment.

Plant immune response in this experiment was monitored following three grapevine defence markers as *VvJAR1*[116], [170], responsible for the synthesis of the jasmonic acid active form, *VvMYB14*, a transcription factor involved in stilbene biosynthesis and secondary metabolism but also in general PRR response [171] and *VvST1*, a gene coding for stilbene synthase involved in the production of phytoalexin as resveratrol [120][119].

Expression of these genes was analysed by RT-qPCR to assess the dynamics of the immune activation and defence across treatments and time points. Simultaneously, the expression of one *B. cinerea* gene *BcKAR2*, was also quantified, an interesting gene described to be involved in the UPR response in other types of fungi[172], [173]. KAR2 was a central protein-folding chaperone identified in the STRING protein-protein interaction network (cluster 1) in the common core of proteins obtained from the EF of both *B. cinerea* strains. This gene was measured only in infected samples, obviously, from both strain B05.10 and T4 at 0, 1, 6, 30 and 54 hpi. A 1 hpi time point was added in accordance with the EF proteome window production set-up in the proteomic analysis.

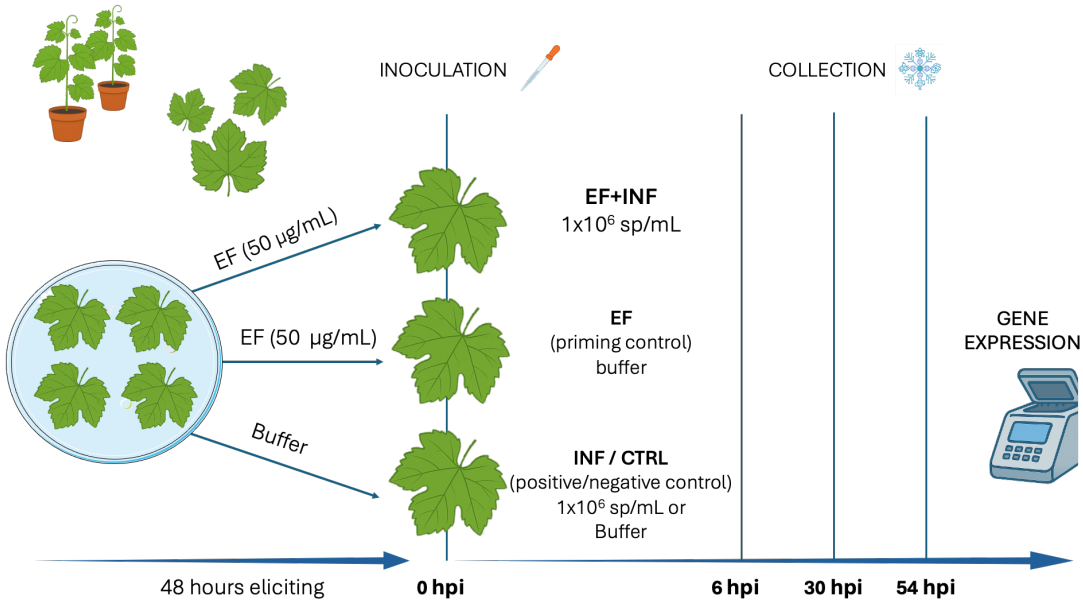

Figure 3.29. Grapevine detached leaves experimental design.

The goal was to evaluate whether *B. cinerea* EF could confer a protective priming effect in grapevine under active pathogen challenge.

Stereomicroscopic imaging revealed an important contrast between the progression of infection in positive controls and in EF-pretreated samples. As illustrated in Figures 3.30 and 3.31 in both B05.10 and T4 infections, respectively, untreated leaves (positive controls) show progressive tissue damage over time. An extensive colonisation is visible at 12 days post-inoculation (Fig 3.31). In contrast, leaves that had been primed with the EF for 48 hours and then inoculated seem to show only minor necrotic symptoms at 54 hours (hpi), more pronounced in T4 than in B05.10. For the more aggressive strain, we had enough leaves to test the macroscopic infection rate at 12 days post-inoculation (dpi), which showed no signs of infection remaining macroscopically comparable to the negative control (Figure 3.32).

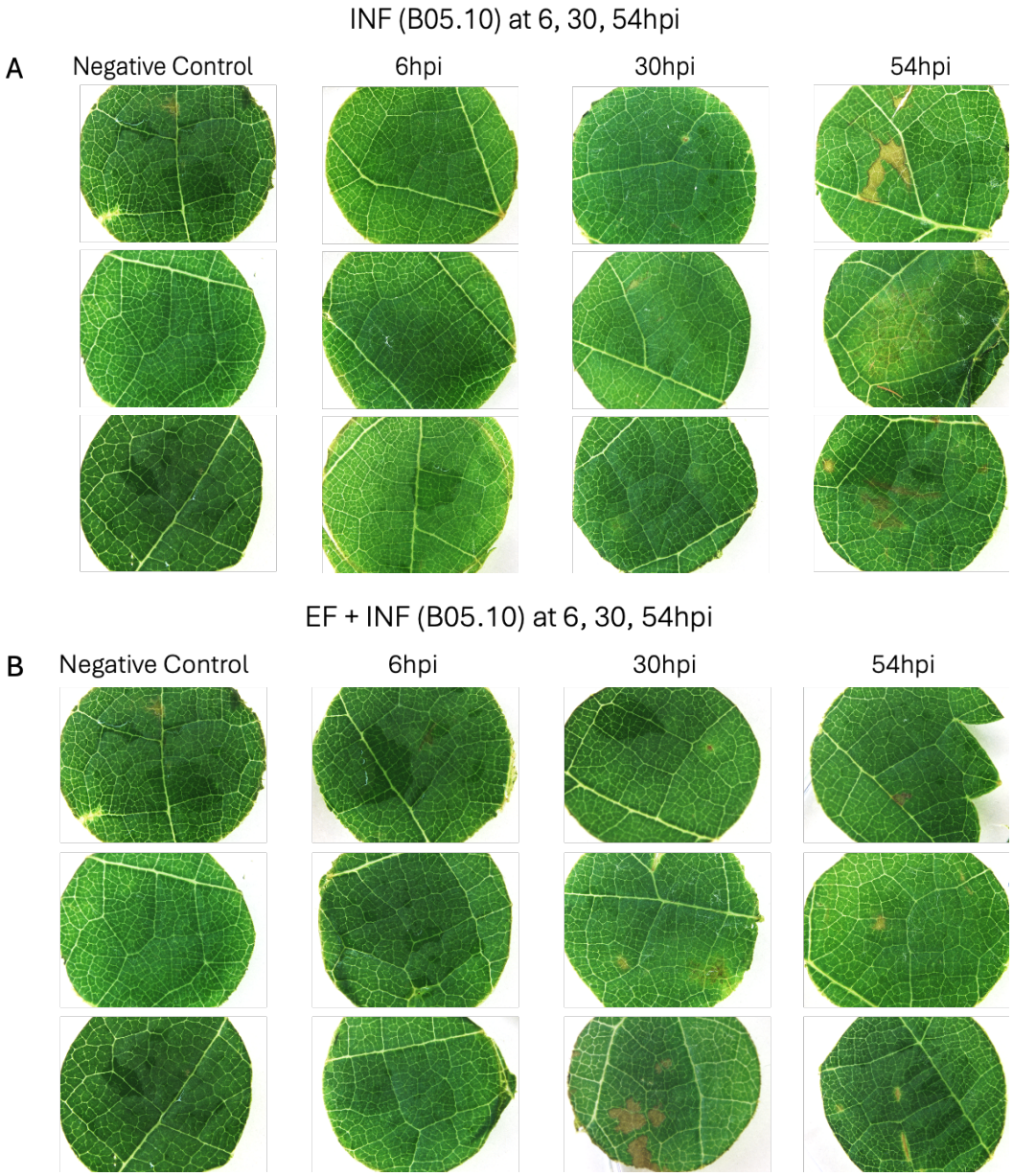
INF (B05.10) at 6, 30, 54hpi
A
Negative Control
6hpi
30hpi
54hpi
EF + INF (B05.10) at 6, 30, 54hpi
B
Negative Control
6hpi
30hpi
54hpi

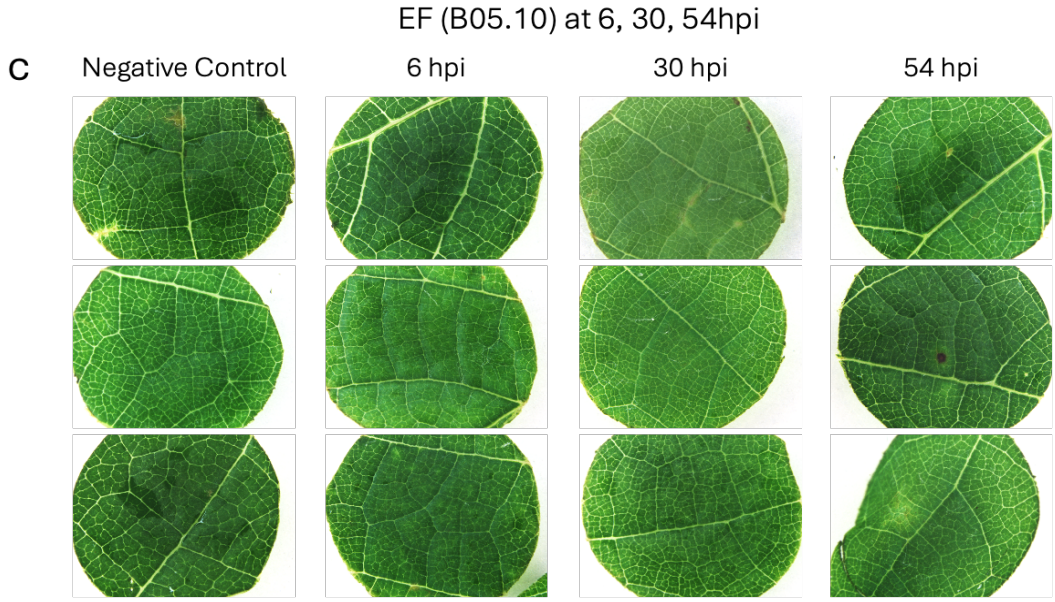

Figure 3.30. Stereomicroscope images of grapevine leaf disc treated over time, where the negative control samples are compared with: (A) B05.10 positive control, leaves were treated with 1x10^6 sp/mL and collected at 6, 30 and 54 hpi (INF). (B) B05.10 EF treatment, leaves were treated at 50ug/mL with EF followed by B05.10 spores inoculation at 1x10^6 sp/mL after 48 hours and collected at 6, 30 and 54 hpi (EF + INF). (C) B0.10 priming control. Leaves were treated with EF at 50 µg/mL and collected at 6, 30 and 54 hpi (EF). Negative control represents leaves treated only with buffer.

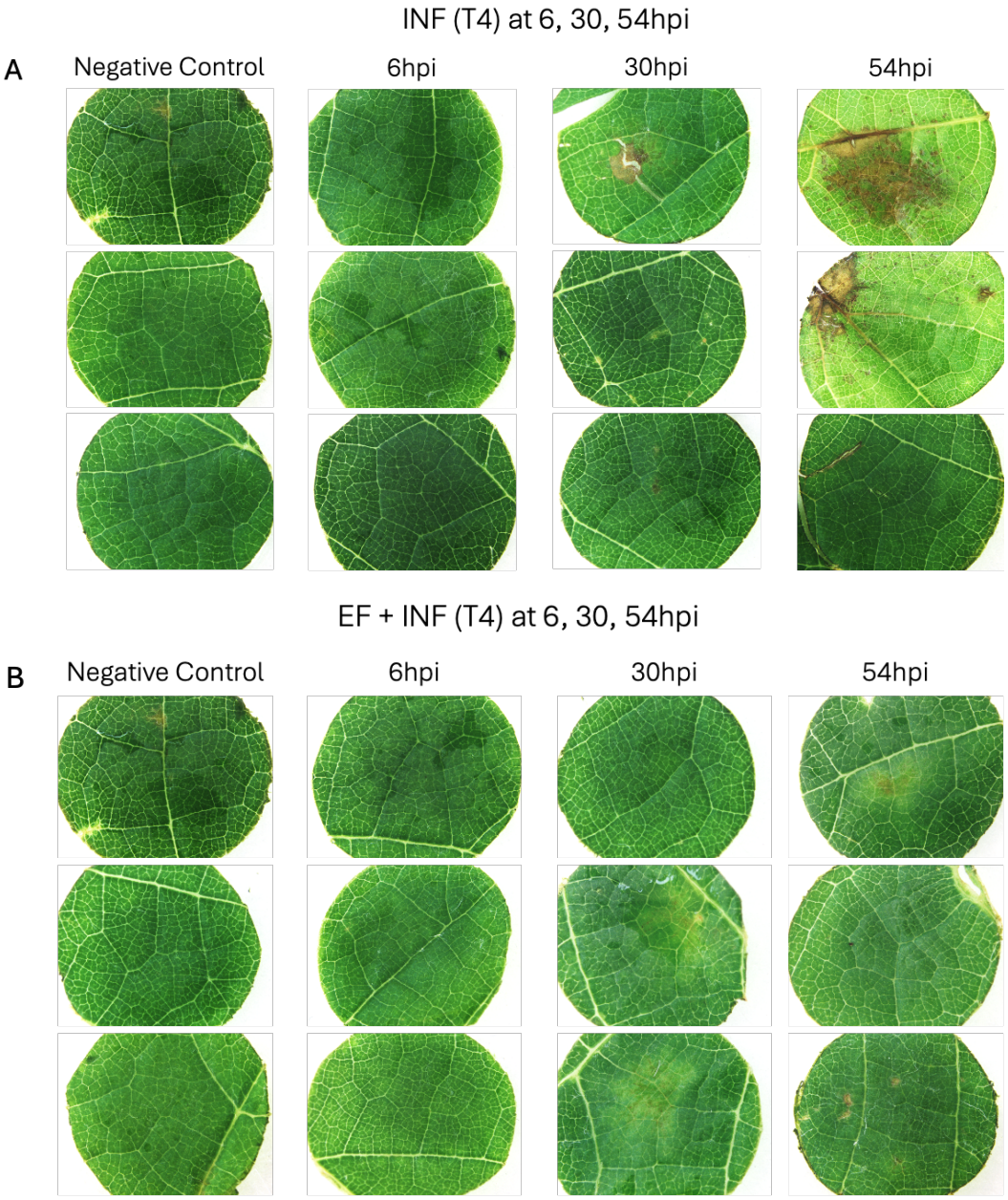
INF (T4) at 6, 30, 54hpi
A
Negative Control
6hpi
30hpi
54hpi
EF + INF (T4) at 6, 30, 54hpi
B
Negative Control
6hpi
30hpi
54hpi

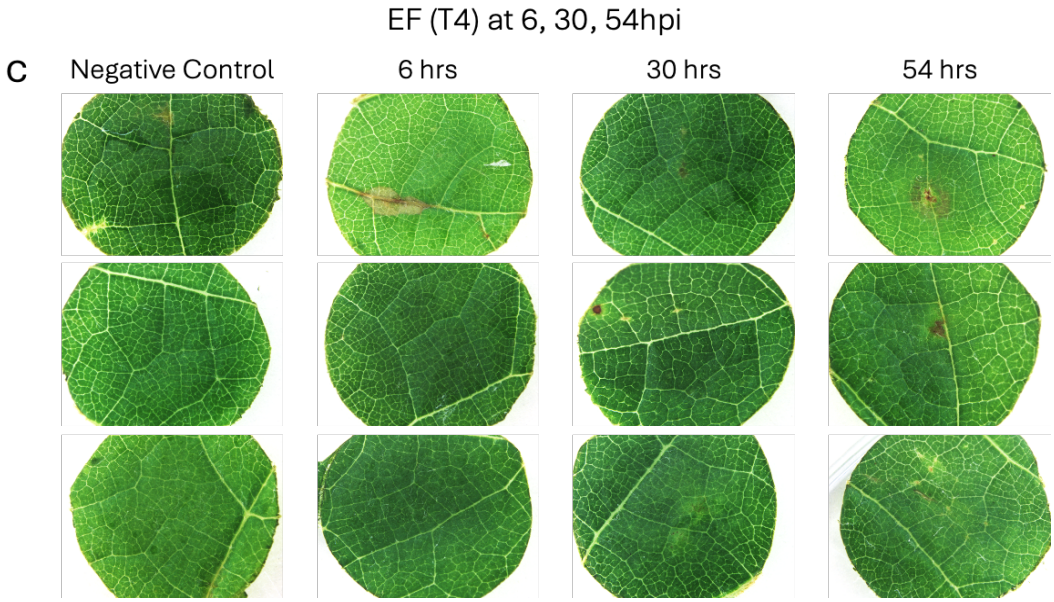

Figure 3.31. Stereomicroscope images of grapevine leaf disc treated over time, where the negative control samples are compared with: (A) T4 positive control, leaves were treated with 1x10^6 sp/mL and collected at 6, 30 and 54 hpi (INF). (B) T4 EF treatment, leaves were treated at 50ug/mL with EF followed by T4 spores inoculation at 1x10^6 sp/mL after 48 hours and collected at 6, 30 and 54 hpi (EF + INF). (C) B0.10 priming control. Leaves were treated with EF at 50 µg/mL and collected at 6, 30 and 54 hpi (EF). Negative control represents leaves treated only with buffer.

Priming controls (EF) similarly did not show major visible lesions or some type of discolouration, as is clearly visible for B05.10 and T4 positive controls (INF), confirming that the fraction itself did not induce any major phytotoxic effect.

Interestingly, in agreement with the tomato assay, the T4 strain seems to trigger a more “aggressive” or faster lesion, especially at 54 hours, larger than the lesion created by B05.10. However, by the final stage of infection (12 days), both strains reach sporulation level, and then the B05.10 lesions appear bigger than the T4 ones similar to the tomato results.

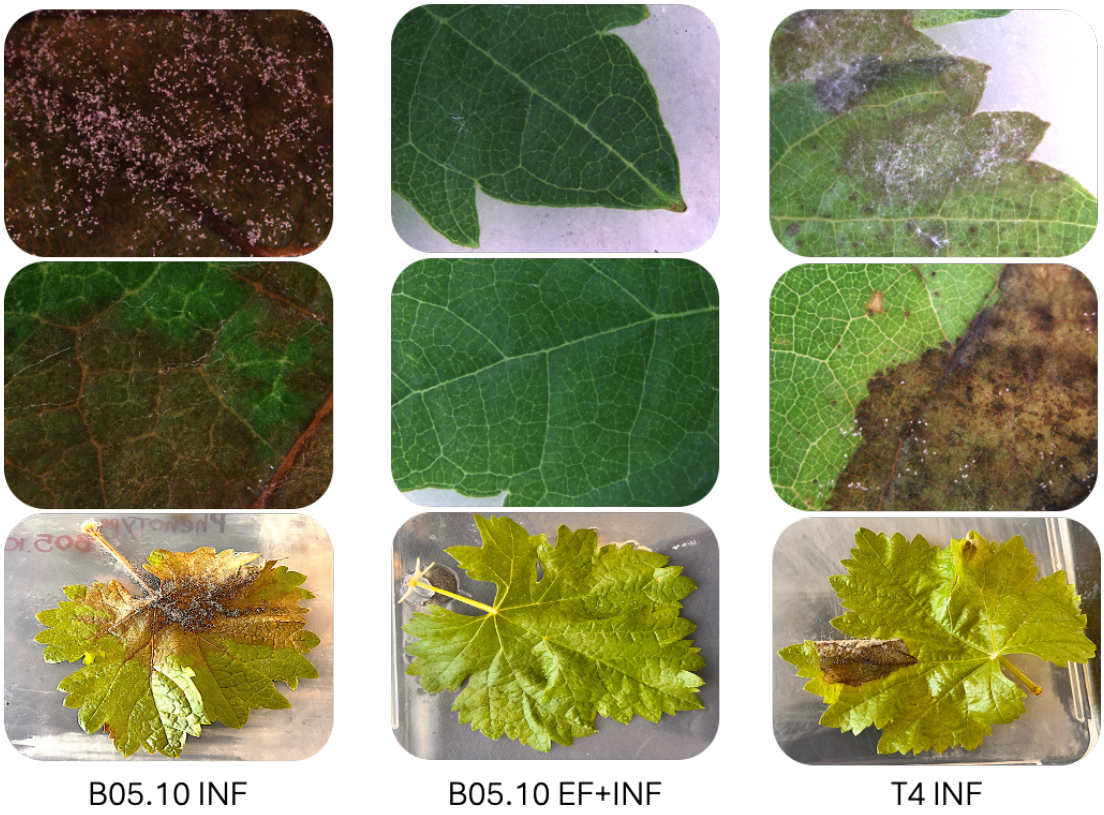

Figure 3.32. Grapevine leaves images after 12 days post-inoculation. INF represent leaves treated with buffer for 48 hours and then challenged with B. cinerea spores. EF + INF represent leaves pre-treated with EF for 48 hours and then challenged with B. cinerea spores.

The protective effect of the EF treatment was further supported by the RT-qPCR gene expression analysis of the three selected defence-related grapevine genes, mentioned earlier. All of them represent key nodes in PRR response, phytoalexin response, stilbene biosynthesis and jasmonate signalling [119], [120], [123], [144].

Figure 3.33 illustrates the relative expression of *VvMYB14*, the transcription factor that regulates [120] stilbene biosynthetic gene as STS1 and is involved in PRR response [174], against necrotrophic pathogens. At 54 hpi, MYB14 was markedly upregulated in all samples except the T4 EF+INF treatment, suggesting a different response to this pathogen after prior immune activation. In the positive control (INF) of T4, in fact, MYB14 reached a fold change expression of 51.2 ± 5.7, indicating strong late expression of this transcription factor, contrary to what was described for STS1 regulation after UV stress.

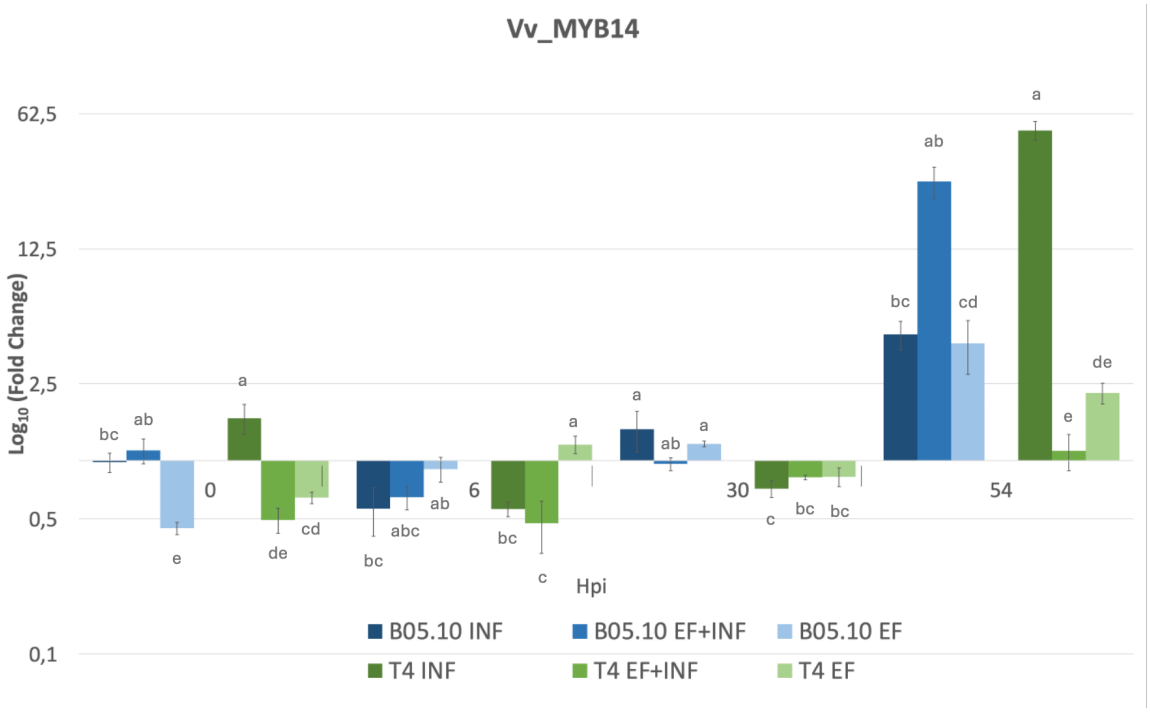

Figure 3.33. Relative expression of the VvMYB14 gene in grapevine. Leaves were treated with EF (50 µg/mL) for 48 hours to activate plant immunity and then inoculated with B. cinerea (EF + INF). Positive control (INF) represents leaves with no immunity but only inoculated at the same time point (0) with the pathogen. Priming control (EF) represents leaves only immune-activated for the first 48 hours but not after being inoculated with the pathogen. Bar plots represent the mean (log10(FC)), and error bars indicate standard deviation (SD) values from three biological replicates. Expression levels were normalised to the reference gene VvEF1a. Statistical differences between treatments were evaluated using the non-parametric Kruskal-Wallis test followed by Bonferroni correction. Different letters indicate significant differences between groups but not between time points (p<0.05).

Conversely, the B05.10 positive control (INF) exhibited a lower but still significant upregulation at 54 hpi. These two strains seem to follow consistently the pattern of the "zig-zag" model of plant immunity [105].

B05.10 positive control (INF) sample seems to be subjected to an initial immune recognition followed by partial immune suppression. Interestingly, when the host was primed with EF prior to infection, MYB14 expression in B05.10 infected leaves increased from 4.5 ± 0.7 to 28.0 ± 5.1. This result supports the role of EF as a priming agent capable of amplifying plant defence activation otherwise attenuated by the pathogen, but in a different way against the two pathogens.

The expression profile of *VvSTS1* (Fig. 3.34), a key gene in the stilbene synthase family, displays a consistent response pattern, confirming the natural engagement of this gene in defence [171]. In EF-treated samples, STS1 seems to spike at 6 hpi, confirming the early recognition by the plant immune system. This

response seems to return to basal levels at later time points. In contrast, both positive controls (INF) exhibited upregulation at the later time point, with T4 increased from 3.3 ± 0.3 at 30 hpi to 72.7 ± 8.0 at 54 hpi, while B05.10 samples reached the maximum 9.3 ± 1.15 at 30 hpi before declining a bit.

Similar to *VvMYB14* at 54 hpiB05.10 EF + INF samples reached a STS1 expression of 34.2 ± 12.6, significantly higher than the unprimed positive control. By contrast, the EF + INF of the T4 strain remains at lower levels. This pattern mirrors that of MYB14 at the same time point, supporting the EF priming activity and suggesting a clearly different pathogenetic approach to the host tissue from these two strains in the first hours of interaction.

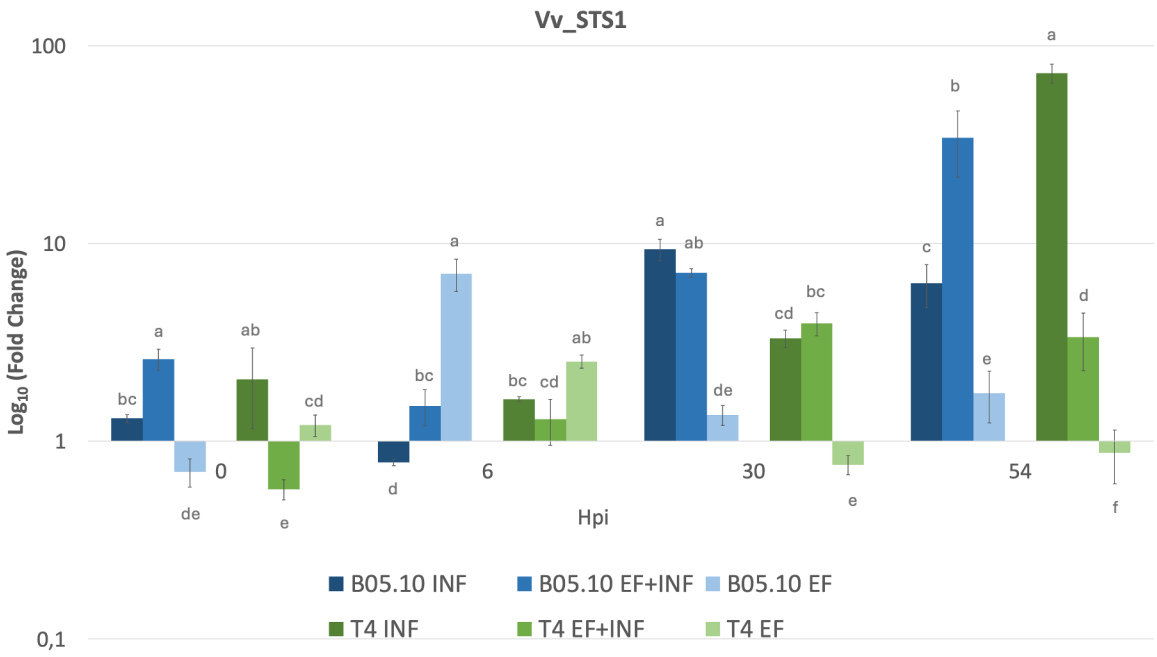

Figure 3.34. Relative expression of the VvSTS1 gene in grapevine. Leaves were treated with EF (50 µg/mL) for 48 hours to activate plant immunity and then inoculated with B. cinerea (EF + INF). Positive control (INF) represents leaves with no immunity but only inoculated at the same time point (0) with the pathogen. Priming control (EF) represents leaves only immune-activated for the first 48 hours but not after being inoculated with the pathogen. Bar plots represent the mean (log10(FC)), and error bars indicate standard deviation (SD) values from three biological replicates. Expression levels were normalised to the reference gene VvEF1a. Statistical differences between treatments were evaluated using the non-parametric Kruskal-Wallis test followed by Bonferroni correction. Different letters indicate significant differences between groups but not between time points (p<0.05).

Another interesting result is illustrated in Figure 3.35, where the expression trend of *VvJAR1* is shown. JAR1 codes for an essential enzyme involved in converting

jasmonic acid (JA) into the bioactive form JA-Ile, a well-described hormone associated with necrotrophic pathogen defence, such as *B. cinerea*. *[175], [176]*. At 0 hpi, *VvJAR1* was downregulated in all samples except in the T4 positive control (INF), where it remained around basal levels, suggesting a different type of contact with the host between these two strains. In contrast, EF treatment mirrored the B05.10 positive control in both pathogens, with a downregulation of the gene.

At 6 hpi, *VvJAR1* was slightly upregulated in all treatments with no significant differences, indicating a similar starting recognition phase from the plant, further showing that the plant recognises the EF treatment in the same way as the pathogen (but with no major visible effects as described above), confirming the priming effect. By 30 hpi, the expression levels reach approximately 2-fold across samples, before returning to baseline at 54 hpi. The EF fraction still at later time seems to act in the same way as the pathogen.

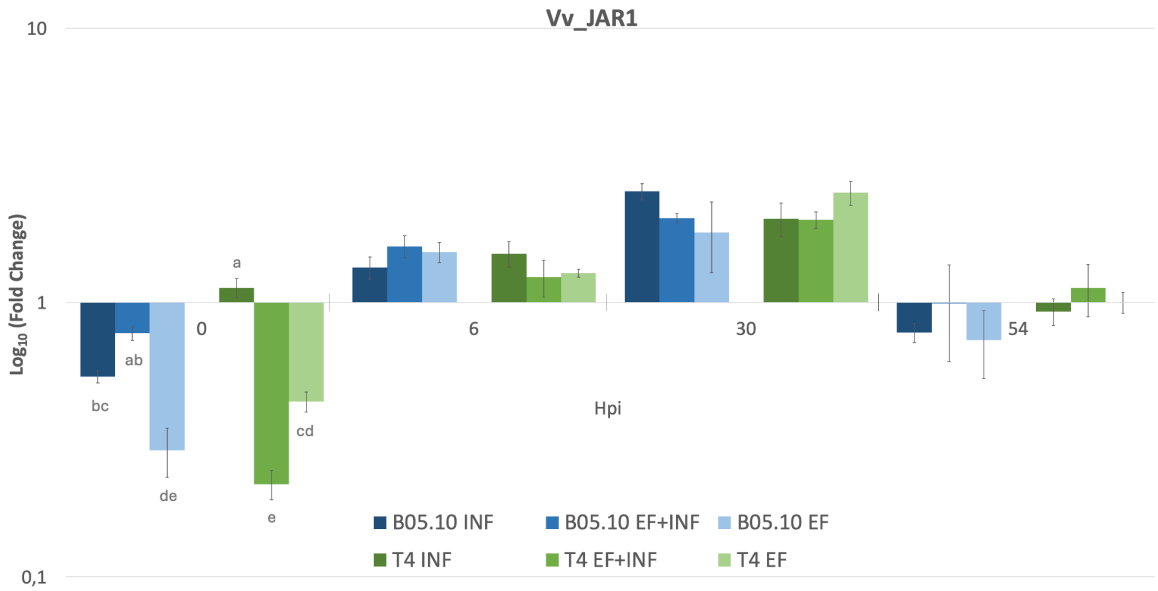

Figure 3.35. Relative expression of the VvJAR1 gene in grapevine. Leaves were treated with EF (50 µg/mL) for 48 hours to activate plant immunity and then inoculated with B. cinerea (EF + INF). Positive control (INF) represents leaves with no immunity but only inoculated at the same time point (0) with the pathogen. Bar plots represent the mean (log10(FC)), and error bars indicate standard deviation (SD) values from three biological replicates. Expression levels were normalised to the reference gene VvEF1a. Statistical differences between treatments were evaluated using the non-parametric Kruskal-Wallis test followed by Bonferroni correction. Different letters indicate significant differences between groups but not between time points (p<0.05).

To complement the expression profile analysis and establish a link with the proteomic analysis, *B. cinerea* gene *BcKAR2* expression was monitored in both strains (Figure 3.36). This gene encodes a chaperone protein identified in the red cluster of the STRING network analysis. This chaperonin is described as involved in protein folding and stress response [8]. Interestingly, *BcKAR2* expression peaked at 1 hpi, particularly in the T4 strain, and then gradually decreased over time. This early peak could suggest a potential role for *BcKAR2* in the fungal adaptation to the host environment, indicating differences between the two strains and suggesting that a host-pathogen interaction begins within the first hour of contact.

These data could also suggest that the EF contains proteins actively secreted, even in an environment without stimuli, that could act as virulence factors or as an environmental sensor for better adaptability, when the pathogen infection wave subsequently occurs.

Figure 3.36. Relative expression of the BcKar2 gene in B. cinerea positive controls. Positive control represents leaves with no immunity but only inoculated at the same time point (0). Bar plots represent the mean (log10(FC)), and error bars indicate standard deviation (SD) values from three biological replicates. Expression levels were normalised to the reference gene VvEF1a. Statistical differences between treatments were evaluated using the non-parametric Mann–Whitney U test. Different letters indicate significant differences between groups but not between time points ($p<0.05$).

4 DISCUSSION

4.1 From Extraction Protocol Optimisation to Proteomic and in Silico Insights

The early stage of *B. cinerea* development in the plant tissue is a crucial moment in the establishment of a successful infection, with a subsequent determinant penetration of the plant tissues that leads either to fungal growth, tissue invasion, rotting and finally sporulation and spread in the environment or a necrotic spot to which the plant restricts the pathogen. Generally, macrospores germinate in a few hours once they meet favourable conditions and within 6 hrs 50% of them present a germ tube. Considering the very limited resources stored in the macrospore for the initial interaction with the host, we thought that the very first hours of interaction between the macrospores and the host tissue could play a key moment determining a successful pathogen infection. This initial phase could enable or disallow the pathogen over very different plant species.

To gain insights on the proteins used by the pathogen in this specific interaction phase, contrary to what described previously for *B. cinerea* "secretome" [51], [53], [54], [87], but also for other relevant pathogens such as *C. albicans* and *S. cerevisiae* [84], [85], our analyses were performed over the macrospores of *B. cinerea*. This is because the macrospores are the very first contact point with the plant tissue as soon as they land over the leaves, fruit or flowers. We wanted to verify the following hypothesis: how does the pathogen sense the environment for appropriate germination conditions and does it prepare itself somehow or not for any type of interaction?

For this, the accurate characterisation of the EF is essential to understand the very early events in host-pathogen interaction.

An important aspect was to find a general *in-vitro*, non-stressing condition for the macrospores to be used during the incubation period, that could allow us to apply the results to a general pathogenic infection situation.

The first part of the study was to establish and optimise appropriate testing conditions, followed by an EF extraction protocol suitable for nanoUPLC-MS/MS analysis coupled with a trypsin-based surface shaving technique. Once these protocols were set in place, we could also test EF extraction for further functional characterisation as cryo-TEM and NTA analysis. The protocol developed for the proteomic analysis, in fact, enables the selective extraction of exoproteome and surfaceome proteins while preserving macrospore and EVs integrity (differently, the SDS-PAGE analysis also revealed the proteins contained within the EVs, due to the effect of the denaturing Laemmli buffer). This methodology is critical, as contamination with intracellular proteins may change the proteome profile, leading to possible false or positive unrelated identifications [177], [178].

The protocol we developed combines mechanical macrospore collection and cleaning by filtration on 40 µm sieves and multiple low-speed centrifugation steps to efficiently remove macrospores from mycelium debris, which are frequently retained after *B. cinerea* macrospores collection. In the same way, after macrospore incubation, high-speed centrifugation and 0.45 µm filtration are extremely important to avoid macrospores and other debris from contaminating the EF fraction. This step is fundamental to ensure the purity of the starting material before EF analysis and testing [54], [85], [87]. Considering the idea of studying what is around/released by the macrospore, we adopted a different strategy with respect to what is found in literature, where generally the extracellular component is studied from the mycelium or from germinated spores [51], [54], [179].

A key aspect of our protocol was the setup of the incubation conditions to maintain macrospore viability well above 95%, generally $\geq$ 98%, as confirmed by trypan blue staining, and that did not stress or provide particular germination stimuli to the macrospores in the presence or absence of trypsin [10].

In literature, trypsin is widely used for cell wall shaving to cut off most of the proteins present on the surface of the cell wall, with several examples in *C. albicans* and many other yeast and non-yeast like pathogens. We set to use a significant amount of trypsin (10 µg/sample) to obtain the highest possible cleavage activity, to counterbalance the slightly lower cleaving efficiency of the enzyme at 25°C to avoid macrospore heat stress [83], [85], [180]. We further optimised the protocol by performing a second overnight trypsin cleavage step after separation of the macrospores from the incubation buffer at the 1 hr time point. Despite the large amount of trypsin used in our protocol, it is well known that this type of enzyme is unable to hydrolyse lipid membranes, such as those of EVs. As a result, the proteomic analysis reveals only the proteins belonging to the exoproteome and surfaceome subgroups.

Our data show a reproducible protein profile from four independent biological replicates for both B. *cinerea* strains. The SDS-PAGE results in fact, display consistent protein patterns of the EF with major bands at 75, 60, between 25-37 and a strong signal around 10 kDa. Although Shah et al. [55], in their work, reported a comparable protein distribution in the *B. cinerea* secretome, our results represent a newly characterised and reproducibly obtained extracellular fraction generated under defined extraction conditions. These findings confirm the robustness and reliability of our EF production protocol for both *B. cinerea* strains.

In particular, during the EF extraction optimisation protocol, two different studies were published in 2023, describing the release from *B. cinerea* B05.10 cultured hyphae of Extracellular vesicles.

Interestingly, these studies on *B. cinerea* extracellular vesicles (EVs) reported consistent enrichment of low molecular weight proteins within vesicle cargo under different growth conditions [73], [74]. Although our study was not aimed at characterising EVs' content, for now, we wanted to check if our EF solution even contained EVs. Thanks to the collaboration with Prof. Lupetti's group at the

University of Siena, we were able to analyse our fraction by cryo-TEM, which revealed EVs presence from EF of both strains, from non-germinate macrscopores as clearly shown in the cryo-TEM images provide.

EVs are small particles secreted by cells across all kingdoms. They generally carry diverse cargo-proteins, RNAs, lipids, metabolites and serve as delivery vehicles for intracellular communication [62]. For pathogen microbes, as *B. cinerea*, EVs enable a cross-kingdom interaction with their host [73], [181].

Recent research in fact confirms that at least *B. cinerea* B05.10 strains produce EVs at the hyphal stage, under both *in vitro* and in planta conditions, describing also a different cargo of EVs based on the environmental conditions [73], [75]. EVs have been described in literature for other fungi pathogens as *Ustilago maydis* [72]*, Colletotrichum higginsianum* [68]*, Fusarium graminearum* [71] and *Fusarium oxysporum* [69]. However, as far as we know, there is no evidence of EVs obtained after just 1 hour of incubation from *B. cinerea* strain B05.10 and T4 macrospores, or just macrospores in general, although it is suspected.

Our results show various EVs populations from both strains B05.10 and T4, because each strain presents a different size distribution with an average size that goes from 100 nm to 250 nm. This is in accordance with different EVs size populations that are described to exist and to be released by fungal pathogen as *Botrytis cinerea [65], [73].*

In particular, NTA from T4 EVs suggest a higher polydispersity of this strain population compared to the B05.10. In fact, T4 EVs appear to be slightly bigger, reaching an average size of around 200 nm instead of 100 nm as for B05.10. Considering the low number of *B. cinerea* EV articles published, such heterogeneity may be due to different biogenesis pathways or may reflect different cargo loading. T4 also seems to suggest a somewhat lower amount of EVs.

Cryo-TEM images show mono-lamellar and multi-lamellar EVs, but also multivesicular bodies (MVBs), at least for T4, but have been described to be released also from the B05.10 strain under hyphal growth [73].

Both strains showed a morphological similarity EVs structure (spherical, structural integrity and a lipid bilayer membrane). In accordance with the MISEV2018 guidelines [182], EVs described as being from 100 to over 200 nm are considered as small EVs and medium EVs, respectively.

Although we did not attempt EV purification from the media, our proteomic analysis seems to reveal some of the proteins characteristically isolated from EV preparations, such as at least one transmembrane or GPI-anchored protein and cytosolic proteins present in more than 40%. Considering that we did not observe cell lysis or mortality, and that the trypsin used in the proteomic analysis was not able to disrupt EVs structure and that our NTA analysis excludes the presence of the larger apoptosomes, this may confirm the possibility of bona-fide targets presence anchored on the outer side of EV (but accessible for enzymatic digestion) or of unconventional secretory pathways as described [65], also for *B. cinerea*.

MVBs and multilamellar vesicles presences may be associated with a differentiated cargo release, potentially implying functional implications [183].

Despite a growing interest in EVs, however, there are not so many publications, especially regarding necrotrophic fungi like *B. cinerea*. Despite this, the knowledge generated from two recent publications on *B. cinerea* B05.10 strain EV proteomic analysis shows that they contain proteins involved in cell wall degradation, transport, stress, metabolism, energy and pathogenicity [13], [17]. Especially in De Vallée et al. 2023 study, it is described that isolated EVs did not show specific toxicity signs over plant tissue, differently from the crude secretome. This is in line with our results, where hypersensitive response signs were obtained from tomato and grapevine treated with EF (which represents a crude secretome). Furthermore, if we consider the last article published on *B. cinerea* EVs in 2023 from Escobar-Niño, A. et al. [74], our identifications overlap (90%) with those representing the entire set of proteins identified after filtration of contaminants, confirming that they are bona fide extracellular proteins [73], [75].

Another study also describes the presence of small RNA, which the pathogen can transfer through EVs to the host to suppress some defence genes, as an RNA silencing method [181], [184]. In particular, He et al. 2023 describe sRNAs from *B. cinerea* vehiculated with tetraspanin decorated EVs and internalised through clathrin-mediated endocytosis (CME) that enter plant cells and hijack defence proteins from the plant to silence host immunity genes. Unfortunately, our protein identification strategy would not allow identification of the EV-specific tetraspanin (*BcPLS1*), because of protein membrane topology and basic amino acid distribution; however, all our data seem in line with published work and extend it.

In fact, differently from all other studies described so far, our data shows the release of EVs after 1 hour incubation in a non-stimulating environment from macrospores of both strains and frames their number to a significantly more contained dataset, separating the extracellularly accessible components from those contained in the EVs.

It also suggests that *B. cinerea* releases factors (proteins, effectors and EVs) immediately and in the absence of particular stimuli [26][27]. The common set of proteins identified from the experiments in B05.10 and T4 strain and the full overlap of the factors identified from the more pathogenic strain to the less pathogenic one, suggests an interesting functional conservation of these factors in the early steps of infection between these two strains while the presence of 51 additional proteins in the less pathogenic strain suggest a higher level of adaptation of the pathogen to the host, possibly justifying the lower pathogenicity and phenotypic differences already documented even for virulence of the two strains [185].

The number of proteins identified considering different methodologies used (macrospores instead of hyphae, a very low incubation period and the absence of a denaturation agent) was lower compared to previous studies [54], [52], [87]. In particular, one of the most recent “surfactome” studies revealed more than one thousand protein IDs identified. These differences, as already said, could be

explained by the lower time of incubation, the use of clean macrospores instead of mycelium, but especially because Escobar-Nino et al.[74] analysed a purified EV fraction, but differently from us, they performed a complete lysis and denaturing procedure of the vesicles before trypsinisation. By contrast, in our study, we specifically targeted the EF but did non introduce any denaturing and lysing agent before trypsinisation, thus vesicles probably remain intact until acidification and organic extraction of the peptides.

Other studies have shown that certain intracellular EV proteins (as actin and tubulin) become detectable by western blot only after treatment with Triton X-100. In contrast, quantitative proteomic analysis of EV samples digested with trypsin in the absence of any denaturing agent typically identified a comparable number of proteins, around 350-400 [152], [186]. This could possibly explain why the cellular component enrichment analysis highlighted a higher proportion of cytosolic annotations (around 40%), as also confirmed by the the SubCello prediction, compared to other "surfactome" analysis that goes around 20% [51], [87], [179] In those studies, however, the samples were subjected to reduction and denaturation prior to trypsinisation. In our case, trypsin digestion was performed directly on intact macrospores, under mild and life-compatible conditions but where the inputs were subjected to reduction and denaturation before trypsinisation. In our study, instead, trypsin digestion happened directly over the macrospores under life-allowing conditions, acting on the released EVs and on soluble proteins accessible to the protease in a slightly reducing environment. This procedure preserved the structural integrity of the EVs, therefore the higher percentage of cytosolic proteins identified in our analysis likely reflects cytoplasmatic components released or associated with the outer membrane of EVs, rather than proteins derived from cell disruption.

Identified proteins were subjected to "in silico" analysis to understand the different categories obtained according to each protein–protein interaction using

STRING, and biological process, molecular function, cellular component and KEGG pathway with GO analysis.

Following the Gene Ontology analysis and the enrichment pathway, the 80 common proteins seem to present a metabolic activity (biosynthesis of organo-nitrogen compounds, amide metabolism, translational elongation and central carbon pathways), with an intracellular origin and a chaperone activity.

STRING analysis revealed an increased size of the predicted network for the common proteins between the two strains, indicating strong functional cohesion within the dataset. This suggests that these proteins interact with each other and are likely secreted for a specific function. The 80 common proteins released by B05.10 and T4, showed 8 different clusters when stringency was set high (score > 0.9).

Cluster 1 was the largest and the most interconnected (9 genes) and was dominated by protein-folding/chaperone factors. GO classification from the Biological Process (BP) point of view, in fact, appeared to be enriched in protein folding, maturation and quality control (26%). Some interesting proteins were founded as *Bcsti1* (A0A384JH41 / G2Y1R0) (AN B05.10 / AN T4). Sti1, known as "Stress-inducible protein 1, in eukaryotes is described as a co-chaperone that links Hsp70 and Hsp90, and is a hub of proteostasis networks. Similar hop/STI1 roles are reported in eukaryotes, but even in plants, as implicated in stress response and facilitating folding of specific regulatory proteins [187], [188].

Bckar2 (A0A384K0D3 / G2YSM3), in fact, is annotated as the ER Hsp70 homolog and described in UniProt as the endoplasmic reticulum chaperone Bip. In other eukaryotes as the yeast *Saccharomyces cerevisiae*, the homologous chaperone Bip is described to take part in translocation, protein folding and ER-associated degradation [189]. The detection in the EF fits with intense secretory pathway traffic or packaging of ER-protein content into vesicles that was subsequently released outside.

Hsp60 (A0A384JNL7 / G2YV39) is the 60-kDa chaperon. This Hsp60 family are involved in protein folding and surface/extracellular interactions relevant to host

responses, as described for *C.albicans*, which is described to be a common surface fungal antigen, as well as involved in virulence and host interaction [190], [191].

Bcin_10g00300 (A0A384JTW8 / G2XPW6) instead was reported to be present on *B. cinerea* EVs/secretome, among other heat-shock proteins, confirming the idea that these chaperone elements are packaged or co-released in early extracellular material [73], [75].

The innovative result from this analysis is probably that the proteostasis/folding pathway seems to be highly active at just 1 hour. This may suggest that the macrospores need a chaperone-rich complex in the very early stage of environment perception, probably to help stabilise the subsequently secreted effectors and help in the rapidly synthesising protein activity. When we look at the BP protein group, the second most characterised group is the “primary metabolism” (24%), organonitrogen compounds and amide biosynthesis plus translational elongation were the most represented. In other fungal pathogen studies, for example, in rice *Magnaporthe oryzae* contact study, a rapid modulation of glycolysis, amino-acid and secondary metabolic pathways was revealed during the first phase of contact [192]. Similarly, in the *Fusarium graminaerum* secretory study, GO enrichments reported pathways involved in metabolism and proteolysis, activities that reflect both housekeeping metabolic activation and development of factors that can act outside the cell [71]. These parallels may suggest that even without a stimulating environment, the fungi mobilise central metabolism and biosynthetic routes early, to generate energy, precursors, and the chaperone-rich complex could be needed to stabilise all these types of activity.

In the same way, enrichment in ATP-dependent protein-folding activity in the Molecular Function (MF) gene ontology confirms this suggestion. Chaperone and heat-shock proteins are recovered in fungal extracellular fractions and EVs [74], generally acting to assist other proteins in folding correctly, especially during protein synthesis. This confirms and may reflect a high metabolic activity and

active protein synthesis even in a non-stimulating environment. Different studies in other ascomycete pathogenic fungi as *C. albicans,* described how important chaperon proteins are for a virulence role linked to better adaptation during infection [193], [194], [195].

Cluster 2 followed this hypothesis. Translational elongation is actively part of the protein synthesis machinery. Translation protein activity in the same way needs a greater demand for chaperones to fold nascent chains, to support protein effectors synthesis for colonisation.

Cluster 3 instead seems to connect carbon metabolism (TCA cycle) with the protective mechanism. *Bcmet6* (A0A384JGC8 / G2XXA6), the methionine synthase, is known in another ascomycete as *Magnaporthe oryzae,* to be crucial for building infection structures as appressorium development

[40]. Connected to this is *Bcsah1*, an S-adenosylhomocysteine hydrolase, fundamental to maintain methylation balance. The homologous gene in *Fusarium graminearium* is described to be required for fungal development and virulence, reinforcing the methionine/methylation pathway around *Bcmet6*[196]. The glutathione S-transferase (GST) *Bcgst24* (A0A384K053 / G2YM70), instead, seems to be implicated in detoxification and oxidative stress tolerance. In eukaryotes, this family is described to take part in the detoxification pathway, even for plants[50], [197]. GTSs in plant pathogens seem to act at the host-pathogen interface to neutralise reactive host defence compounds. This seems to be in line with our hypothesis, macrospores seem to prepare the environment for germination and structure biosynthesis, but also release factors involved in a possible host defence, even before the real host presence.

This hypothesis could be confirmed by Cluster 4; proteins in this cluster, in fact, supply NADPH and ribose 5,5-phosphate by the Pentose Phosphate Pathway (PPP). In plant pathogens, this pathway seems to be crucial for oxidative stress survival, lipid and nucleotide biosynthesis [47]. In plant pathogen fungi as *B. cinerea* or *Magnaporthe oryzae,* PPP activation and NADPH production are described to be important for oxidative stress defence as well as virulence

activity [198]. Seeing PPP enriched together with folding and detox proteins in the 1-hour EF set, could suggest a primed oxidative-stress and virulence metabolism preparation even before host stimulus. Another important cluster, above cluster 5 that groups four genes involved in seleno-compound metabolism, is Cluster 6. This set includes *BcSOD1* (A0A384JBV7 / G2YHA8), *Bcatp1* (A0A384K3Z3 / G2Y4C1) and *Bcatp16* (A0A384JVG5 / G2YH36). This set of proteins is tied to mitochondrial energy metabolism and redox homeostasis. The very first theme that emerges is the reactive oxygen species (ROS) defence by SOD1. It's widely described how this protein, superoxide dismutase 1, converts superoxide (O_2^-) to hydrogen peroxide for defence, but it's also been known to play important roles as a nuclear transcription factor and RNA-binding protein[48]. Its presence in the EF after only 1 hour indicates that macrospores are already exporting ROS detoxification capability in the environment at an early phase. This may suggest two biological implications. The first is that the fungus is probably preparing to survive oxidative challenges, as reactive oxygen species generated by the plant's innate immune system, even before contact. Second, as indicated by Effector P 3.0, SOD1 is defined as an apoplastic effector. In fact, analysis Effector P 3.0, showed a high proportion of proteins described as "cytoplasmatic effectors". It is widely known that effector proteins are no longer restricted to small cysteine-rich but can include diverse protein types with properties that could favour host translocation or intracellular activity [132]. Presence of predicted cytoplasmic effectors, metabolic enzymes, and chaperons is in line with the assumption that EVs and unconventional secretory pathways (confirmed by a low % presence of GPI-anchored proteins) release a mixed cargo of molecules and effectors capable of entering plant cells [70], [71], [73], [74], [76].

Extracellular SOD activity (secreted, vesicle-associated, or even exposed) can directly modulate apoplastic ROS levels and signalling, reducing the plant oxidative burst and therefore improving subsequent colonisation. It's described in fact, how *B. cinerea* virulence is reduced when *BcSOD1* is missing [49].

The other two proteins comprise the catalytic core for ATP synthesis from ADP and inorganic phosphate using the proton motive force. Their detection confirms the idea of macrospores that seem to be metabolically active. The presence of ATP synthase, in fact, aligns with the metabolic-readiness idea: spores require ATP production to fuel germination, membrane trafficking, biosynthesis of effectors and any other process that requires energy. In particular, the deleted mutant of the ATP δ subunit of the F1Fo-ATP synthase (ATP16) in another ascomycete fungi pathogen as *C. albicans*, leads to downregulation of virulence factors production and reduced pathogenicity [199].

From a pathogenic point of view, a spore that rapidly activates mitochondria, while simultaneously releasing antioxidant defences, is probably better equipped to survive subsequent oxidative conditions on the host surface after contact.

KEGG pathway enrichment analysis revealed that the 80 proteins shared by both strains are primarily involved in central carbon metabolism, including glycolysis/gluconeogenesis, the pentose phosphate pathway, the TCA cycle, and secondary metabolism. Such metabolic enrichment suggests that these proteins sustain essential cellular functions by providing ATP and biosynthetic precursors. In particular, Espino et al. suggest how glycolysis and gluconeogenesis, together with the TCA cycle, can indicate how macrospores are ready to move energy reserves up to the germination phase preparation, even if they seem to be in a dormant phase [54]. In parallel, the enrichment of the pentose phosphate pathway highlights an active redox metabolism, supporting NADPH production required for macromolecule biosynthesis and oxidative stress defence [200], [201]. This may suggest how the macrospores are trying to prepare themselves for colonisation of the environment.

Taken together, GO annotation and pathway analyses delineate a coordinated program and a sequential waypoint wave. This includes the early activation of biosynthetic and translational processes, proteostasis and metabolic activity, mobilisation of intracellular cargo via EVs and unconventional secretory routes,

and the presence of effectors in the EF that could modulate the environment or a potential host. Such a conserved early-phase strategy suggests that the pathogen invests in preparing for colonisation even prior to direct host contact. This conserved program represents an interesting target for novel phytochemical strategies, not only against *B. cinerea* strains but potentially also against other pathogens with comparable infection biology.

4.2 Priming the Plant Immune System: Insights from *In Vivo* Assays

The preliminary detached-leaf assay on tomato plants clearly indicates that the EF extracted from *B. cinerea* strains (B05.10 and T4) is capable of triggering immune-associated leaf responses in tomato without any extensive damage, as observed in spores-inoculated controls. As shown from the photos, by 48 hours, leaves treated with EF exhibit small dark point lesions (known as “black spot”) while positive controls develop progressively expanding necrotrophic lesions that, after 7 days, lead to sporulation. The EF-induced phenotype on tomato leaves may be consistent with a localised hypersensitive response (HR) previously described in *Arabidopsis thaliana*. HR is characterised by a rapid and localised cell death at the inoculation site (or contact site) as a resistance reaction against pathogen attacks. The spatial restriction of cell death (to contain the size of the infection) is a typical feature of a strong effector or pattern recognition [202]. Considering the limited experimental design of this test, this suggests that the HR-like response elicited by EF may result from *B. cinerea* secreted proteins acting as elicitors, similar to what is caused by members of the cerato-platanin family and cell death-inducing proteins (CDIP) [203], [204]. In particular, the recombinant protein *BcCDI1* is reported to trigger cell death when infiltrated at 100 µg/mL. This study supports the idea that a secreted mixture of proteins in our EF extracted after 1 hour of incubation carries sufficient PAMP/effectors to activate the HR in tomato.

Interestingly, in our assay, T4 produced a relatively larger early lesion than B05.10 at 48 hours in the positive control. This observation may suggest that aggressiveness can vary depending on timing and host tissue, as already described with 97 different strains of *B. cinerea* on wild and domesticated tomato genotypes [205].

The 25-100 µg/mL concentration range used in this study seems to be inside the common range used for priming plant tests. For instance, *BcCDI1* has been tested at 100 µg/mL, while chitin and chitosan oligomers are described to be active between 50-300 µg/mL in tomato tissue. Additionally, the droplet application method has been previously employed with purified *B. cinerea* proteins at the microgram scale to induce HR-like responses [162], [203], [206]. Although in nature *B. cinerea* does not secrete a single protein or elicitors at microgram doses during real-life infection, and none of the CDIP described in literature was identified in our work, our results provide a preliminary indication that additional factors present in the EF can induce an HR. Further studies at lower concentrations and on the single components will be required to understand if a threshold exists between a functional immune stimulation of the host and the development of an HR, or whether specific factors are toxic to the host.

To further investigate the elicitation activity of EF, a gene expression analysis was performed over 5 different pathogenic defence-related genes.
(i) *SlWRKY1* a transcription factors that play key roles in regulating defence responses [207]; (ii) *SlPTI5* an ERF transcription factors involved in activation of PR/defence gene [208]; (iii) *SlPR1* a gene involved in SA pathway response activated by WRKY TF [99]; (iv) *SlSOD1*, encoding superoxide dismutase, a key gene controlling ROS levels and (v) *SlJAR1* that encodes for an enzyme that conjugates JA to Ile (JA-Ile), generating the bioactive form that is a key jasmonate signal, especially for necrotrophic pathogen defence in tomato [209].
Gene expression analysis shows that *SlPTI5* appeared to be similar at 24 hpi between EF treatment and pathogen but then remained slightly activated or slightly downregulated to basal levels at 48 hpi in EF samples, compared to positive controls at 48hpi, where consistent upregulation appeared (±12 fold change). Contrary, *SlWRKY1* appear to be consistent between EF and positive controls, both at 24 and 48 hpi in all EF concentrations. This could be explained

by the fact that SA-mediated defences are not always strongly activated against *B. cinerea,* as described [210], or maybe because, in our case, WRKY1 is not the major TF for defence. On the other side, *SlPR1* appeared to be very less induced by the EF treatment, where it is instead heavily upregulated by the pathogen, as for PTI5. This suggests a partial activation mechanism for PTI5 and PR1 genes when the plant is subjected to EF. By contrast, when the pathogen is present, the continuous release of effectors and the increase of damage may activate the defence marker genes as demonstrated at 48 hpi. Even if necrotrophs primarily induce a JA/ET response, however, a hormonal crosstalk during pathogen infection, between JA and SA pathways, is also described against pathogens such as *B. cinerea* [113][211], explaining at least partial upregulation in WRKY1 and PR1 and PTI5 at 48hpi.

Our results show that *SlSOD* expression, instead, remained near basal levels at both time points, in nearly every condition. Tang et al. (2022) reported increased SOD levels 24 hours after *B. cinerea* infection in tomato [166]. In contrast, our results show that *SlSOD* expression remained near basal levels at both time points. However, a transient ROS burst may be more rapid and precede our first sampling point in small leaves as the tomato one, especially with a purified fraction such as EF. Notably, the presence of SOD1 in the EF, described in cluster 6, may act as a local shield in the apoplast, rapidly converting superoxide before it diffuses. Similarly, the presence of PPP enzymes, described in cluster 4, may supply NADPH, supporting fungal (and potentially even host) ROS-scavenging enzymes. The outcome could explain the containment of ROS to micro-lesions (black spot visible), allowing *B. cinerea* to protect itself, but at the same time benefits from the localised death and expansion.

Interestingly, despite experimental limitations of this analysis, *SlJAR1expression* showed a slight upregulation trend at 48 hpi in EF-treated leaves from the more pathogenic strain, particularly at 50 µg/mL, whereas it decreased in infection controls. These data suggest the possibility that the pathogen, in some way, transiently suppresses JA biosynthesis to facilitate colonisation. It's widely

described how *B. cinerea* can suppress host immune response, delivering small RNA effectors into host cells [212]. In contrast, EF, lacking CDPI but carrying EV cargos and chaperones, may prime JA signalling, supporting the early defence readiness hypothesis.

Overall, these results suggest that EF activate the expression of defence gene markers, probably shifting the tomato leaves into a ready-to-respond state, favouring JA/ER-mediated defences rather than SA-mediated responses. In ongoing infections, instead, JA signalling may be suppressed while SA responses emerge as a secondary line of defence [163], [213].

This indicates that the early infection strategy of these two strains, B05.10 and T4, may be conserved, as no significant differences were noticed at least for the tomato plant infection.

After the preliminary tomato experiment, where EF activity was confirmed as a boost for the plant immunity system, we wanted to check and test the fraction in grapevine leaves. The rationale was to evaluate whether EF, even outside the context of an infection, could prime the grapevine leaf immunity and improve the defence, or in some way alter the disease trajectory. Different studies already described how plants such as Arabidopsis or tomato can be primed using different extracts and enhance their resistance against phytopathogens such as *Botrytis cinerea* or *Fusarium graminearum* [214], [215]. In another study, a specific extract from *B. cinerea* was sprayed on grapevine plants, triggering the induction of genes involved in pathogenic stress response as PR and phytoalexin synthesis, as well as PAL and STS. Consequently, the extract treatment increased the protection of the plant towards *Plasmopora viticola* [216].

In this experiment, grapevine leaves from the strain *Trincadeira* were pre-treated with the same EF, extracted from *B. cinerea* from both strains used for the tomato experiment and subsequently challenged with the pathogen using both B05.10 and T4.

Gene expression analysis focused on three marker genes as *VvMYB14*, a TF described as activating stilbene biosynthesis; *VvSTS1*, encoding stilbene synthase (a key factor for phytoalexin production in grapevine); and *VvJAR1* involved in JA-Ile synthesis and jasmonate pathway signalling. In particular, stilbene accumulation mediated by MYB14 and STS1 represents one of the most effective defence barriers in grapevine against *Botrytis cinerea [120], [175], [217]*. *VvJAR1* instead was selected because it is widely known that the JA/ET pathway is the main defence line against necrotrophic pathogens [112], [175].

Regarding *VvMYB14*, the expression gene revealed how the profile remains largely close to basal levels, with no significant up- or downregulation until later time points. This could be explained by the "zig-zag" model of plant immunity [105], where early perception phases maintain defence genes at basal levels until recognition events trigger transcriptional activation. In positive infection controls, *VvMYB14* increased significantly at late time points after the infection, especially in T4 (51.2-fold change), whereas B05.10 was significantly lower (4.5-fold change). Contrary to what is seen from tomato analysis, this may suggest a different infective strategy adopted by the two pathogens, at least for this grapevine cultivar, and when the plant is not prepared, B05.10 seems able to somehow reduce stilbene-associated defence [41]. In this phase B05.10, then, could spread more easily due to the lower defence activation with respect to T4, which triggers a high response in both the TF and the stilbene gene, possibly as a result of the greater and earlier tissue damage observed. Alternatively, B05.10 interferes with the defensive pathway in a way we have not attempted to characterise in the current work. A similar pattern, in fact, seems to happen in STS1, where T4 induces a significantly stronger late gene induction in the INF samples compared to the moderate increase induced by B05.10. Notably, the transcriptional activation of the TF appeared later than the STS1 gene in all time points analysed.

It is also extremely interesting to note that the most aggressive strain (B05.10) induced a significantly lower defence activation at 30 and/or 54 hpi with respect to the less aggressive strain (T4) when looking at STS1 and MYB14 transcription, respectively, while the opposite is true when infection is preceded by EF priming. The aggressive strain may be able in some way to avoid or reduce grapevine stilbene-defence lines.
After EF stimulation, however, the plant is probably able to mount a significantly stronger induction of both genes against the more aggressive strain when challenged, while the less aggressive strain seems to induce significantly lower priming, as if the EF content of the two strains differed in their priming effect. B05.10-EF appear as a stronger priming agent, as it seems confirmed by the results of the primed samples, where the EF-B05.10 samples showed a higher transcriptional activation.

In line with the above observation, it is interesting to note that at 54 hpi, the STS1 transcriptional activation in the more aggressive strain (B05.10) was comparable between the infected positive control (INF) (6.27–fold change) with the EF control (7.02–fold change) at 6 hpi (that corresponds to 54 hours post stimulation with EF). This indicates and confirms a very similar priming effect, at least in the stilbene defence activation pathway, which was nevertheless significantly lower than that observed in the infection positive control of the less aggressive strain (T4), where STS1 activation was much higher (72.7–fold change).
In the case of the less aggressive T4 strain, the situation seems to be reversed: the transcriptional activation observed in the EF control at 6hpi (3.3-fold change) was comparable to that of the infection post-priming sample at 54 hpi (2.53-fold change), rather than to the infection positive control as occurred with the B05.10 strain, further confirming the presence of a lower priming potential of the less pathogenic strain. This also could be explained by the zig-zag model, considering that the EF was inoculated 48 hours earlier than the pathogen.

These results suggest that the complete set of proteins, molecules, metabolites and EVs contained in the EF induces a stilbene-based defence response that returns to baseline levels by the third day after stimulation, probably due to the limited half-life of EF or the absence of a subsequent wave attack by the pathogen, which is not present. The stronger transcriptional activation induced by the B05.10 infection post-priming samples shows how the plant is able to more effectively trigger the stilbene-based defence response when previously primed, thereby enhancing its resistance against B05.10, as also confirmed by the outcome at 12 dpi. This observation aligns with the mechanism described by Conrath et al. [39], who reported how plants can accumulate and increase the cellular level of inactive proteins involved in cellular signal amplification when stimulated by elicitors. Subsequently, when exposed to pathogen effectors, plants activate these dormant signalling proteins more efficiently in primed cells than in non-primed cells, leading to a stronger and more robust response.

For T4, instead, the plant appears able to detect and mount a strong defence directly against the pathogen, even without prior EF priming, as demonstrated by the 72- and 51-fold change value in the positive control for STS1 and MYB14, respectively.

It is therefore possible that, differently from B05.10, the T4 strain is less effective in suppressing or evading grapevine defence responses, although it is still able to complete the infection with a milder infection strategy, as demonstrated by the 12dpi sporulation results.

The lower priming effect observed for T4 may therefore suggest a distinct way in which the grapevine *cv. Trincadeira* recognises and responds to the two *B. cinerea* strains, even when exposed only to EF stimulation. At the same time, considering the different infection strategy of the two strains, it is also plausible that the plant does not need to rely on stilbene-mediated defence when previously primed against T4.

Similar results observed in B05.10 have been described in *Vitis vinifera*, treated with laminarin or chitosan oligomers, where an early STS1 stimulation before the pathogen confers protection, whereas unprimed infections elicit a delayed stilbene burst that does not stop the infection progression [218], [219].

Finally, *VvJAR1* was analysed. At 0 hpi, the gene was downregulated in all samples except T4 positive controls, where it remained at a basal level. By 6 hpi, all treatments (infected post-priming or primed and infected controls) showed an increase, reaching the top at 30 hpi (2-fold change), before declining again at 54 hpi. However, in this gene, primed and infection controls seem to follow the same trend. This contrasts with the preliminary tomato results, where *SlJAR1* was maintained or upregulated in the EF samples but downregulated in the infected samples. Here, the early down-regulation may reflect a transient suppression of the JA-Ile synthesis, maybe by a possible activation of the SA pathway in a first phase, or a remodulation of the hormonal crosstalk between SA-JA and ET [220], [221]. Another hypothesis could be that the grapevine kept the specific JA pathway in a low-cost and suppressed mode, in this first phase of interaction, as the gene expression seems to be the same between the EF and the real infection. This would allow the plant to rapidly activate the pathway when the infection and the damage really occur, confirmed by the fact that other pathways as stilbene biosynthesis, are instead activated [222]. An additional hypothesis could be that the pathogen suppressed or kept at basal levels in the first hours JA signalling, as a stealth infection mechanism, thanks to some molecules present in the EF. Fungal small RNAs are described to ride EVs to enter plant cells [76], [212], and at the same time, *B. cinerea* is described to suppress plant defence genes by cross-kingdom RNAi [212]. These results could suggest a different defence strategy used by the plants for the JA-Ile pathway activation, as shown from tomato and grapevine results or even suggest again a different infection strategy used by the two strains of *B. cinerea* for different plant species as tomato and grapevine.

Nevertheless, in grapevine, the EF fraction appeared to act as a real priming agent. In the first 54 hours of interaction, the EF gene expression result was totally comparable to the pathogen control result. This would allow, in future, the use of *B. cinerea* extract to better study the molecular patterns involved in plant defence, without damaging the plant.

The differing fold changes in MYB14 and STS1 between B05.10 and T4 demonstrate how EF differentially stimulate the host's responses depending on strain-specific interactions and likely infection strategies. B05.10 appears more suppressive in unprimed conditions, but priming activates higher and stronger stilbene transcription. T4 triggers stronger late responses in unprimed infection control, but priming seems to attenuate the need for a stronger response for this less aggressive strain, contrary to the more aggressive one, suggesting again, even a different infection strategy that could be used by the two pathogens, for the cv. *Trincadeira* (considering the outcome at 12Dpi). In the case of JAR1, EF treatment does not trigger a sustained JA activation, but instead induces brief early peaks, preparing the plant for rapid responses when needed without maintaining prolonged and costly JA signalling.

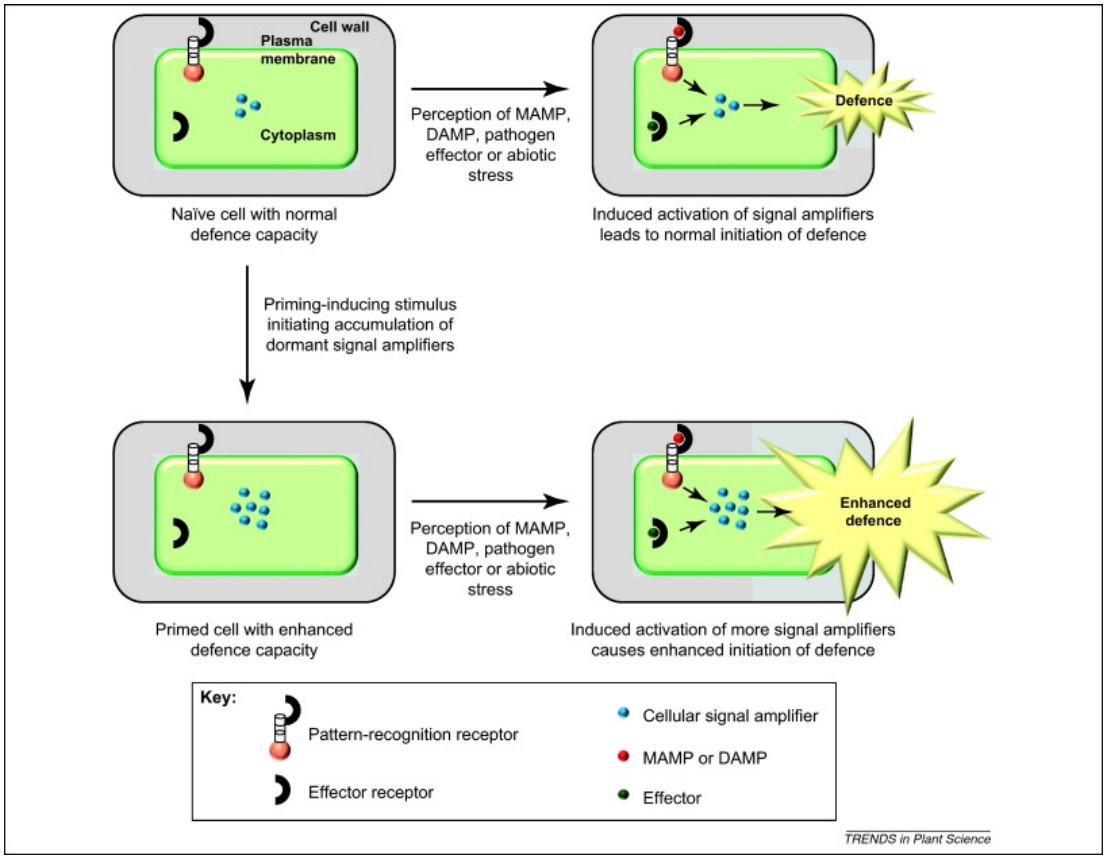

Figura 4.1 Accumulation of dormant cellular signal amplifiers as a possible mechanism of priming in plants. An inducing stimulus as the EF, could enhance the intracellular level of dormant proteins with an important role in cellular signalling amplification. The subsequent exposures to pathogen effectors, PAMPs, abiotic effectors, etc... activate more of these signalling proteins in primed cells than in non-primed cells, enhancing a strong signal amplification and a better defence response. Adapted from Conrath, 2011 [106].

Functionally, EF can pre-arm early signalling, accelerate or amplify stilbene gene activation upon challenge as described for other single-molecule elicitors [216], [218], [219], and reduce symptom development. Rather than a single elicitor, however, our fraction provides a protein-rich, EV-compatible mixture including, as already described, HSPs, UPR proteins as Bip/KAR2 and redox/metabolic proteins.

To further connect the proteomic results with gene expression analysis, we chose to follow the transcription fate of one of the most intriguing proteins identified in our experiments from the most represented cluster. This *B. cinerea* gene *BcKAR2* (A0A384K0D3 / G2YSM3) codes for KAR2, a 73kDa protein part of the HSPs 70 family. KAR2, it's also called ER chaperone BiP. Together with several other ER-

associated proteins, viruses, as well as bacterial and fungal pathogens, target BiP; similarly, overexpression or suppression in any of these proteins has an effect connected to resistance to pathogens of different natures.

While *BcKAR2* protein is not widely described in *B. cinerea,* its central role in controlling the unfolded protein stress response (UPR) on one side and its importance as a target for fungal and bacterial plant pathogens on the other side, makes it a very interesting target to explore. For instance, it has been shown that *Phytoptora capsici* and *P. sojae* express Avh262 in the host, inducing host's BiP stabilisation and subsequent susceptibility to the pathogen; similarly host's BiP overexpression increases susceptibility, while BiP silencing induces resistance to the pathogen in *Nicotiana benthamiana[223]*. Similarly, in *Oryzae sativa,* BiP overexpression compromised resistance to *Xanthomonas oryzae* by interfering with the stability/maturation of the XA21 PRR[224]. In *Solanum Lycopersicum,* instead, BiP silencing compromised resistance to *Verticillum dahliae* by interfering with its receptor-like protein (RLP-PRR) Ve1 [225].

In our experiments, *BcKAR2* expression profiles revealed an interesting peak already 1 hpi, and remained upregulated up to 30 hpi, especially in the T4 strain, and then gradually decreased.

Overexpression of *BcKAR2* and its identification in the EF may represent two sides of the same coin. On one side, it is well known that upon infection, both the host and the pathogen engage in a fight that requires a fit UPR system to sustain defence against the other organism, and BiP in general is central to this in both organisms. Probably the fungus needed a strong hub of UPR to support effectors, energy and secondary metabolic production to prepare the plant environment for the infection at the right moment. On the other side, based on literature data, the identification of *BcKAR2* in the EF may suggest a role in the attack of the host by interfering with the pathogen's detection in a way we have not attempted to characterise yet, due to time constraints, but similar to what is described for the Oomycetes and bacteria described above. Different fold changes between T4 and B05.10 could reflect different infection strategies. B05.10, as the more

aggressive strain, shows a lower KAR2 induction compatible with a lower interference with a putative Vitis' PRR and a consequent stronger STS1 transcriptional activation in all the EF and EF-INF samples, while T4 always showed a lower STS1 activation in all time points, returning to an un-induced state by 30 hpi in the EF sample set. Many other hypotheses are possibly supported by our observations that will be tested in the future.

Finally, the visual observations across all the time points provide clear evidence that this fraction has a biologically meaningful priming effect. At the earliest time point of 6 hours, primed and unprimed leaves appear with no significant differences. However, in positive inoculated controls, the first microscopic signs of tissue lesion and damage started to appear within the first 30 hours, more prominent in the T4 strain. This suggests that T4, as already observed in the tomato experiment, may trigger an earlier oxidative burst, necrosis and higher amount of elicitors even if it's described as less aggressive, but probably more "early acting" [226]. In contrast, primed leaves remain symptom-free. This, again, aligns with the classic model of plant defence priming, where pre-exposure with elicitors or priming agents launch the host into a ready-to-respond state, enhancing resistance involving earlier, faster and/or stronger responses upon pathogen attacks [227].

Between 30 and 54 hpi, especially, differences become more pronounced. Unprimed leaves started to show the first sign of necrosis and lesion expansion, especially in the T4 strain, as described earlier. Primed leaves, by contrast, maintained an intact tissue. This stage probably corresponds to the pathogen's transition into the active necrotrophy phase, starting to secrete CWDE and damaging effectors to facilitate local host cell death, switching from autophagic cell death suppression to induction of regulated cell death and necrotic cell death [41]. The ability of primed leaves to suppress these processes is probably based on the recognition of PAMPs, by PRRs, contained in the EF before the real

presence of the pathogen [114], as suggested by enhanced or better-timed activation of defence genes consistent with the gene expression data.

The most evident contrast is observed at 12 dpi. Positive controls collapsed and showed dense sporulation and spread necrosis all over the leaves in both strains, indicating that the pathogen has completed its reproductive cycle. In primed leaves, however, host tissue integrity was maintained, and no sporulation occurred. This seems to suggest that priming not only delayed symptoms but also prevented disease establishment in the long term. Similar protection, but with reduced lesion progression or disease severity, has been demonstrated in grapevine plants against *Botrytis cinerea*, but using different types of elicitors. A protein-based composition obtained from meat and yeast, oligandrin a 10-kDa protein synthesised by *Phytophthora* and beta-1,3-glucan laminarin derived from algae *Laminaria digitata [228], [229], [230]*.

Under control conditions, T4 shows faster early lesion initiation, while B05.10 leads to more extensive infection and sporulation over a long time. However, despite the differences, EF priming activity enhances leaves' resistance for both T4 (until 54 hpi) and B05.10. This suggests that EF for each strain activates a defensive program that overcomes each specific strategy [126].

5 CONCLUSIONS

In this research work, we aimed to understand how *Botrytis cinerea* senses the surrounding environment and prepares for infection by looking at the very early factors expressed/released on its interface with the environment. Differently from previous literature that looked at filamentous hyphae grown in liquid under agitation after a few days of incubation, we established and applied a different strategy and concentrated our effort on the ungerminated macrospores, the structure used by the pathogen to restart the infection cycle every year. We focused on the largely unexplored contribution of the EF from ungerminated macroconidia with the aim of capturing the very first moment of contact with the environment. This, in fact, is generally a state overlooked in favour of hyphal analyses, providing a novel window on the molecular arsenal deployed at infection onset.

First, we successfully optimised a macrospore shaving method. By carefully controlling incubation conditions to prevent germination and preserve cell viability, we were able to perform trypsin digestion of all the accessible proteins actively or passively released on the external or present on the outer macrospore cell wall surface (exoproteome and surfaceome). In particular, our methodical centrifugations/filtration steps enabled us to obtain fully viable and mostly contaminant-free macroconidia.

This methodological approach enabled the direct capture of molecular players exposed at the surface or directly released into the outside that could be involved in the earliest interaction with the environment and the plant.

Thanks to this method, we were able to demonstrate that ungerminated macroconidia from two differently aggressive *B. cinerea* strains (B05.10 and T4), even after one hour incubation, actively released extracellular vesicles and several proteins. Using NTA and cryo-TEM analysis, we revealed a heterogeneous population of vesicles from 50 to 200 nm, including multilamellar structures and MVBs similar to those described recently to be released from young hyphae, but

here described for the first time as released by the macrospore, similar to what happens in other ascomycetes in the yeast phase. These findings are in line with recent reports of fungal EVs, but extend them to the macrospore stage, highlighting as well that unconventional secretion and vesicle trafficking are mobilised immediately, even in the absence of any germination stimuli. Further studies will be needed, but these observations support the view that the EF fraction could serve as an essential immediate toolbox needed for establishing infection.

By applying a bottom-up proteomic approach to both strains, B05.10 and T4, we revealed a highly conserved core of 80 proteins dominated by chaperons, heat shock proteins, glycolytic enzymes and several metabolic effectors. In silico analyses and related predictors further indicate a potential metabolic activity, even in anticipation of a possible environmental contact, suggesting non-conventional export routes (by the low number of proteins endowed of a signal peptide), consistent with EV-mediated trafficking. The existence of such a conserved exoproteome and surfaceome backbone suggests and highlights that *B. cinerea* could use a stable set of proteins that could represent a universal "toolkit" for early perception and interaction with diverse hosts.

Furthermore, several of these proteins were also recently identified by Sing S. et al. (2025) from *in vivo* infection analysis, further confirming that our approach at least partially mimics real life [52].

The functional dimension of this work was also explored by testing the immunomodulatory activity of the EF on two model plant systems, such as tomato and grapevine. In tomato, the detached leaf assay demonstrated that EF from both strains activate key marker genes of plant immunity with similarities and differences with respect to the pathogen. Gene associated with pathogen-triggered immunity and jasmonic acid signalling, all respond to EF exposure, confirming that EF proteins are recognised as elicitors.

In grapevine, pre-treatment with EF revealed an even more interesting effect. The stilbene biosynthesis gene and the MYB14 transcription factor were both induced, especially in the presence of the B05.10 EF fraction. These gene expression patterns correlated with no necrotic lesion after challenge inoculation in both strains at 12 days post-infection (T4 results not shown), suggesting that EF not only primes host defence but also confers a degree of protection against subsequent infection.

Considering EF's capability to prime plant immunity, we hypothesise that the proteins released very early by *B. cinerea*, even in a non-stimulating environment, after 1 hour incubation, are probably double-edged molecules.

From the host perspective, we demonstrated how this fraction put in contact with the host could act as an elicitor stimulating defence in two different plant species (WRKY1, PTI5, MYB14 and STS1). From the pathogen perspective, instead, these proteins could also be essential for establishing the right extracellular environment to spread, penetrate and initiate infection, as clearly demonstrated by the discovery that six of the proteins described in our work have been previously identified as covering different essential roles needed for infection by studying KO mutants or similar. Anyway, the true infection happens only when, after the first wave of effectors released by the pathogen, is followed by another or more waves of effectors and enzymes continuously released during the host-pathogen battle. This duality underlines a probable central role of these proteins in the outcome of the interaction. They may be indispensable for pathogenesis, but at the same time, they expose the pathogen to recognition. Further studies are needed to better understand the complex interaction between *B. cinerea* and the plant host, in the early phase of the interaction, and to better characterise the molecular patterns that are activated by the EF.

With this idea, it was interesting the identification of *BcKAR2*, a Bip-like HSP70 chaperone, within the highly conserved protein core. The extracellular presence of this protein, central to UPR in fungi, could suggest a hypothesis: fungal Bip protein might be internalised or perceived by the host cells, in some way

perturbing ER homeostasis. Such interference could mimic or overload the host's own Bip network, effectively modulating UPR capacity and weakening the plant defence. Comparable strategies are known in viruses, bacteria and oomycetes.

In conclusion, in the complex battles against pathogenic fungi such as *B. cinerea*, our study highlighted an interesting central role of the EF in *B. cinerea* pathogenicity, revealing it as both conserved and rich in modulators of plant immunity. By illuminating early infection processes, this study opens a new window on the plant-pathogen interaction too often not considered. Rather than being just a list of proteins, the EF appears as a dynamic system at the core of the ongoing battle between plants and pathogens. Beyond its immediate findings, this thesis contributes to the debate on how even necrotrophic pathogens rely on a molecular dialogue at the host surface.

Understanding the EF activity also opens new opportunities to design new environmentally friendly agrochemicals that can target pathogen plant interactions.

6 References

[1] R. J. Bennett and B. G. Turgeon, " Fungal Sex: The Ascomycota ," *Microbiol Spectr*, vol. 4, no. 5, Oct. 2016, doi: 10.1128/microbiolspec.funk-0005-2016.

[2] T. N. Taylor, H. Hass, H. Kerp, M. Krings, and R. T. Hanlin, "Perithecial ascomycetes from the 400 million year old Rhynie chert: an example of ancestral polymorphism," 2017, doi: 10.1080/15572536.2006.11832862.

[3] D. Liu, "Classification of medically important fungi," *Molecular Medical Microbiology, Third Edition*, pp. 2763–2777, Jan. 2024, doi: 10.1016/B978-0-12-818619-0.00034-4.

[4] J. W. Bennett, "Mycotechnology: the role of fungi in biotechnology," *J Biotechnol*, vol. 66, no. 2–3, pp. 101–107, Dec. 1998, doi: 10.1016/S0168-1656(98)00133-3.

[5] J. W. Bennett and M. Klich, "Mycotoxins," *Encyclopedia of Microbiology, Third Edition*, pp. 559–565, Jan. 2009, doi: 10.1016/B978-012373944-5.00333-3.

[6] N. A. Sahasrabudhe and N. V. Sankpal, "Production of organic acids and metabolites of fungi for food industry," *Applied Mycology and Biotechnology*, vol. 1, no. C, pp. 387–425, Jan. 2001, doi: 10.1016/S1874-5334(01)80016-2.

[7] S. Honda *et al.*, "Establishment of Neurospora crassa as a model organism for fungal virology", doi: 10.1038/s41467-020-19355-y.

[8] M. D. Bolton, B. P. H. J. Thomma, and B. D. Nelson, "Sclerotinia sclerotiorum (Lib.) de Bary: biology and molecular traits of a cosmopolitan pathogen," *Mol Plant Pathol*, vol. 7, no. 1, pp. 1–16, Jan. 2006, doi: 10.1111/J.1364-3703.2005.00316.X.

[9] C. G. Pressete *et al.*, "Sclerotinia Sclerotiorum (White Mold): Cytotoxic, Mutagenic, and Antimalarial Effects In Vivo and In Vitro," *J Food Sci*, vol. 84, no. 12, pp. 3866–3875, Dec. 2019, doi: 10.1111/1750-3841.14910.

[10] J. Tan, H. Zhao, J. Li, Y. Gong, and X. Li, "The Devastating Rice Blast Airborne Pathogen Magnaporthe oryzae—A Review on Genes Studied with Mutant Analysis," *Pathogens*, vol. 12, no. 3, p. 379, Mar. 2023, doi: 10.3390/PATHOGENS12030379/S1.

[11] Z. Caracuel-Rios and N. J. Talbot, "Cellular differentiation and host invasion by the rice blast fungus Magnaporthe grisea," *Curr Opin Microbiol*, vol. 10, no. 4, pp. 339–345, Aug. 2007, doi: 10.1016/j.mib.2007.05.019.

[12] Te Beest, "Rice Blast," *The Plant Health Instructor*, 2007, doi: 10.1094/PHI-I-2007-0313-07.

[13] W. Sakulkoo *et al.*, "A single fungal MAP kinase controls plant cell-to-cell invasion by the rice blast fungus," *Science (1979)*, vol. 359, no. 6382, pp. 1399–1403, Mar. 2018, doi: 10.1126/SCIENCE.AAQ0892/SUPPL_FILE/AAQ0892S5.MP4.

[14] E. Oliveira-Garcia, X. Yan, M. Oses-Ruiz, S. de Paula, and N. J. Talbot, “Effector-triggered susceptibility by the rice blast fungus Magnaporthe oryzae,” *New Phytol*, vol. 241, no. 3, pp. 1007–1020, Feb. 2024, doi: 10.1111/NPH.19446.
[15] M. Li, R. Yu, X. Bai, H. Wang, and H. Zhang, “Fusarium: a treasure trove of bioactive secondary metabolites,” *Nat Prod Rep*, vol. 37, no. 12, pp. 1568–1588, Dec. 2020, doi: 10.1039/D0NP00038H.
[16] L. J. Ma *et al.*, “Fusarium pathogenomics,” *Annu Rev Microbiol*, vol. 67, pp. 399–416, Sep. 2013, doi: 10.1146/ANNUREV-MICRO-092412-155650.
[17] J. A. L. van Kan, “Licensed to kill: the lifestyle of a necrotrophic plant pathogen,” *Trends Plant Sci*, vol. 11, no. 5, pp. 247–253, May 2006, doi: 10.1016/J.TPLANTS.2006.03.005.
[18] R. Dean *et al.*, “The Top 10 fungal pathogens in molecular plant pathology,” *Mol Plant Pathol*, vol. 13, no. 4, pp. 414–430, May 2012, doi: 10.1111/J.1364-3703.2011.00783.X.
[19] Y. Elad, M. Vivier, and S. Fillinger, “Botrytis, the Good, the Bad and the Ugly,” *Botrytis - The Fungus, the Pathogen and its Management in Agricultural Systems*, pp. 1–15, Jan. 2016, doi: 10.1007/978-3-319-23371-0_1.
[20] P. L. T U D Z Y N S K I and A. N. D J A N A L Va N K A N, “Botrytis cinerea : the cause of grey mould disease,” *Mol Plant Pathol*, vol. 8, no. 5, pp. 561–580, 2007, doi: 10.1111/J.1364-3703.2007.00417.X.
[21] R. Dean *et al.*, “The Top 10 fungal pathogens in molecular plant pathology,” 2012, doi: 10.1111/J.1364-3703.2011.00783.X.
[22] H. Da *et al.*, “From Genes to Molecules, Secondary Metabolism in Botrytis cinerea: New Insights into Anamorphic and Teleomorphic Stages,” 2023, doi: 10.3390/plants12030553.
[23] G. Holz, S. Coertze, and B. Williamson, “The Ecology of Botrytis on Plant Surfaces,” *Botrytis: Biology, Pathology and Control*, pp. 9–27, 2007, doi: 10.1007/978-1-4020-2626-3_2.
[24] Y. Fukumori, M. Nakajima, and K. Akutsu, “Microconidia act the role as spermatia in the sexual reproduction of Botrytis cinerea,” *FUNGAL DISEASES J Gen Plant Pathol*, vol. 70, pp. 256–260, 2004, doi: 10.1007/s10327-004-0124-9.
[25] Z. M. Haile *et al.*, “Molecular analysis of the early interaction between the grapevine flower and Botrytis cinerea reveals that prompt activation of specific host pathways leads to fungus quiescence,” *Plant Cell Environ*, vol. 40, no. 8, pp. 1409–1428, Aug. 2017, doi: 10.1111/pce.12937.
[26] E. N. K. Sowley, M. W. Shaw, and F. M. Dewey, “Persistent, symptomless, systemic, and seed-borne infection of lettuce by Botrytis cinerea,” *Eur J Plant Pathol*, vol. 126, no. 1, pp. 61–71, Jan. 2010, doi: 10.1007/S10658-009-9524-1/METRICS.
[27] J. Karkowska-Kuleta and A. Kozik, “Cell wall proteome of pathogenic fungi,” 2015, *Polskie Towarzystwo Biochemiczne*. doi: 10.18388/abp.2015_1032.

[28] A. Beauvais and J. P. Latgé, “Special issue: Fungal cell wall,” Sep. 01, 2018, *MDPI AG*. doi: 10.3390/jof4030091.
[29] D. Cantu, L. Carl Greve, J. M. Labavitch, and A. L. T. Powell, “Characterization of the cell wall of the ubiquitous plant pathogen Botrytis cinerea,” *Mycol Res*, vol. 113, no. 12, pp. 1396–1403, Dec. 2009, doi: 10.1016/J.MYCRES.2009.09.006.
[30] E. Liñeiro, C. Chiva, J. M. Cantoral, E. Sabidó, and F. J. Fernández-Acero, “Modifications of fungal membrane proteins profile under pathogenicity induction: A proteomic analysis of Botrytis cinerea membranome,” *Proteomics*, vol. 16, no. 17, pp. 2363–2376, Sep. 2016, doi: 10.1002/PMIC.201500496.
[31] A. Escobar-Niño *et al.*, “Proteomic study of the membrane components of signalling cascades of Botrytis cinerea controlled by phosphorylation,” *Sci Rep*, vol. 9, no. 1, p. 9860, Dec. 2019, doi: 10.1038/S41598-019-46270-0.
[32] F. Fan *et al.*, “Mitochondrial Inner Membrane ABC Transporter Bcmdl1 Is Involved in Conidial Germination, Virulence, and Resistance to Anilinopyrimidine Fungicides in Botrytis cinerea,” *Microbiol Spectr*, vol. 11, no. 4, Aug. 2023, doi: 10.1128/SPECTRUM.00108-23.
[33] J. Tang *et al.*, “The Gβ-like protein Bcgbl1 regulates development and pathogenicity of the gray mold Botrytis cinerea via modulating two MAP kinase signaling pathways,” *PLoS Pathog*, vol. 19, no. 12, Dec. 2023, doi: 10.1371/JOURNAL.PPAT.1011839.
[34] G. Wang, J. Zou, Y. Wang, W. Liang, and D. Li, “The small GTPase BcSec4 is involved in conidiophore development, membrane integrity, and autophagy in Botrytis cinerea,” *Phytopathology Research*, vol. 4, no. 1, pp. 1–13, Dec. 2022, doi: 10.1186/S42483-022-00131-3/FIGURES/8.
[35] C. P. Kubicek, T. L. Starr, and N. L. Glass, “Plant cell wall-degrading enzymes and their secretion in plant-pathogenic fungi,” *Annu Rev Phytopathol*, vol. 52, no. Volume 52, 2014, pp. 427–451, Aug. 2014, doi: 10.1146/ANNUREV-PHYTO-102313-045831/CITE/REFWORKS.
[36] J. Ruiz-Herrera, M. Victoria Elorza, E. Valentín, and R. Sentandreu, “Molecular organization of the cell wall of Candida albicans and its relation to pathogenicity,” *FEMS Yeast Res*, vol. 6, no. 1, pp. 14–29, Jan. 2006, doi: 10.1111/J.1567-1364.2005.00017.X.
[37] P. W. J. de Groot, K. J. Hellingwerf, and F. M. Klis, “Genome-wide identification of fungal GPI proteins,” *Yeast*, vol. 20, no. 9, pp. 781–796, Jul. 2003, doi: 10.1002/YEA.1007.
[38] R. Garcia-Rubio, H. C. de Oliveira, J. Rivera, and N. Trevijano-Contador, “The Fungal Cell Wall: Candida, Cryptococcus, and Aspergillus Species,” *Front Microbiol*, vol. 10, p. 492056, Jan. 2020, doi: 10.3389/FMICB.2019.02993/XML.
[39] M. Choquer *et al.*, “Botrytis cinerea virulence factors: new insights into a necrotrophic and polyphageous pathogen,” *FEMS Microbiol Lett*, vol. 277, no. 1, pp. 1–10, Dec. 2007, doi: 10.1111/J.1574-6968.2007.00930.X.

[40] M. E. Saint-Macary *et al.*, “Methionine biosynthesis is essential for infection in the rice blast fungus Magnaporthe oryzae,” *PLoS One*, vol. 10, no. 4, Apr. 2015, doi: 10.1371/JOURNAL.PONE.0111108.
[41] K. Bi, Y. Liang, T. Mengiste, and A. Sharon, “Killing softly: a roadmap of Botrytis cinerea pathogenicity,” *Trends Plant Sci*, vol. 28, no. 2, pp. 211–222, Feb. 2023, doi: 10.1016/J.TPLANTS.2022.08.024.
[42] C. González, N. Brito, and A. Sharon, “Infection Process and Fungal Virulence Factors,” *Botrytis - The Fungus, the Pathogen and its Management in Agricultural Systems*, pp. 229–246, Jan. 2016, doi: 10.1007/978-3-319-23371-0_12.
[43] G. Doehlemann, B. Ökmen, W. Zhu, and A. Sharon, “Plant Pathogenic Fungi,” *The Fungal Kingdom*, pp. 701–726, Sep. 2017, doi: 10.1128/9781555819583.CH34.
[44] H. da Silva Ripardo-Filho, V. Coca Ruíz, I. Suárez, J. Moraga, J. Aleu, and I. G. Collado, “From Genes to Molecules, Secondary Metabolism in Botrytis cinerea: New Insights into Anamorphic and Teleomorphic Stages,” *Plants 2023, Vol. 12, Page 553*, vol. 12, no. 3, p. 553, Jan. 2023, doi: 10.3390/PLANTS12030553.
[45] G. Billon-Grand, C. Rascle, M. Droux, J. A. Rollins, and N. Poussereau, “pH modulation differs during sunflower cotyledon colonization by the two closely related necrotrophic fungi Botrytis cinerea and Sclerotinia sclerotiorum,” *Mol Plant Pathol*, vol. 13, no. 6, pp. 568–578, Aug. 2012, doi: 10.1111/J.1364-3703.2011.00772.X.
[46] N. Müller *et al.*, “Investigations on VELVET regulatory mutants confirm the role of host tissue acidification and secretion of proteins in the pathogenesis of Botrytis cinerea,” *New Phytol*, vol. 219, no. 3, pp. 1062–1074, Aug. 2018, doi: 10.1111/NPH.15221.
[47] M. Breitenbach, M. Weber, M. Rinnerthaler, T. Karl, and L. Breitenbach-Koller, “Oxidative Stress in Fungi: Its Function in Signal Transduction, Interaction with Plant Hosts, and Lignocellulose Degradation,” *Biomolecules*, vol. 5, no. 2, p. 318, Apr. 2015, doi: 10.3390/BIOM5020318.
[48] W. H. Chung, “Unraveling new functions of superoxide dismutase using yeast model system: Beyond its conventional role in superoxide radical scavenging,” *J Microbiol*, vol. 55, no. 6, pp. 409–416, Jun. 2017, doi: 10.1007/S12275-017-6647-5.
[49] J. López-Cruz, C. S. Óscar, F. C. Emma, G. A. Pilar, and G. B. Carmen, “Absence of Cu–Zn superoxide dismutase BCSOD1 reduces Botrytis cinerea virulence in Arabidopsis and tomato plants, revealing interplay among reactive oxygen species, callose and signalling pathways,” *Mol Plant Pathol*, vol. 18, no. 1, pp. 16–31, Jan. 2017, doi: 10.1111/MPP.12370.
[50] G. Gullner, T. Komives, L. Király, and P. Schröder, “Glutathione S-Transferase Enzymes in Plant-Pathogen Interactions,” *Front Plant Sci*, vol. 9, p. 1836, 2018, doi: 10.3389/FPLS.2018.01836.

[51] A. Escobar-Niño, R. Carrasco-Reinado, I. M. Morano, J. M. Cantoral, and F. J. Fernandez-Acero, “Unravelling the initial triggers of Botrytis cinerea infection: First description of its surfactome,” *Journal of Fungi*, vol. 7, no. 12, p. 1021, Dec. 2021, doi: 10.3390/JOF7121021/S1.

[52] S. Singh, M. Hegde, I. Kaur, and N. Adlakha, “Temporal proteome profiling of Botrytis cinerea reveals proteins involved in plant invasion and survival,” *Scientific Reports 2025 15:1*, vol. 15, no. 1, pp. 1–11, Apr. 2025, doi: 10.1038/s41598-025-92683-5.

[53] K. Liu *et al.*, “Identification of virulence-related proteins during Botrytis cinerea – fruit interaction at early phase,” *Postharvest Biol Technol*, vol. 204, p. 112443, Oct. 2023, doi: 10.1016/J.POSTHARVBIO.2023.112443.

[54] J. J. Espino, G. Gutiérrez-Sánchez, N. Brito, P. Shah, R. Orlando, and C. González, “The Botrytis cinerea early secretome,” *Proteomics*, vol. 10, no. 16, pp. 3020–3034, Aug. 2010, doi: 10.1002/PMIC.201000037.

[55] P. Shah, J. A. Atwood, R. Orlando, H. El Mubarek, G. K. Podila, and M. R. Davis, “Comparative proteomic analysis of botrytis cinerea secretome,” *J Proteome Res*, vol. 8, no. 3, pp. 1123–1130, Mar. 2009, doi: 10.1021/pr8003002.

[56] C. Viotti, “ER to Golgi-Dependent Protein Secretion: The Conventional Pathway,” *Methods Mol Biol*, vol. 1459, pp. 3–29, Sep. 2016, doi: 10.1007/978-1-4939-3804-9_1.

[57] R. González-Fernández, J. Valero-Galván, F. J. Gómez-Gálvez, and J. V. Jorrín-Novo, “Unraveling the in vitro secretome of the phytopathogen Botrytis cinerea to understand the interaction with its hosts,” *Front Plant Sci*, vol. 6, no. OCTOBER, p. 151048, Oct. 2015, doi: 10.3389/FPLS.2015.00839/BIBTEX.

[58] M. C. Giraldo and B. Valent, “Filamentous plant pathogen effectors in action,” *Nat Rev Microbiol*, vol. 11, no. 11, pp. 800–814, Nov. 2013, doi: 10.1038/NRMICRO3119.

[59] M. Tang *et al.*, “Establishment of a Mutant Library for Infection Cushion Development and Identification of a Key Regulatory Gene in Botrytis cinerea,” *Journal of Fungi 2025, Vol. 11, Page 16*, vol. 11, no. 1, p. 16, Dec. 2024, doi: 10.3390/JOF11010016.

[60] A. A. Sakekar, S. R. Gaikwad, and N. S. Punekar, “Protein expression and secretion by filamentous fungi,” *Journal of Biosciences 2021 46:1*, vol. 46, no. 1, pp. 1–18, Feb. 2021, doi: 10.1007/S12038-020-00120-8.

[61] J. M. Wolf, J. Espadas, J. Luque-Garcia, T. Reynolds, and A. Casadevall, “Lipid biosynthetic genes affect Candida albicans extracellular vesicle morphology, cargo, and immunostimulatory properties,” *Eukaryot Cell*, vol. 14, no. 8, pp. 745–754, Aug. 2015, doi: 10.1128/EC.00054-15/FORMAT/EPUB.

[62] V. da S. C. Parreira, L. G. C. Santos, M. L. Rodrigues, and F. Passetti, “ExVe: The knowledge base of orthologous proteins identified in fungal extracellular vesicles,” *Comput Struct Biotechnol J*, vol. 19, pp. 2286–2296, Jan. 2021, doi: 10.1016/j.csbj.2021.04.031.

[63] E. Celińska and J. M. Nicaud, “Filamentous fungi-like secretory pathway strayed in a yeast system: peculiarities of Yarrowia lipolytica secretory pathway underlying its extraordinary performance,” *Appl Microbiol Biotechnol*, vol. 103, no. 1, p. 39, Jan. 2018, doi: 10.1007/S00253-018-9450-2.
[64] R. Kalluri and V. S. LeBleu, “The biology , function , and biomedical applications of exosomes,” *Science*, vol. 367, no. 6478, Feb. 2020, doi: 10.1126/SCIENCE.AAU6977.
[65] Z. Wang *et al.*, “Pathogen-Derived Extracellular Vesicles: Emerging Mediators of Plant-Microbe Interactions,” *Molecular Plant-Microbe Interactions*, vol. 36, no. 4, pp. 218–227, Apr. 2023, doi: 10.1094/MPMI-08-22-0162-FI/ASSET/IMAGES/LARGE/MPMI-08-22-0162-FIF2-1681986242815.JPEG.
[66] M. Mathieu, L. Martin-Jaular, G. Lavieu, and C. Théry, “Specificities of secretion and uptake of exosomes and other extracellular vesicles for cell-to-cell communication,” *Nature Cell Biology 2019 21:1*, vol. 21, no. 1, pp. 9–17, Jan. 2019, doi: 10.1038/s41556-018-0250-9.
[67] J. C. Akers, D. Gonda, R. Kim, B. S. Carter, and C. C. Chen, “Biogenesis of extracellular vesicles (EV): Exosomes, microvesicles, retrovirus-like vesicles, and apoptotic bodies,” *J Neurooncol*, vol. 113, no. 1, pp. 1–11, May 2013, doi: 10.1007/S11060-013-1084-8/METRICS.
[68] B. D. Rutter, T. T. H. Chu, J. F. Dallery, K. K. Zajt, R. J. O’Connell, and R. W. Innes, “The development of extracellular vesicle markers for the fungal phytopathogen Colletotrichum higginsianum,” *J Extracell Vesicles*, vol. 11, no. 5, p. e12216, May 2022, doi: 10.1002/JEV2.12216.
[69] M. R. Bleackley *et al.*, “Extracellular Vesicles From the Cotton Pathogen Fusarium oxysporum f. sp. vasinfectum Induce a Phytotoxic Response in Plants,” *Front Plant Sci*, vol. 10, p. 488444, Jan. 2020, doi: 10.3389/FPLS.2019.01610/BIBTEX.
[70] D. Garcia-Ceron, M. R. Bleackley, and M. A. Anderson, “Fungal Extracellular Vesicles in Pathophysiology,” *Subcell Biochem*, vol. 97, pp. 151–177, 2021, doi: 10.1007/978-3-030-67171-6_7.
[71] D. Garcia-Ceron *et al.*, “Extracellular vesicles from fusarium graminearum contain protein effectors expressed during infection of corn,” *Journal of Fungi*, vol. 7, no. 11, p. 977, Nov. 2021, doi: 10.3390/JOF7110977/S1.
[72] S. Kwon *et al.*, “Mrna inventory of extracellular vesicles from ustilago maydis,” *Journal of Fungi*, vol. 7, no. 7, p. 562, Jul. 2021, doi: 10.3390/JOF7070562/S1.
[73] A. De Vallée *et al.*, “Extracellular Vesicles of the Plant Pathogen Botrytis cinerea,” *Journal of Fungi*, vol. 9, no. 4, Apr. 2023, doi: 10.3390/jof9040495.
[74] A. Escobar-Niño, A. Harzen, S. C. Stolze, H. Nakagami, and F. J. Fernández-Acero, “The Adaptation of Botrytis cinerea Extracellular Vesicles Proteome to Surrounding Conditions: Revealing New Tools for Its

Infection Process," *Journal of Fungi*, vol. 9, no. 9, Sep. 2023, doi: 10.3390/jof9090872.
[75] A. Escobar-Niño, A. Harzen, S. C. Stolze, H. Nakagami, and F. J. Fernández-Acero, "The Adaptation of Botrytis cinerea Extracellular Vesicles Proteome to Surrounding Conditions: Revealing New Tools for Its Infection Process," *Journal of Fungi*, vol. 9, no. 9, Sep. 2023, doi: 10.3390/jof9090872.
[76] B. He *et al.*, "Fungal small RNAs ride in extracellular vesicles to enter plant cells through clathrin-mediated endocytosis," *Nat Commun*, vol. 14, no. 1, Dec. 2023, doi: 10.1038/s41467-023-40093-4.
[77] A. Weiberg *et al.*, "Fungal small RNAs suppress plant immunity by hijacking host RNA interference pathways," *Science*, vol. 342, no. 6154, pp. 118–123, Oct. 2013, doi: 10.1126/SCIENCE.1239705.
[78] J. Armengaud, J. A. Christie-Oleza, G. Clair, V. Malard, and C. Duport, "Exoproteomics: Exploring the world around biological systems," Oct. 2012. doi: 10.1586/epr.12.52.
[79] D. E. Levin, "Regulation of Cell Wall Biogenesis in Saccharomyces cerevisiae: The Cell Wall Integrity Signaling Pathway," *Genetics*, vol. 189, no. 4, pp. 1145–1175, Dec. 2011, doi: 10.1534/GENETICS.111.128264.
[80] A. Gil-Bona *et al.*, "Candida albicans cell shaving uncovers new proteins involved in cell wall integrity, yeast to hypha transition, stress response and host–pathogen interaction," *J Proteomics*, vol. 127, pp. 340–351, Sep. 2015, doi: 10.1016/J.JPROT.2015.06.006.
[81] W. Zhang, B. B. Ge, Z. Y. Lv, K. S. Park, L. M. Shi, and K. C. Zhang, "Membrane Protein Bcest Is Involved in Hyphal Growth, Virulence and Stress Tolerance of Botrytis cinerea," *Microorganisms*, vol. 11, no. 5, May 2023, doi: 10.3390/microorganisms11051225.
[82] A. Olaya-Abril, L. Gómez-Gascón, I. Jiménez-Munguía, I. Obando, and M. J. Rodríguez-Ortega, "Another turn of the screw in shaving Gram-positive bacteria: Optimization of proteomics surface protein identification in Streptococcus pneumoniae," *J Proteomics*, vol. 75, no. 12, pp. 3733–3746, Jun. 2012, doi: 10.1016/J.JPROT.2012.04.037.
[83] E. Marín *et al.*, "Candida albicans Shaving to Profile Human Serum Proteins on Hyphal Surface," *Front Microbiol*, vol. 6, no. DEC, p. 1343, 2015, doi: 10.3389/FMICB.2015.01343.
[84] M. R. Insenser, M. L. Hernáez, C. Nombela, M. Molina, G. Molero, and C. Gil, "Gel and gel-free proteomics to identify Saccharomyces cerevisiae cell surface proteins," *J Proteomics*, vol. 73, no. 6, pp. 1183–1195, Apr. 2010, doi: 10.1016/J.JPROT.2010.02.005.
[85] M. L. Hernáez, P. Ximénez-Embún, M. Martínez-Gomariz, M. D. Gutiérrez-Blázquez, C. Nombela, and C. Gil, "Identification of Candida albicans exposed surface proteins in vivo by a rapid proteomic approach," *J Proteomics*, vol. 73, no. 7, pp. 1404–1409, May 2010, doi: 10.1016/j.jprot.2010.02.008.

[86] S. Esteves, I. Costa, S. Luelmo, N. Santarém, and A. Cordeiro-Da-Silva, “microorganisms Leishmania Vesicle-Depleted Exoproteome: What, Why, and How?,” 2022, doi: 10.3390/microorganisms10122435.
[87] R. González-Fernández, K. Aloria, J. Valero-Galván, I. Redondo, J. M. Arizmendi, and J. V. Jorrín-Novo, “Proteomic analysis of mycelium and secretome of different Botrytis cinerea wild-type strains,” *J Proteomics*, vol. 97, pp. 195–221, Jan. 2014, doi: 10.1016/J.JPROT.2013.06.022.
[88] R. González-Fernández, J. Valero-Galván, F. J. Gómez-Gálvez, and J. V. Jorrín-Novo, “Unraveling the in vitro secretome of the phytopathogen Botrytis cinerea to understand the interaction with its hosts,” *Front Plant Sci*, vol. 6, no. OCTOBER, p. 151048, Oct. 2015, doi: 10.3389/FPLS.2015.00839/BIBTEX.
[89] R. Singh, C. Caseys, and D. J. Kliebenstein, “Genetic and molecular landscapes of the generalist phytopathogen Botrytis cinerea,” *Mol Plant Pathol*, vol. 25, no. 1, p. e13404, Jan. 2024, doi: 10.1111/MPP.13404.
[90] J. Veloso and J. A. L. van Kan, “Many Shades of Grey in Botrytis-Host Plant Interactions.,” *Trends Plant Sci*, vol. 23, no. 7, pp. 613–622, Apr. 2018, doi: 10.1016/J.TPLANTS.2018.03.016.
[91] Z. Li, R. Wu, F. Guo, Y. Wang, P. Nick, and X. Wang, “Advances in the molecular mechanism of grapevine resistance to fungal diseases,” *Molecular Horticulture 2025 5:1*, vol. 5, no. 1, pp. 1–19, Jan. 2025, doi: 10.1186/S43897-024-00119-X.
[92] “Agri-environmental indicator - consumption of pesticides - Statistics Explained - Eurostat.” Accessed: Aug. 27, 2025. [Online]. Available: https://ec.europa.eu/eurostat/statistics-explained/index.php?title=Agri-environmental_indicator_-_consumption_of_pesticides
[93] “Pesticides use and trade,” 1990, Accessed: Aug. 27, 2025. [Online]. Available: http://www.fao.org/faostat/en/#data/RP.
[94] “EU trends in the use and risk of chemical pesticides (Indicator) | European zero pollution dashboards.” Accessed: Aug. 27, 2025. [Online]. Available: https://www.eea.europa.eu/en/european-zero-pollution-dashboards/indicators/eu-trends-in-the-use-and-risk-of-chemical-pesticides
[95] “STATE OF THE WORLD VINE AND WINE SECTOR IN 2023”.
[96] “Vino italiano: 2024 da record nelle esportazioni, a 8,1 miliardi di euro (+5,5% sul 2023) - WineNews.” Accessed: Aug. 28, 2025. [Online]. Available: https://winenews.it/it/vino-italiano-2024-da-record-nelle-esportazioni-a-81-miliardi-di-euro-55-sul-2023_551770/?utm_source=chatgpt.com
[97] K. E. Hammond-Kosack and J. E. Parker, “Deciphering plant–pathogen communication: fresh perspectives for molecular resistance breeding,” *Curr Opin Biotechnol*, vol. 14, no. 2, pp. 177–193, Apr. 2003, doi: 10.1016/S0958-1669(03)00035-1.

[98] M. El Oirdi *et al.*, “Botrytis cinerea Manipulates the Antagonistic Effects between Immune Pathways to Promote Disease Development in Tomato C W OA,” 2011, doi: 10.1105/tpc.111.083394.
[99] S. Tian *et al.*, “Unraveling the Molecular Mechanisms of Tomatoes’ Defense against Botrytis cinerea: Insights from Transcriptome Analysis of Micro-Tom and Regular Tomato Varieties,” 2023, doi: 10.3390/plants12162965.
[100] P. A. G. Elmer and T. J. Michailides, “Epidemiology of Botrytis cinerea in Orchard and Vine Crops,” *Botrytis: Biology, Pathology and Control*, pp. 243–272, 2007, doi: 10.1007/978-1-4020-2626-3_14.
[101] D. Prusky, N. Alkan, T. Mengiste, and R. Fluhr, “Quiescent and necrotrophic lifestyle choice during postharvest disease development,” *Annu Rev Phytopathol*, vol. 51, no. Volume 51, 2013, pp. 155–176, Aug. 2013, doi: 10.1146/ANNUREV-PHYTO-082712-102349/CITE/REFWORKS.
[102] M. Kabbage, B. Williams, and M. B. Dickman, “Cell death control: the interplay of apoptosis and autophagy in the pathogenicity of Sclerotinia sclerotiorum,” *PLoS Pathog*, vol. 9, no. 4, Apr. 2013, doi: 10.1371/JOURNAL.PPAT.1003287.
[103] N. Shlezinger *et al.*, “Anti-apoptotic machinery protects the necrotrophic fungus Botrytis cinerea from host-induced apoptotic-like cell death during plant infection,” *PLoS Pathog*, vol. 7, no. 8, Aug. 2011, doi: 10.1371/JOURNAL.PPAT.1002185.
[104] J. Guo and Y. Cheng, “Advances in Fungal Elicitor-Triggered Plant Immunity,” *Int J Mol Sci*, vol. 23, no. 19, p. 12003, Oct. 2022, doi: 10.3390/IJMS231912003.
[105] J. D. G. Jones and J. L. Dangl, “The plant immune system,” *Nature 2006 444:7117*, vol. 444, no. 7117, pp. 323–329, Nov. 2006, doi: 10.1038/nature05286.
[106] U. Conrath, “Molecular aspects of defence priming,” *Trends Plant Sci*, vol. 16, no. 10, pp. 524–531, Oct. 2011, doi: 10.1016/J.TPLANTS.2011.06.004.
[107] M. Yuan *et al.*, “Pattern-recognition receptors are required for NLR-mediated plant immunity,” *Nature 2021 592:7852*, vol. 592, no. 7852, pp. 105–109, Mar. 2021, doi: 10.1038/s41586-021-03316-6.
[108] B. P. M. Ngou, P. Ding, and J. D. G. Jones, “Thirty years of resistance: Zig-zag through the plant immune system,” *Plant Cell*, vol. 34, no. 5, pp. 1447–1478, May 2022, doi: 10.1093/PLCELL/KOAC041.
[109] A. S. Zvereva and M. M. Pooggin, “Silencing and Innate Immunity in Plant Defense Against Viral and Non-Viral Pathogens,” *Viruses 2012, Vol. 4, Pages 2578-2597*, vol. 4, no. 11, pp. 2578–2597, Oct. 2012, doi: 10.3390/V4112578.
[110] N. Aerts, M. Pereira Mendes, and S. C. M. Van Wees, “Multiple levels of crosstalk in hormone networks regulating plant defense,” *The Plant Journal*, vol. 105, no. 2, p. 489, Jan. 2020, doi: 10.1111/TPJ.15124.

[111] A. Corina Vlot, D. A. Dempsey, and D. F. Klessig, “Salicylic Acid, a multifaceted hormone to combat disease,” *Annu Rev Phytopathol*, vol. 47, pp. 177–206, Sep. 2009, doi: 10.1146/ANNUREV.PHYTO.050908.135202.
[112] J. Kelloniemi *et al.*, “Analysis of the molecular dialogue between gray mold (botrytis cinerea) and grapevine (vitis vinifera) reveals a clear shift in defense mechanisms during berry ripening,” *Molecular Plant-Microbe Interactions*, vol. 28, no. 11, pp. 1167–1180, Nov. 2015, doi: 10.1094/MPMI-02-15-0039-R/SUPPL_FILE/MPMI-02-15-0039-R.ST7.PDF.
[113] N. Li, X. Han, D. Feng, D. Yuan, and L. J. Huang, “Signaling Crosstalk between Salicylic Acid and Ethylene/Jasmonate in Plant Defense: Do We Understand What They Are Whispering?,” *Int J Mol Sci*, vol. 20, no. 3, p. 671, Feb. 2019, doi: 10.3390/IJMS20030671.
[114] C. J. Liao, S. Hailemariam, A. Sharon, and T. Mengiste, “Pathogenic strategies and immune mechanisms to necrotrophs: Differences and similarities to biotrophs and hemibiotrophs,” Oct. 01, 2022, *Elsevier Ltd*. doi: 10.1016/j.pbi.2022.102291.
[115] C. Wasternack and B. Hause, “Jasmonates: biosynthesis, perception, signal transduction and action in plant stress response, growth and development. An update to the 2007 review in Annals of Botany,” *Ann Bot*, vol. 111, no. 6, pp. 1021–1058, Jun. 2013, doi: 10.1093/AOB/MCT067.
[116] A. Guerreiro, J. Figueiredo, M. Sousa Silva, and A. Figueiredo, “Linking jasmonic acid to grapevine resistance against the biotrophic oomycete Plasmopara viticola,” *Front Plant Sci*, vol. 7, no. APR2016, Apr. 2016, doi: 10.3389/FPLS.2016.00565/ABSTRACT.
[117] R. Roychowdhury *et al.*, “Jasmonic Acid (JA) in Plant Immune Response: Unravelling Complex Molecular Mechanisms and Networking of Defence Signalling Against Pathogens,” *J Plant Growth Regul*, vol. 44, no. 1, pp. 89–114, Jan. 2025, doi: 10.1007/S00344-024-11264-4/TABLES/1.
[118] M. Ghorbel, F. Brini, A. Sharma, and M. Landi, “Role of jasmonic acid in plants: the molecular point of view,” *Plant Cell Reports 2021 40:8*, vol. 40, no. 8, pp. 1471–1494, Apr. 2021, doi: 10.1007/S00299-021-02687-4.
[119] L. Fang, Y. Hou, L. Wang, H. Xin, N. Wang, and S. Li, “Myb14, a direct activator of STS, is associated with resveratrol content variation in berry skin in two grape cultivars,” *Plant Cell Rep*, vol. 33, no. 10, pp. 1629–1640, Oct. 2014, doi: 10.1007/s00299-014-1642-3.
[120] J. Höll *et al.*, “The R2R3-MYB transcription factors MYB14 and MYB15 regulate stilbene biosynthesis in Vitis vinifera,” *Plant Cell*, vol. 25, no. 10, pp. 4135–4149, 2013, doi: 10.1105/TPC.113.117127.
[121] F. Caruso *et al.*, “Antifungal activity of resveratrol against Botrytis cinerea is improved using 2-furyl derivatives,” *PLoS One*, vol. 6, no. 10, Oct. 2011, doi: 10.1371/JOURNAL.PONE.0025421.
[122] M. Dubois, L. Van den Broeck, and D. Inzé, “The Pivotal Role of Ethylene in Plant Growth,” *Trends Plant Sci*, vol. 23, no. 4, pp. 311–323, Apr. 2018, doi: 10.1016/J.TPLANTS.2018.01.003/ASSET/590679E3-178C-4C0F-8818-0170A4EA1BAD/MAIN.ASSETS/GR2.JPG.

[123] C. M. J. Pieterse, D. Van Der Does, C. Zamioudis, A. Leon-Reyes, and S. C. M. Van Wees, "Hormonal modulation of plant immunity," *Annu Rev Cell Dev Biol*, vol. 28, pp. 489–521, 2012, doi: 10.1146/ANNUREV-CELLBIO-092910-154055.
[124] B. Mauch-Mani, I. Baccelli, E. Luna, and V. Flors, "Defense Priming: An Adaptive Part of Induced Resistance," *Annu Rev Plant Biol*, vol. 68, pp. 485–512, Apr. 2017, doi: 10.1146/ANNUREV-ARPLANT-042916-041132.
[125] A. Martinez-Medina *et al.*, "Recognizing Plant Defense Priming," *Trends Plant Sci*, vol. 21, no. 10, pp. 818–822, Oct. 2016, doi: 10.1016/J.TPLANTS.2016.07.009.
[126] U. Conrath, G. J. M. Beckers, C. J. G. Langenbach, and M. R. Jaskiewicz, "Priming for Enhanced Defense," *Annu Rev Phytopathol*, vol. 53, no. Volume 53, 2015, pp. 97–119, Aug. 2015, doi: 10.1146/ANNUREV-PHYTO-080614-120132/CITE/REFWORKS.
[127] A. Balmer, V. Pastor, J. Gamir, V. Flors, and B. Mauch-Mani, "The 'primeome': Towards a holistic approach to priming," *Trends Plant Sci*, vol. 20, no. 7, pp. 443–452, Jul. 2015, doi: 10.1016/J.TPLANTS.2015.04.002/ASSET/4AA3B30A-A6F6-4319-B96E-F977E2B41619/MAIN.ASSETS/GR2.JPG.
[128] M. Van Hulten, M. Pelser, L. C. Van Loon, C. M. J. Pieterse, and J. Ton, "Costs and benefits of priming for defense in Arabidopsis," *Proceedings of the National Academy of Sciences*, vol. 103, no. 14, pp. 5602–5607, Apr. 2006, doi: 10.1073/PNAS.0510213103.
[129] S. Gelibter *et al.*, "The impact of storage on extracellular vesicles: A systematic study," *J Extracell Vesicles*, vol. 11, no. 2, Feb. 2022, doi: 10.1002/jev2.12162.
[130] H. Heberle, V. G. Meirelles, F. R. da Silva, G. P. Telles, and R. Minghim, "InteractiVenn: A web-based tool for the analysis of sets through Venn diagrams," *BMC Bioinformatics*, vol. 16, no. 1, pp. 1–7, May 2015, doi: 10.1186/S12859-015-0611-3/FIGURES/4.
[131] L. V. Bozhilova, A. V. Whitmore, J. Wray, G. Reinert, and C. M. Deane, "Measuring rank robustness in scored protein interaction networks," *BMC Bioinformatics*, vol. 20, no. 1, p. 446, Aug. 2019, doi: 10.1186/S12859-019-3036-6.
[132] J. Sperschneider and P. N. Dodds, "EffectorP 3.0: Prediction of Apoplastic and Cytoplasmic Effectors in Fungi and Oomycetes," *Molecular Plant-Microbe Interactions*, vol. 35, no. 2, pp. 146–156, Feb. 2022, doi: 10.1094/MPMI-08-21-0201-R/ASSET/IMAGES/LARGE/MPMI-08-21-0201-RT6-1644488731661.JPEG.
[133] J. Hallgren *et al.*, "DeepTMHMM predicts alpha and beta transmembrane proteins using deep neural networks," *bioRxiv*, p. 2022.04.08.487609, Apr. 2022, doi: 10.1101/2022.04.08.487609.
[134] Y. Mao, H. Fan, and C. Lu, "Immunoproteomic assay of extracellular proteins in Streptococcus equi ssp. zooepidemicus," *FEMS Microbiol Lett*,

vol. 286, no. 1, pp. 103–109, Sep. 2008, doi: 10.1111/J.1574-6968.2008.01259.X.
[135] M. H. Gíslason, H. Nielsen, J. J. Almagro Armenteros, and A. R. Johansen, "Prediction of GPI-anchored proteins with pointer neural networks," *Curr Res Biotechnol*, vol. 3, pp. 6–13, Jan. 2021, doi: 10.1016/J.CRBIOT.2021.01.001.
[136] F. E. El-Rami and A. E. Sikora, "Bioinformatics Workflow for Gonococcal Proteomics," *Methods Mol Biol*, vol. 1997, pp. 185–205, 2019, doi: 10.1007/978-1-4939-9496-0_12.
[137] S. Lu *et al.*, "CDD/SPARCLE: the conserved domain database in 2020," *Nucleic Acids Res*, vol. 48, no. D1, pp. D265–D268, Jan. 2020, doi: 10.1093/NAR/GKZ991.
[138] D. Binns, E. Dimmer, R. Huntley, D. Barrell, C. O'Donovan, and R. Apweiler, "QuickGO: a web-based tool for Gene Ontology searching," *Bioinformatics*, vol. 25, no. 22, pp. 3045–3046, Nov. 2009, doi: 10.1093/BIOINFORMATICS/BTP536.
[139] F. Supek, M. Bošnjak, N. Škunca, and T. Šmuc, "REVIGO Summarizes and Visualizes Long Lists of Gene Ontology Terms," *PLoS One*, vol. 6, no. 7, p. e21800, 2011, doi: 10.1371/JOURNAL.PONE.0021800.
[140] G. Laureano *et al.*, "The interplay between membrane lipids and phospholipase A family members in grapevine resistance against Plasmopara viticola," *Sci Rep*, vol. 8, no. 1, Dec. 2018, doi: 10.1038/S41598-018-32559-Z.
[141] J. Lian, H. Han, J. Zhao, and C. Li, "In-vitro and in-planta Botrytis cinerea Inoculation Assays for Tomato," *Bio Protoc*, vol. 8, no. 8, p. e2810, 2018, doi: 10.21769/BIOPROTOC.2810.
[142] J. Hellemans, G. Mortier, A. De Paepe, F. Speleman, and J. Vandesompele, "qBase relative quantification framework and software for management and automated analysis of real-time quantitative PCR data," *Genome Biol*, vol. 8, no. 2, pp. 1–14, Feb. 2008, doi: 10.1186/GB-2007-8-2-R19/FIGURES/5.
[143] B. Eisenmann *et al.*, "Rpv3-1 mediated resistance to grapevine downy mildew is associated with specific host transcriptional responses and the accumulation of stilbenes," *BMC Plant Biol*, vol. 19, no. 1, pp. 1–17, Aug. 2019, doi: 10.1186/S12870-019-1935-3/TABLES/1.
[144] F. Monteiro, M. Sebastiana, M. S. Pais, and A. Figueiredo, "Reference Gene Selection and Validation for the Early Responses to Downy Mildew Infection in Susceptible and Resistant Vitis vinifera Cultivars," *PLoS One*, vol. 8, no. 9, p. e72998, Sep. 2013, doi: 10.1371/JOURNAL.PONE.0072998.
[145] L. Castillo, V. Plaza, L. F. Larrondo, and P. Canessa, "Recent Advances in the Study of the Plant Pathogenic Fungus Botrytis cinerea and its Interaction with the Environment," *Curr Protein Pept Sci*, vol. 18, no. 10, pp. 976–989, Aug. 2016, doi: 10.2174/1389203717666160809160915/CITE/REFWORKS.

[146] S. N. A. Abdullah and M. S. Akhtar, “Plant and Necrotrophic Fungal Pathogen Interaction: Mechanism and Mode of Action,” *Plant, Soil and Microbes: Volume 1: Implications in Crop Science*, pp. 29–53, Jan. 2016, doi: 10.1007/978-3-319-27455-3_3.
[147] A. De Cal, P. Melgarejo, and M. D. M. Jimenez-Gasco, “Editorial: Necrotrophic Fungal Plant Pathogens,” *Front Plant Sci*, vol. 13, p. 839674, Feb. 2022, doi: 10.3389/FPLS.2022.839674/BIBTEX.
[148] M. J. Rodríguez-Ortega *et al.*, “Characterization and identification of vaccine candidate proteins through analysis of the group A Streptococcus surface proteome,” *Nature Biotechnology 2006 24:2*, vol. 24, no. 2, pp. 191–197, Jan. 2006, doi: 10.1038/nbt1179.
[149] P. T. Wingfield, “Use of Protein Folding Reagents,” *Current protocols in protein science / editorial board, John E. Coligan ... [et al.]*, vol. APPENDIX 3, no. 1, p. Appendix, Jun. 2001, doi: 10.1002/0471140864.PSA03AS00.
[150] G. Fedele, C. Brischetto, and V. Rossi, “Biocontrol of Botrytis cinerea on Grape Berries as Influenced by Temperature and Humidity,” *Front Plant Sci*, vol. 11, p. 1232, Aug. 2020, doi: 10.3389/FPLS.2020.01232.
[151] P. F. Lebeau, J. Chen, J. H. Byun, K. Platko, and R. C. Austin, “The trypan blue cellular debris assay: a novel low-cost method for the rapid quantification of cell death,” *MethodsX*, vol. 6, pp. 1174–1180, Jan. 2019, doi: 10.1016/J.MEX.2019.05.010.
[152] D. Choi *et al.*, “Quantitative proteomic analysis of trypsin-treated extracellular vesicles to identify the real-vesicular proteins; Quantitative proteomic analysis of trypsin-treated extracellular vesicles to identify the real-vesicular proteins,” 2020, doi: 10.1080/20013078.2020.1757209.
[153] D. Szklarczyk *et al.*, “The STRING database in 2023: protein-protein association networks and functional enrichment analyses for any sequenced genome of interest,” *Nucleic Acids Res*, vol. 51, no. D1, pp. D638–D646, Jan. 2023, doi: 10.1093/NAR/GKAC1000.
[154] R. M. Patel, J. A. L. Van Kan, A. M. Bailey, and G. D. Foster, “Inadvertent gene silencing of argininosuccinate synthase (bcass1) in Botrytis cinerea by the pLOB1 vector system,” *Mol Plant Pathol*, vol. 11, no. 5, pp. 613–624, Sep. 2010, doi: 10.1111/J.1364-3703.2010.00632.X.
[155] A. K. Pandey, P. Jain, G. K. Podila, B. Tudzynski, and M. R. Davis, “Cold induced Botrytis cinerea enolase (BcEnol-1) functions as a transcriptional regulator and is controlled by cAMP,” *Mol Genet Genomics*, vol. 281, no. 2, pp. 135–146, Feb. 2009, doi: 10.1007/S00438-008-0397-3.
[156] W. Zhang, B. B. Ge, Z. Y. Lv, K. S. Park, L. M. Shi, and K. C. Zhang, “Membrane Protein Bcest Is Involved in Hyphal Growth, Virulence and Stress Tolerance of Botrytis cinerea,” *Microorganisms*, vol. 11, no. 5, p. 1225, May 2023, doi: 10.3390/MICROORGANISMS11051225/S1.
[157] B. An, B. Li, H. Li, Z. Zhang, G. Qin, and S. Tian, “Aquaporin8 regulates cellular development and reactive oxygen species production, a critical component of virulence in Botrytis cinerea,” *New Phytologist*, vol. 209, no. 4, pp. 1668–1680, Mar. 2016, doi: 10.1111/NPH.13721.

[158] Q. Yang, J. Jiang, C. Mayr, M. Hahn, and Z. Ma, “Involvement of two type 2C protein phosphatases BcPtc1 and BcPtc3 in the regulation of multiple stress tolerance and virulence of Botrytis cinerea,” *Environ Microbiol*, vol. 15, no. 10, pp. 2696–2711, Oct. 2013, doi: 10.1111/1462-2920.12126.
[159] J. López-Cruz, C. S. Óscar, F. C. Emma, G. A. Pilar, and G. B. Carmen, “Absence of Cu-Zn superoxide dismutase BCSOD1 reduces Botrytis cinerea virulence in Arabidopsis and tomato plants, revealing interplay among reactive oxygen species, callose and signalling pathways,” *Mol Plant Pathol*, vol. 18, no. 1, pp. 16–31, Jan. 2017, doi: 10.1111/MPP.12370.
[160] A. Schamber, M. Leroch, J. Diwo, K. Mendgen, and M. Hahn, “The role of mitogen-activated protein (MAP) kinase signalling components and the Ste12 transcription factor in germination and pathogenicity of Botrytis cinerea,” *Mol Plant Pathol*, vol. 11, no. 1, pp. 105–119, Jan. 2010, doi: 10.1111/J.1364-3703.2009.00579.X.
[161] A. R. Santamaria, N. Mulinacci, A. Valletta, M. Innocenti, and G. Pasqua, “Effects of elicitors on the production of resveratrol and viniferins in cell cultures of vitis vinifera L. cv Italia,” *J Agric Food Chem*, vol. 59, no. 17, pp. 9094–9101, Sep. 2011, doi: 10.1021/JF201181N/ASSET/IMAGES/LARGE/JF-2011-01181N_0007.JPEG.
[162] L. Lucini, G. Baccolo, Y. Rouphael, G. Colla, L. Bavaresco, and M. Trevisan, “Chitosan treatment elicited defence mechanisms, pentacyclic triterpenoids and stilbene accumulation in grape (Vitis vinifera L.) bunches,” *Phytochemistry*, vol. 156, pp. 1–8, Dec. 2018, doi: 10.1016/J.PHYTOCHEM.2018.08.011.
[163] O. Windram *et al.*, “Arabidopsis defense against Botrytis cinerea: Chronology and regulation deciphered by high-resolution temporal transcriptomic analysis,” *Plant Cell*, vol. 24, no. 9, pp. 3530–3557, 2012, doi: 10.1105/TPC.112.102046/DC1.
[164] B. Liu *et al.*, “Tomato WRKY transcriptional factor SlDRW1 is required for disease resistance against Botrytis cinerea and tolerance to oxidative stress,” *Plant Science*, vol. 227, pp. 145–156, 2014, doi: 10.1016/j.plantsci.2014.08.001.
[165] F. Mo *et al.*, “Identification of the small auxin up-regulated RNA in tomato and investigation of SlSAUR50 as a positive regulator of tomato resistance to Botrytis cinerea,” *Int J Biol Macromol*, vol. 306, p. 141738, May 2025, doi: 10.1016/J.IJBIOMAC.2025.141738.
[166] Q. TANG, X. dong ZHENG, J. GUO, and T. YU, “Tomato SlPti5 plays a regulative role in the plant immune response against Botrytis cinerea through modulation of ROS system and hormone pathways,” *J Integr Agric*, vol. 21, no. 3, pp. 697–709, Mar. 2022, doi: 10.1016/S2095-3119(21)63630-4.
[167] C. Zhou *et al.*, “WRKY Transcription Factor OsWRKY29 Represses Seed Dormancy in Rice by Weakening Abscisic Acid Response,” *Front Plant Sci*, vol. 11, May 2020, doi: 10.3389/FPLS.2020.00691.

[168] B. Blanco-Ulate, E. Vincenti, A. L. T. Powell, and D. Cantu, “Tomato transcriptome and mutant analyses suggest a role for plant stress hormones in the interaction between fruit and Botrytis cinerea,” *Front Plant Sci*, vol. 4, no. MAY, p. 142, May 2013, doi: 10.3389/FPLS.2013.00142/ABSTRACT.
[169] R. Wan *et al.*, “Resistance evaluation of Chinese wild Vitis genotypes against Botrytis cinerea and different responses of resistant and susceptible hosts to the infection,” *Front Plant Sci*, vol. 6, no. October, p. 854, Oct. 2015, doi: 10.3389/FPLS.2015.00854.
[170] V. A. Rapisarda *et al.*, “Academic Editors: Luciana Cerioni A Comparative Transcriptomic Study Reveals Temporal and Genotype-Specific Defense Responses to Botrytis cinerea in Grapevine,” 2025, doi: 10.3390/jof11020124.
[171] J. Chong, A. Poutaraud, and P. Hugueney, “Metabolism and roles of stilbenes in plants,” *Plant Science*, vol. 177, no. 3, pp. 143–155, Sep. 2009, doi: 10.1016/J.PLANTSCI.2009.05.012.
[172] B. Ramírez-Zavala, I. Krüger, C. Dunker, I. D. Jacobsen, and J. Morschhäuser, “The protein kinase Ire1 has a Hac1-independent essential role in iron uptake and virulence of Candida albicans,” *PLoS Pathog*, vol. 18, no. 2, p. e1010283, Feb. 2022, doi: 10.1371/JOURNAL.PPAT.1010283.
[173] M. Yu, X. Zhou, D. Chen, Y. Jiao, G. Han, and F. Tao, “HacA, a key transcription factor for the unfolded protein response, is required for fungal development, aflatoxin biosynthesis and pathogenicity of Aspergillus flavus,” *Int J Food Microbiol*, vol. 417, Jun. 2024, doi: 10.1016/j.ijfoodmicro.2024.110693.
[174] Y. Luo *et al.*, “The Effect of Transcription Factor MYB14 on Defense Mechanisms in Vitis quinquangularis-Pingyi,” *Int J Mol Sci*, vol. 21, no. 3, p. 706, Feb. 2020, doi: 10.3390/IJMS21030706.
[175] P. Agudelo-Romero *et al.*, “Transcriptome and metabolome reprogramming in Vitis vinifera cv. Trincadeira berries upon infection with Botrytis cinerea,” *J Exp Bot*, vol. 66, no. 7, pp. 1769–1785, 2015, doi: 10.1093/jxb/eru517.
[176] Z. M. Haile *et al.*, “Dual Transcriptome and Metabolic Analysis of Vitis vinifera cv. Pinot Noir Berry and Botrytis cinerea During Quiescence and Egressed Infection,” *Front Plant Sci*, vol. 10, Jan. 2020, doi: 10.3389/FPLS.2019.01704/FULL.
[177] M. Braaksma, E. S. Martens-Uzunova, P. J. Punt, and P. J. Schaap, “An inventory of the Aspergillus niger secretome by combining in silico predictions with shotgun proteomics data,” *BMC Genomics*, vol. 11, no. 1, pp. 1–11, Oct. 2010, doi: 10.1186/1471-2164-11-584/TABLES/5.
[178] M. Rasheed, N. Kumar, and R. Kaur, “Global Secretome Characterization of the Pathogenic Yeast Candida glabrata,” *J Proteome Res*, vol. 19, no. 1, pp. 49–63, Jan. 2020, doi: 10.1021/ACS.JPROTEOME.9B00299.

[179] S. Singh, M. Hegde, I. Kaur, and N. Adlakha, “Temporal proteome profiling of Botrytis cinerea reveals proteins involved in plant invasion and survival”, doi: 10.1038/s41598-025-92683-5.
[180] A. Gil-Bona *et al.*, “Candida albicans cell shaving uncovers new proteins involved in cell wall integrity, yeast to hypha transition, stress response and host-pathogen interaction,” *J Proteomics*, vol. 127, no. 0 0, p. 340, Sep. 2015, doi: 10.1016/J.JPROT.2015.06.006.
[181] Q. Cai *et al.*, “Plants send small RNAs in extracellular vesicles to fungal pathogen to silence virulence genes,” *Science (1979)*, vol. 360, no. 6393, pp. 1126–1129, Jun. 2018, doi: 10.1126/SCIENCE.AAR4142/ASSET/106A1632-CE8D-4958-94A0-E89E2970DF20/ASSETS/GRAPHIC/360_1126_F4.JPEG.
[182] C. Théry *et al.*, “Minimal information for studies of extracellular vesicles 2018 (MISEV2018): a position statement of the International Society for Extracellular Vesicles and update of the MISEV2014 guidelines,” *J Extracell Vesicles*, vol. 7, no. 1, Jan. 2018, doi: 10.1080/20013078.2018.1535750.
[183] J. D. Petersen, E. Mekhedov, S. Kaur, D. D. Roberts, and J. Zimmerberg, “Endothelial cells release microvesicles that harbour multivesicular bodies and secrete exosomes,” *Journal of Extracellular Biology*, vol. 2, no. 4, p. e79, Apr. 2023, doi: 10.1002/JEX2.79.
[184] B. He *et al.*, “Botrytis cinerea small RNAs are associated with tomato AGO1 and silence tomato defense-related target genes supporting cross-kingdom RNAi”, doi: 10.1101/2022.12.30.522274.
[185] J. Schumacher *et al.*, “Natural variation in the VELVET gene bcvel1 affects virulence and light-dependent differentiation in Botrytis cinerea,” *PLoS One*, vol. 7, no. 10, Oct. 2012, doi: 10.1371/JOURNAL.PONE.0047840.
[186] A. Cvjetkovic *et al.*, “Detailed Analysis of Protein Topology of Extracellular Vesicles-Evidence of Unconventional Membrane Protein Orientation,” 2016, doi: 10.1038/srep36338.
[187] R. Toribio, S. Mangano, N. Fernández-Bautista, A. Muñoz, and M. M. Castellano, “HOP, a Co-chaperone Involved in Response to Stress in Plants,” *Front Plant Sci*, vol. 11, p. 591940, Oct. 2020, doi: 10.3389/FPLS.2020.591940/BIBTEX.
[188] A. Röhl *et al.*, “Hop/Sti1 phosphorylation inhibits its co-chaperone function,” *EMBO Rep*, vol. 16, no. 2, pp. 240–249, Feb. 2015, doi: 10.15252/EMBR.201439198/SUPPL_FILE/EMBR201439198.REVIEWER_COMMENTS.PDF.
[189] M. Griesemer, C. Young, A. S. Robinson, and L. Petzold, “BiP clustering facilitates protein folding in the endoplasmic reticulum,” *PLoS Comput Biol*, vol. 10, no. 7, 2014, doi: 10.1371/JOURNAL.PCBI.1003675.
[190] Y. Gong, T. Li, C. Yu, and S. Sun, “Candida albicans Heat Shock Proteins and Hsps-Associated Signaling Pathways as Potential Antifungal Targets,” *Front Cell Infect Microbiol*, vol. 7, no. DEC, p. 520, Dec. 2017, doi: 10.3389/FCIMB.2017.00520.

[191] R. A. Bryan *et al.*, “Toward developing a universal treatment for fungal disease using radioimmunotherapy targeting common fungal antigens,” *Mycopathologia*, vol. 173, no. 5–6, pp. 463–471, Jun. 2012, doi: 10.1007/S11046-011-9476-9.
[192] Q. Meng *et al.*, “Proteomics of Rice—Magnaporthe oryzae Interaction: What Have We Learned So Far?,” *Front Plant Sci*, vol. 10, p. 1383, Oct. 2019, doi: 10.3389/FPLS.2019.01383.
[193] L. Neckers and U. Tatu, “Molecular Chaperones in Pathogen Virulence: Emerging New Targets for Therapy,” *Cell Host Microbe*, vol. 4, no. 6, p. 519, Dec. 2008, doi: 10.1016/J.CHOM.2008.10.011.
[194] N. Robbins and L. E. Cowen, “Roles of Hsp90 in Candida albicans morphogenesis and virulence,” *Curr Opin Microbiol*, vol. 75, Oct. 2023, doi: 10.1016/J.MIB.2023.102351.
[195] L. C. Horianopoulos and J. W. Kronstad, “Chaperone Networks in Fungal Pathogens of Humans,” *Journal of Fungi 2021, Vol. 7, Page 209*, vol. 7, no. 3, p. 209, Mar. 2021, doi: 10.3390/JOF7030209.
[196] D. Shi *et al.*, “S-adenosyl-L-homocysteine hydrolase FgSah1 is required for fungal development and virulence in Fusarium graminearum,” *Virulence*, vol. 12, no. 1, pp. 2171–2185, 2021, doi: 10.1080/21505594.2021.1965821/ASSET/5A11DBE8-CEF6-4428-92F7-C4AD97444F68/ASSETS/GRAPHIC/KVIR_A_1965821_F0008_OC.JPG.
[197] M. Morel, A. A. Ngadin, M. Droux, J. P. Jacquot, and E. Gelhaye, “The fungal glutathione S-transferase system. Evidence of new classes in the wood-degrading basidiomycete Phanerochaete chrysosporium,” *Cell Mol Life Sci*, vol. 66, no. 23, p. 3711, 2009, doi: 10.1007/S00018-009-0104-5.
[198] R. Singh, C. Caseys, and D. J. Kliebenstein, “Genetic and molecular landscapes of the generalist phytopathogen Botrytis cinerea,” *Mol Plant Pathol*, vol. 25, no. 1, p. e13404, Jan. 2024, doi: 10.1111/MPP.13404.
[199] S. Li *et al.*, “The δ subunit of F1Fo-ATP synthase is required for pathogenicity of Candida albicans,” *Nat Commun*, vol. 12, no. 1, p. 6041, Dec. 2021, doi: 10.1038/S41467-021-26313-9.
[200] A. Masi, R. L. Mach, and A. R. Mach-Aigner, “The pentose phosphate pathway in industrially relevant fungi: crucial insights for bioprocessing,” *Appl Microbiol Biotechnol*, vol. 105, no. 10, p. 4017, May 2021, doi: 10.1007/S00253-021-11314-X.
[201] P. C. Albuquerque *et al.*, “Vesicular transport in Histoplasma capsulatum: an effective mechanism for trans-cell wall transfer of proteins and lipids in ascomycetes,” 2008, doi: 10.1111/j.1462-5822.2008.01160.x.
[202] S. Froidurea *et al.*, “AtsPLA2-α nuclear relocalization by the Arabidopsis transcription factor AtMYB30 leads to repression of the plant defense response,” *Proc Natl Acad Sci U S A*, vol. 107, no. 34, pp. 15281–15286, Aug. 2010, doi: 10.1073/PNAS.1009056107/SUPPL_FILE/PNAS.201009056SI.PDF.

[203] W. Zhu *et al.*, "Botrytis cinerea BcCDI1 protein triggers both plant cell death and immune response," *Front Plant Sci*, vol. 14, p. 1136463, Apr. 2023, doi: 10.3389/FPLS.2023.1136463/BIBTEX.
[204] M. Frías, C. González, and N. Brito, "BcSpl1, a cerato-platanin family protein, contributes to Botrytis cinerea virulence and elicits the hypersensitive response in the host," *New Phytologist*, vol. 192, no. 2, pp. 483–495, Oct. 2011, doi: 10.1111/J.1469-8137.2011.03802.X.
[205] N. E. Soltis *et al.*, "Interactions of Tomato and Botrytis cinerea Genetic Diversity: Parsing the Contributions of Host Differentiation, Domestication, and Pathogen Variation," *Plant Cell*, vol. 31, no. 2, p. 502, Feb. 2019, doi: 10.1105/TPC.18.00857.
[206] Z. Czékus, N. Iqbal, B. Pollák, A. Martics, A. Ördög, and P. Poór, "Role of ethylene and light in chitosan-induced local and systemic defence responses of tomato plants," *J Plant Physiol*, vol. 263, p. 153461, Aug. 2021, doi: 10.1016/J.JPLPH.2021.153461.
[207] X. Liu *et al.*, "An effector essential for virulence of necrotrophic fungi targets plant HIRs to inhibit host immunity," *Nature Communications 2024 15:1*, vol. 15, no. 1, pp. 1–16, Oct. 2024, doi: 10.1038/s41467-024-53725-0.
[208] Y. Q. Gu *et al.*, "Tomato Transcription Factors Pti4, Pti5, and Pti6 Activate Defense Responses When Expressed in Arabidopsis," *Plant Cell*, vol. 14, no. 4, p. 817, 2002, doi: 10.1105/TPC.000794.
[209] W. P. Suza, M. L. Rowe, M. Hamberg, and P. E. Staswick, "A tomato enzyme synthesizes (+)-7-iso-jasmonoyl-L-isoleucine in wounded leaves," *Planta*, vol. 231, no. 3, pp. 717–728, Jan. 2010, doi: 10.1007/S00425-009-1080-6.
[210] J. Glazebrook, "Contrasting mechanisms of defense against biotrophic and necrotrophic pathogens," *Annu Rev Phytopathol*, vol. 43, pp. 205–227, 2005, doi: 10.1146/ANNUREV.PHYTO.43.040204.135923.
[211] J. Yang *et al.*, "The Crosstalks Between Jasmonic Acid and Other Plant Hormone Signaling Highlight the Involvement of Jasmonic Acid as a Core Component in Plant Response to Biotic and Abiotic Stresses," *Front Plant Sci*, vol. 10, p. 458580, Oct. 2019, doi: 10.3389/FPLS.2019.01349/XML.
[212] M. Wang, A. Weiberg, E. Dellota, D. Yamane, and H. Jin, "Botrytis small RNA Bc-siR37 suppresses plant defense genes by cross-kingdom RNAi," *RNA Biol*, vol. 14, no. 4, pp. 421–428, Apr. 2017, doi: 10.1080/15476286.2017.1291112.
[213] J. S. Thaler, P. T. Humphrey, and N. K. Whiteman, "Evolution of jasmonate and salicylate signal crosstalk," *Trends Plant Sci*, vol. 17, no. 5, pp. 260–270, May 2012, doi: 10.1016/J.TPLANTS.2012.02.010/ASSET/BEDF0AEF-F5CE-4CC6-B944-1C8468BDA8C5/MAIN.ASSETS/GR1.JPG.
[214] M. Greco *et al.*, "Upcycling olive pomace into pectic elicitors for plant immunity and disease protection," *Plant Physiology and Biochemistry*, vol. 217, p. 109213, Dec. 2024, doi: 10.1016/J.PLAPHY.2024.109213.

[215] M. Greco *et al.*, “Phenolic compounds-enriched extract recovered from two-phase olive pomace serves as plant immunostimulants and broad-spectrum antimicrobials against phytopathogens including Xylella fastidiosa,” *Plant Stress*, vol. 14, p. 100655, Dec. 2024, doi: 10.1016/J.STRESS.2024.100655.
[216] C. Saigne-Soulard *et al.*, “Oligosaccharides from Botrytis cinerea and Elicitation of Grapevine Defense,” *Polysaccharides: Bioactivity and Biotechnology*, pp. 939–958, Jan. 2015, doi: 10.1007/978-3-319-16298-0_8.
[217] A. Vannozzi, I. B. Dry, M. Fasoli, S. Zenoni, and M. Lucchin, “Genome-wide analysis of the grapevine stilbene synthase multigenic family: genomic organization and expression profiles upon biotic and abiotic stresses,” *BMC Plant Biol*, vol. 12, no. 1, pp. 1–22, Aug. 2012, doi: 10.1186/1471-2229-12-130/FIGURES/7.
[218] A. Aziz, A. Heyraud, and B. Lambert, “Oligogalacturonide signal transduction, induction of defense-related responses and protection of grapevine against Botrytis cinerea,” *Planta*, vol. 218, no. 5, pp. 767–774, Mar. 2004, doi: 10.1007/S00425-003-1153-X/FIGURES/5.
[219] S. Trouvelot *et al.*, “A beta-1,3 glucan sulfate induces resistance in grapevine against Plasmopara viticola through priming of defense responses, including HR-like cell death,” *Mol Plant Microbe Interact*, vol. 21, no. 2, pp. 232–243, Feb. 2008, doi: 10.1094/MPMI-21-2-0232.
[220] A. Koornneef *et al.*, “Kinetics of salicylate-mediated suppression of jasmonate signaling reveal a role for redox modulation,” *Plant Physiol*, vol. 147, no. 3, pp. 1358–1368, 2008, doi: 10.1104/PP.108.121392.
[221] A. Robert-Seilaniantz, M. Grant, and J. D. G. Jones, “Hormone crosstalk in plant disease and defense: more than just jasmonate-salicylate antagonism,” *Annu Rev Phytopathol*, vol. 49, pp. 317–343, Sep. 2011, doi: 10.1146/ANNUREV-PHYTO-073009-114447.
[222] S. C. Hoo *et al.*, “Regulation and Function of Arabidopsis JASMONATE ZIM-Domain Genes in Response to Wounding and Herbivory,” *Plant Physiol*, vol. 146, no. 3, pp. 952–964, Mar. 2008, doi: 10.1104/PP.107.115691.
[223] M. Jing *et al.*, “A Phytophthora sojae effector suppresses endoplasmic reticulum stress-mediated immunity by stabilizing plant Binding immunoglobulin Proteins,” *Nature Communications 2016 7:1*, vol. 7, no. 1, pp. 1–17, Jun. 2016, doi: 10.1038/ncomms11685.
[224] C. J. Park, R. Bart, M. Chern, P. E. Canlas, W. Bai, and P. C. Ronald, “Overexpression of the Endoplasmic Reticulum Chaperone BiP3 Regulates XA21-Mediated Innate Immunity in Rice,” *PLoS One*, vol. 5, no. 2, p. e9262, Feb. 2010, doi: 10.1371/JOURNAL.PONE.0009262.
[225] T. W. H. Liebrand *et al.*, “Chaperones of the endoplasmic reticulum are required for Ve1-mediated resistance to Verticillium,” *Mol Plant Pathol*, vol. 15, no. 1, pp. 109–117, Jan. 2014, doi: 10.1111/MPP.12071/SUPPINFO.

[226] J. P. Derckel *et al.*, “Differential Induction of Grapevine Defenses by Two Strains of Botrytis cinerea,” *Phytopathology*, vol. 89, no. 3, pp. 197–203, 1999, doi: 10.1094/PHYTO.1999.89.3.197.
[227] M. Hönig, V. M. Roeber, T. Schmülling, and A. Cortleven, “Chemical priming of plant defense responses to pathogen attacks,” *Front Plant Sci*, vol. 14, p. 1146577, 2023, doi: 10.3389/FPLS.2023.1146577.
[228] A. Nesler, M. Perazzolli, G. Puopolo, O. Giovannini, Y. Elad, and I. Pertot, “A complex protein derivative acts as biogenic elicitor of grapevine resistance against powdery mildew under field conditions,” *Front Plant Sci*, vol. 6, no. September, Sep. 2015, doi: 10.3389/FPLS.2015.00715.
[229] N. Mohamed *et al.*, “Defense Responses in Grapevine Leaves Against Botrytis cinerea Induced by Application of a Pythium oligandrum Strain or Its Elicitin, Oligandrin, to Roots,” *Phytopathology*, vol. 97, no. 5, pp. 611–620, May 2007, doi: 10.1094/PHYTO-97-5-0611.
[230] A. Aziz *et al.*, “Laminarin elicits defense responses in grapevine and induces protection against Botrytis cinerea and Plasmopara viticola,” *Mol Plant Microbe Interact*, vol. 16, no. 12, pp. 1118–1128, 2003, doi: 10.1094/MPMI.2003.16.12.1118.